Collectives excitations in nuclei

P. Chomaz

Collective excitations in nuclei.

Ph. CHOMAZ
GANIL, BP 5027,
14076 CAEN Cedex 5,
FRANCE,
chomaz@ganil.fr

Abstract:

In these lectures we will describe several aspects of giant resonances observed in nuclei. We will present the theoretical tools in order to describe collective vibrations in hot and cold, stable or unstable, nuclei. This presentation will be illustrated by many experimental results.

Resumer :

Dans ce cours nous abordons les différents aspects des résonances géantes observées dans les noyaux. Qu'ils soient chauds, qu'ils soient froids, qu'ils soient exotiques, qu'ils soient stables, qu'ils soient instables nous nous attacherons à discuter les méthodes théoriques employées pour les décrire. Cette présentation sera illustrée par de nombreux resultats expérimentaux.

Chapter 1 Introduction

Collective behaviors are a general property of systems with many degrees of freedom. Often they describe how they react to an external stress. It is a general observation that complex systems are often able to self-organize in simple collective motion while they are expected to present disorder and chaos because of their intrinsic complexity. This paradox is well illustrated by the atomic nucleus. On the one hand, following the Bohr ideas, this strongly interacting system can be seen as the prototype of quantum chaos. On the other hand, other experimental evidences, such as the existence of magic numbers and the presence of giant resonances, are pleading in favor of a strongly organized system. The study of this amazing self-organization and its transition from order to chaos is one of the subject of the present article.

Of particular interest are the collective motions that can be interpreted in terms of vibration. If the associated string constant is positive the motion corresponds to an oscillation around an equilibrium or more generally around a stable solution. Conversely, when the string constant is negative this is the signature of the presence of instabilities in the system. Both cases correspond to typical situations encountered in many different physical systems. In this article we will discuss these two different aspects of collective vibrations taking as an example the nuclear systems.

In quantum mechanics, stable vibrations are associated with boson degrees of freedom. At first glance, this may seem surprising, particularly when considering excitations of macroscopic systems formed with fermions. Collective oscillations have been observed in mesoscopic systems such as zero-sound phonons in helium-3 fluids or plasmons in metallic clusters. Also, the nucleus is known to exhibit a large variety of collective vibrations usually called phonons. These giant resonances are understood as the first oscillator quanta of the collective vibrations. In particular, the giant dipole resonance corresponds to a collective motion of the protons against the neutrons which is akin to the plasmons in metals, the monopole vibration is a compression mode analogous to the zero- sound in Fermi liquids, and the giant quadrupole resonance is understood as a surface vibration which resembles the wave at the interface of two liquids.

From the microscopic point of view, these bosons can be understood as being built from fermion pairs, which carry boson quantum numbers. However, the number of possible pairs much be large enough to insure that the effects of the fermion antisymmetrization do not introduce significant deviations from a boson behavior. Moreover, the excitations of small fermionic systems are not expected to be well described by a boson picture, in particular, because the Pauli exclusion principle imposes constraints that cannot be accounted for in a boson representation. In this article we will present some properties of giant resonances and we will discuss the above questions. We will also investigate their properties at zero and at finite temperature and we will discuss their role in the dynamics of nuclear reactions.

Until recently, the second and higher quanta, the so-called multiphonons states, remained unobserved. Therefore, the observation of multiple excitations of giant resonances was an important missing piece in the puzzle of collective excitations. The non-existence of multiple excitations would have undermined our understanding of giant resonances. In the early seventy's it has been proposed that multiphonons states might be excited during heavy ion reactions. It was proposed that the multiphonon excitations might be responsible for part of the energy lost observed in deep-inelastic reactions. In 1977, structures were observed in heavy ion inelastic spectra and it was suggested that these structures might be due to multiple excitations of giant resonances. However, it is only recently that an unambiguous signature of the multiphonon nature of the structures observed in heavy ion reactions have been reported. This study about multiphonon states will also be part of the present article.

Finally, in the recent years it has been increasingly evident that the systems formed during nuclear collisions might run across instabilities. Of particular interest are the instabilities related with the transition from liquid to gas because it might be a way to get information about the nuclear equation of state. From a more general point of view, the creation of domains during a phase transition might be thought as a highly collective motion. Therefore it is important to understand the possible links between phase transitions and collective motions. This will also be a subject of the present article.

Chapter 2 Phenomenology of Giant Resonances

Before proceeding to a study of giant resonances in many different contexts, it is necessary to briefly review their phenomenology. The subject of giant resonance excitations in nuclei has been treated extensively in many review articles (see for example [Be75a, Sp81, Be76a, Wo87]) to which one can refer for a detailed information.

2.1 An example: the Giant Dipole Resonance

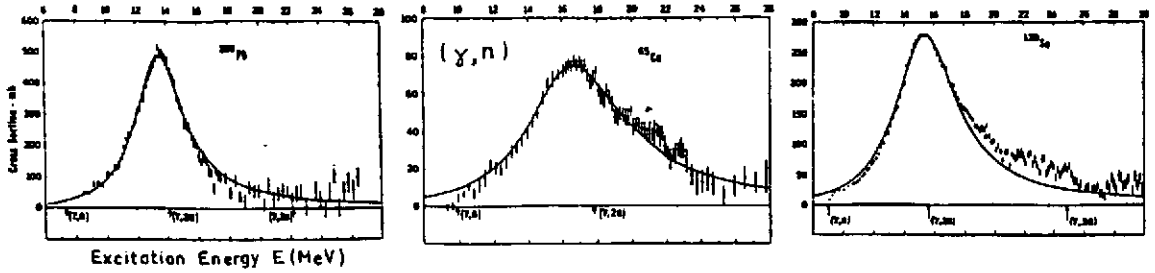

Figure 1 Giant Dipole Resonance in (γ,n) Reactions: The total photo neutron cross section for three nuclei ^{208}Pb, ^{120}Sn, and ^{65}Cu from ref. [Be75b] showing the strong resonance associated with a dipole vibration of the nucleus, the so-called Giant Dipole Resonance.

In 1947, Baldwin and Klaiber [Ba47] carried out photon-induced reactions and observed that at high excitation energies of about 15 to 20 MeV, the nucleus acts as a strong absorber of the incident photons (see Fig. 1). This phenomenon was named the nuclear giant resonance. In fact, this possibility of a resonant γ absorption was mention 10 years before in a paper by Bothe and Gentner who noticed that some γ capture probabilities were much higher than expected. The observed peak in the photo-absorption probability was interpreted by Goldhaber and Teller[Go48] as the excitation of a collective nuclear vibration in which all the protons in the nucleus move collectively against all the neutrons providing a separation between the centers of mass and charge, thus creating an electric dipole moment.

2.1.1 Experimental systematics about the GDR

Experimentally, the GDR is well established as a general feature of all nuclei. It has been observed in nuclei as light as ^3He and as heavy as ^{232}Th. Nearly all the systematic information comes from photoabsorption experiments because of the high selectivity of this reaction to E_1 transitions. An example of spectra from photonuclear reactions on three different targets is shown in Fig.1. However, complementary information has been obtained more recently in electron, proton or heavy ion inelastic scattering associated with coincidence measurements.

2.1.1.1 Cross section

In spherical nuclei, the cross section σ_{abs} of photoabsorption can be approximated by a Lorentzian distribution

$$\sigma_{abs}(E_\gamma) = \frac{\sigma_R E_\gamma^2 \Gamma_{GDR}^2}{(E_\gamma^2 - E_{GDR}^2)^2 + E_\gamma^2 \Gamma_{GDR}^2} \quad , \tag{2.1}$$

where σ_R is the maximum of the distribution, E_{GDR} and Γ_{GDR} the energy and width of the GDR. In nuclei with a large static deformation the GDR splits into two components corresponding to oscillations along and perpendicular to the symmetry axis (see Fig.2).

In that case, the GDR cross section is well reproduced by the sum of two Lorentzian components. Both for spherical and deformed nuclei, the Lorentzian parametrization provides a good description of the shape of the GDR in medium and heavy nuclei by treating the resonance energy, width and strength as energy independent empirically adjustable parameters.

2.1.1.2 Excitation energy

Using this method, it has been shown that the A dependence of the excitation energy of the dipole is intermediate between $A^{-1/6}$ and $A^{-1/3}$ and can be reproduced by a two parameter expression [Be75a]: (see Fig.3).

$$E_{GDR} = 31.2A^{-1/3} + 20.6A^{-1/6}\ (MeV) \quad . \tag{2.2}$$

However, as far as medium and heavy nuclei are concerned, the energy of the GDR can be fairly reproduced by the simple law, $E_{GDR} \approx 80A^{-1/3}\ (MeV)$.

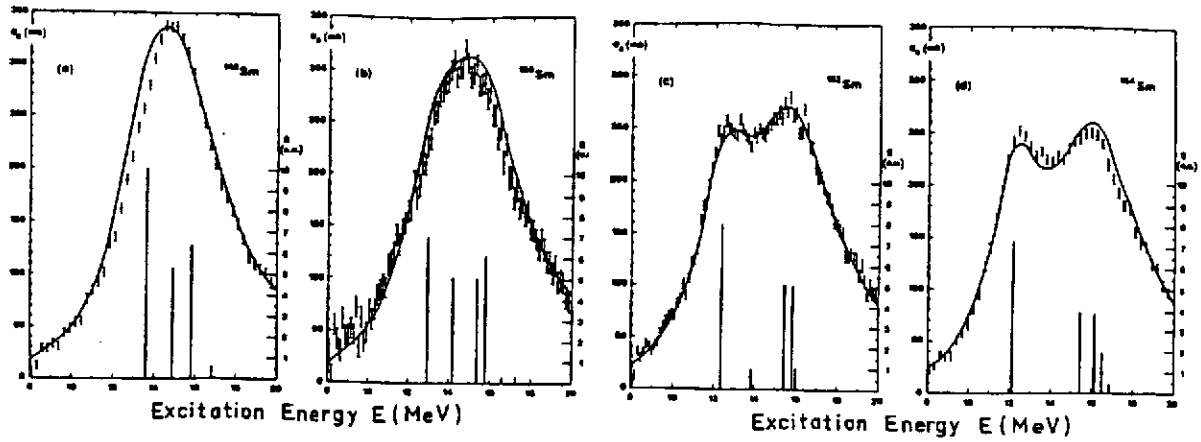

Figure 2 Evolution of the GDR with Deformation: Total photo neutron cross section for Sm isotopes showing the evolution of the giant dipole resonance in going from the spherical nucleus ^{148}Sm to the deformed nucleus ^{154}Sm(see ref. [Ma84])

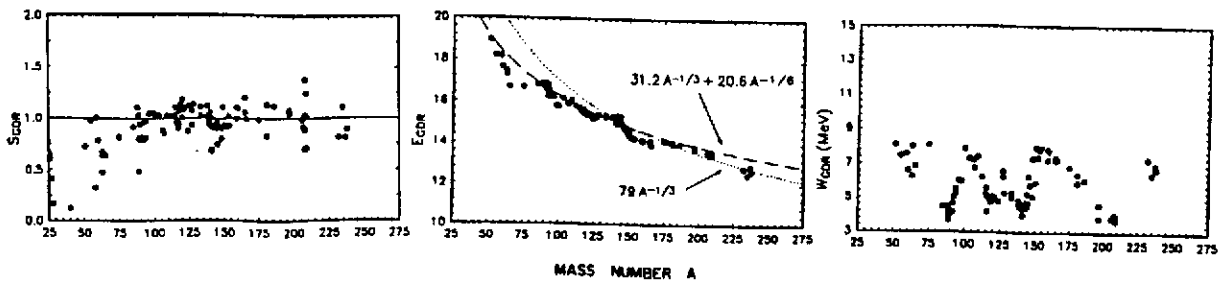

Figure 3 Properties of the GDR : Systematics for the excitation energy E_x, width Γ and fraction of the E_1 energy sum rule strength of the GDR as a function of the nucleus mass A.(see ref. [Ga92]).

2.1.1.3 Width

The observed width Γ_{GDR} of the resonance, varies from 4 to 8 MeV with the narrowest width found in magic nuclei (see Fig.3). As giant resonances are excited at energies above the particle emission threshold, their total width is, apart from the effects of the possible deformation, a sum of three terms the escape width $\Gamma^{\uparrow}$, the Landau damping $\Delta\Gamma$, and the spreading width $\Gamma^{\downarrow}$. The escape width $\Gamma^{\uparrow}$ is due to the coupling of the 1p-1h state to the continuum which gives rise to the direct decay of a particle into hole states of the residual nucleus and can provide an experimental probe into the microscopic description of the giant resonances. It is the dominant contribution for light nuclei. The Landau damping $\Delta\Gamma$ results from the fragmentation of the p-h strength due to shell structure effects and is also mainly apparent in light nuclei. The spreading width $\Gamma^{\downarrow}$ arises from the coupling of the 1p-1h doorway states to nuclear compound states, eventually, leading to the emission of low energy particles. With increasing mass number, the decay proceeds mainly via mixing with more complicated states, so, for heavy nuclei, the total width is dominated by the spreading width.

2.1.1.4 Collectivity and excitation properties

The collectivity of the excitation which is related to the number of participating nucleons, can be measured by the fraction of the energy weighted sum rule (EWSR) exhausted. For example, the dipole strength integrated up to E_γ=30 MeV can be expressed in terms of Thomas Reiche-Kuhn sum rule[Le50]:

$$m_1 = \frac{2\pi e^2 h}{mc}\frac{NZ}{A} \sim 60\frac{NZ}{A} MeV.mb \quad , \tag{2.3}$$

where N and Z are the neutron and proton number of the nucleus respectively, A=N+Z and m is the nucleon mass. The fraction of the EWSR observed in the various nuclei is shown in figure 3.

2.1.2 Macroscopic description

The giant dipole resonance (GDR) is considered today as the prototype of giant resonances which are considered as highly collective nuclear excitations in which an appreciable fraction of the nucleons of a nucleus move together.

In such a context, it is appropriate to think about these modes of excitation in hydrodynamical terms as the oscillation of a liquid drop. To explain the observation of the GDR, different models were proposed. In the Steinwedel and Jensen model[St50], the total nucleus density is incompressible but the neutron and proton densities vary independently. In that case, the restoring force is proportional to the volume energy coefficient of the Bethe and Weiszacker formula. This model gives the energy of the vibration proportional to $A^{-1/3}$. In the Goldhaber and Teller model[Go48], the GDR is considered as an oscillation of a non-deformed neutron sphere against a proton one. In this case, the restoring force is proportional to the surface energy coefficient of the Bethe and Weizacker formula and the excitation energy of the GDR vary as $A^{-1/6}$.

Let us discuss in a little bit more details these macroscopic models in order to introduce the basic concepts about collective vibrations.

2.1.2.1 The Goldhaber and Teller model[Go48]

In this model the protons and the neutrons are simply assumed to oscillate with opposite phases. Let us consider a system with equal number of protons and neutrons, $N = Z = A/2$. If we call $z(t)$ the displacement of each protons and $-z(t)$ the displacement of each neutrons (so that the center of mass is kept constant) in the $\vec{u}_0$ direction we can easily compute the total kinetic energy

$$T = \sum_{protons} 1/2 m_p \dot{z}^2 + \sum_{neutrons} 1/2 m_n \dot{z}^2 = 1/2 A m \dot{z}^2 \tag{2.4}$$

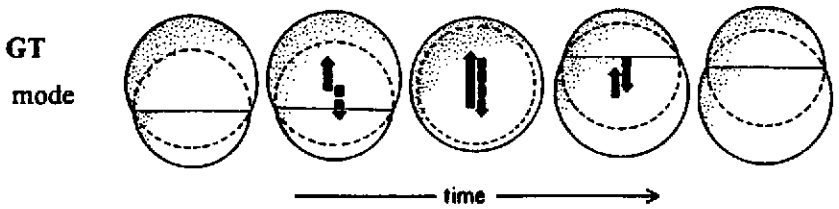

Figure 4 GDR vibration: Shematic picture of the GDR in the Goldhaber and Teller model [Go48].

In order to compute the variation of binding energy induced by the displacement z Goldhaber and Teller assumed that the potential energy depends upon the difference of the neutron and proton densities and that for symmetry reasons only the quadratic power of this difference appears in the symmetry energy

$$E_{sym} = \int d^3 r \mathcal{V}_{sym} \left[\rho_p(r) - \rho_n(r)\right] \tag{2.5}$$

For example introducing the symmetry density

$$\rho_{sym} = \rho_p - \rho_n \tag{2.6}$$

the symmetry term of the binding energy may be approximated by the liquid-drop formulation

$$E_{sym} = \frac{1}{2} b_{sym} \int d^3 r \frac{\rho_{sym}^2}{\rho_0} \tag{2.7}$$

where b_{sym} is a coefficient with an empirical value about 50 MeV.

Introducing the displaced densities and assuming that proton and neutron densities are equal the half of the matter density ρ^0we can write

$$\begin{aligned} \rho_p(\vec{r}) &= \rho_p^0(\vec{r} - z\,\vec{u}_0) = \tfrac{1}{2}\rho^0(\vec{r} - z\,\vec{u}_0) = \tfrac{1}{2}\left(\rho^0(\vec{r}) - z\,\vec{u}_0 \cdot \vec{\nabla}\rho^0(\vec{r})\right) \\ \rho_n(\vec{r}) &= \rho_n^0(\vec{r} + z\,\vec{u}_0) = \tfrac{1}{2}\rho^0(\vec{r} + z\,\vec{u}_0) = \tfrac{1}{2}\left(\rho^0(\vec{r}) + z\,\vec{u}_0 \cdot \vec{\nabla}\rho^0(\vec{r})\right) \end{aligned} \tag{2.8}$$

Then the potential energy reads

$$E_{sym} = \frac{1}{2} z^2 \int d^3 r \left(\nabla_{\vec{u}_0}\rho^0\right)^2 \frac{\partial^2 \mathcal{V}_{sym}}{\partial \rho^2} = \frac{b_{sym}}{\rho_0} z^2 \int d^3 r \left(\nabla_{\vec{u}_0}\rho^0\right) \tag{2.9}$$

where the last equality comes from the liquid-drop approximation. If the density ρ^0 is assumed to be spherically symmetric[1] we can chose $\vec{u}_0$ on the z axis and we can use the fact that $\partial\rho^0/\partial z = \partial\rho^0/\partial r\ \partial r/\partial z = \cos\theta\ \partial\rho^0/\partial r$ in order to write.

[1] From this model, it is clear that the restauring force depends upon the shape of the system, as we will discuss later.

$$E_{sym} = \frac{1}{2} z^2 \frac{4\pi}{3} \int r^2 dr \left(\frac{d\rho^0}{dr} \right)^2 \frac{\partial^2 \mathcal{V}_{sym}}{\partial \rho^2} \tag{2.10}$$

Now we can write the total energy variation associated with the dipole motion as

$$\Delta E = T + E_{sym} = \frac{1}{2} M \dot{z}^2 + \frac{1}{2} K z^2 \tag{2.11}$$

where the inertia parameter is noting but the total mass of the system

$$M = Am \tag{2.12}$$

and the spring constant is given by

$$K = \int d^3r \left(\nabla_{\vec{u}_0} \rho^0 \right)^2 \frac{\partial^2 \mathcal{V}_{sym}}{\partial \rho^2} = \frac{b_{sym}}{\rho_0} \int d^3r \left(\nabla_{\vec{u}_0} \rho^0 \right)^2 \tag{2.13}$$

From these equations it is clear that M is proportional to the total mass of the system while K is proportional to $A^{2/3}$ because $\nabla_{\vec{u}_0} \rho^0$ is picked at the surface. Equation 2.11 can be recognized as an harmonic oscillator Hamiltonian which is the collective Hamiltonian for the vibration.

2.1.2.2 Classical vibration

To get a deeper insight into the dynamics associated with the Hamiltonian 2.11 we can solve the classical equation of motion which simply reads

$$M \frac{d^2 z}{dt^2} = -K z \tag{2.14}$$

The corresponding free motion is a harmonic oscillation of frequency

$$\omega = \sqrt{\frac{K}{M}} \tag{2.15}$$

Considering the mass dependence of the string constant and of the inertia parameter on gets

$$\omega(A) = \omega_0 A^{-1/6} \tag{2.16}$$

We have seen that this dependence is confirmed by the experimental results only in light nuclei. Therefore on needs other models to describe dipole vibrations in larger nuclei.

2.1.2.3 Steinwedel and Jensen model

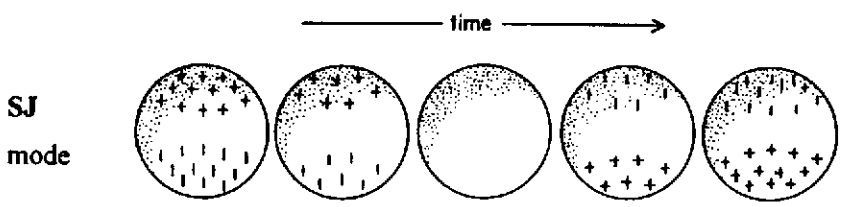

Figure 5 GDR vibration : Shematic picture of the GDR in the Steinwedel and Jensen model [St50].

From the above derivation it appears that the GDR frequency should be a function of $A^{-1/6}$ while experimentally the frequency appears to be closer to $A^{-1/3}$. It appears that because of the strong force characteristics and in particular of the strong short range attraction between protons and neutrons it is energetically not favorable to introduce a displacement of the proton surface against the neutron one as it is assumed in the Goldhaber and Teller model. To overcome this difficulty Steinwedel and Jensen have proposed to introduce a displacement field (i.e. it is not as before a global displacement of the proton or the neutrons but a local one) which vanishes at the surface. This can be done by introducing the following displacement of protons

$$\mathbf{u}(\mathbf{r}) = Q_{l,m}(t) \tau_Z \nabla \left(j_l(qr) Y_{l,m}(\hat{r}) \right) \tag{2.17}$$

where τ_Z is the third component of isospin operator (-1 for protons +1 for neutrons)and where j_1 is the spherical Bessel function[2]. Requiring that the motion at the surface is 0 means that the surface radius, R, should be associated with a zero of the derivative of the Bessel function. The first zero being around 2.46 this condition leads to

$$q = 2.46/R \tag{2.18}$$

In infinite medium the collective oscillations of protons against neutrons look like sound waves with a sound velocity almost independent of q

$$c = \frac{\omega}{q} \tag{2.19}$$

so that we get for the frequency

$$\omega \propto \frac{1}{R} \propto A^{-1/3} \tag{2.20}$$

which exhibits the proper behavior as a function of A.

2.1.2.4 Electromagnetic excitations

Let us now how this mode can be excited through electromagnetic excitations and in particular let discuss relativistic Coulomb excitations such as the ^{136}Xe excitation during the reaction $^{208}Pb + ^{136}Xe$ at E/A = 700 MeV which has been studied in refs [Ri93, Sc93a]. In such relativistic reaction between heavy ions the strong transverse electric field

$$E_\perp(t) = -\frac{Z_p e \gamma b}{(b^2 + \gamma^2 v^2 t^2)^{\frac{3}{2}}} \tag{2.21}$$

dominates. In eq. (2.21) it is assumed that the projectile of charge Z_p is travelling on a straight line trajectory defined by an impact parameter b and a constant velocity v [Ba88a].

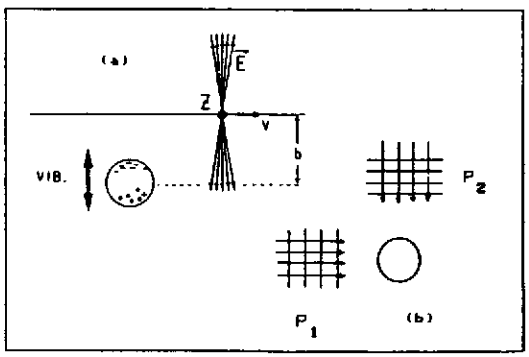

Figure 6 Schematic illustration of the electric field create by a relaticvistic heavy ion traveling on a straight line. This electric field may excite the giant dipole mode [Ba88a].

Therefore, the excitation of the transverse GDR degrees of freedom in a nucleus of mass A, charge Z and neutron number N, is simply due to the interaction of the protons with the constant electric field. Therefore, the interaction energy associated with the displacement z in the transverse direction simply reads

$$W(t) = Ze\ E_\perp(t)\ z = F_{ext}(t)\ z \tag{2.22}$$

Then this energy can be used in conjugation with the collective Hamiltonian in order to write the dynamical equations for the dipole moment in presence of an external field

$$M\frac{d^2 z}{dt^2} - K\ z = F_{ext}(t) \tag{2.23}$$

where $F_{ext}(t) = Ze\ E_\perp(t)$. In order to understand the resonant shape of the dipole excitation we should add to this equation a term taking into account the damping of the GDR. This can be done by introducing a simple frictional force conventionally written $F_{fric} = -M\gamma\ \dot{z}$. Then the classical equations reads

$$M\frac{d^2 z}{dt^2} + M\gamma\ \frac{d\ z}{dt} - K\ z = F_{ext}(t) \tag{2.24}$$

[2]This can be justified assuming a potential flow $\mathbf{u} = \chi$ where the displacement potential is assumed to be the dipole term of the multipole expention of a plane wave with the momentum q.

This equation can be easily solved going to the Fourier representation and introducing the field frequency ω_{ext}

$$F_{ext}(t) = F_0 e^{-i\omega_{ext} t} \tag{2.25}$$

However, one should remember that Physical external forces are real so that only the real part of the expression we will derived are meaning full. With the above field the motion of the dipole reads

$$z(t) = \frac{1/M}{\omega^2 - \omega_{ext}^2 - i\gamma\omega_{ext}} F_0 e^{-i\omega_{ext} t} \equiv \Pi(\omega_{ext})\ F_0 e^{-i\omega_{ext} t} \tag{2.26}$$

where the operator $\Pi(\omega_{ext})$ gives the response of the system to an external field at the frequency ω_{ext}. In order to compute the average rate of energy lost per unit time we should compute

$$P = \overline{\mathrm{Re}\left(F_{ext}(t)\right) \mathrm{Re}\left(\dot{z}(t)\right)} \tag{2.27}$$

where the $\overline{\ldots}$ means the average over time. Because of the time averaging only the imaginary part of $\Pi(\omega_{ext})$ contributes and one gets

$$P = \frac{F_0^2}{M} \frac{\gamma\omega_{ext}^2}{\left(\omega^2 - \omega_{ext}^2\right)^2 + \gamma^2\omega_{ext}^2} \tag{2.28}$$

which is nothing but the Lorentzian shape.

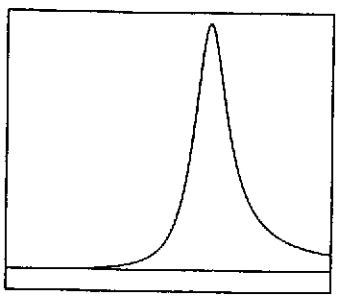

Figure 7 Lorentzian resonance profile.

Here we took as an example the Coulomb excitation but the same arguments hold for the photoabsorption and indeed this shape correctly describe the observed GDR data in heavy nuclei.

2.1.2.5 Quantization of the motion

In order to built a quantum version of the vibration in absence of friction we can first introduce $P = M\dot{Q}$ the momentum conjugated of the coordinate Q (in the simple models of the GDR above this collective coordinate was z the displacement on the z axis of the proton against neutrons). Then, the total Hamiltonian,

$$H = \frac{1}{2M}P^2 + \frac{K}{2}Q^2 \quad , \tag{2.29}$$

can now be quantized as a harmonic oscillator with the frequency:

$$\omega_\lambda = \sqrt{\frac{K_\lambda}{M_\lambda}} \quad . \tag{2.30}$$

To do so we consider P and Q as operators, $\hat{P}$ and $\hat{Q}$ and we introduce the creation and annihilation operators for the phonons, $\hat{O}^\dagger$ and $\hat{O}$, defined by the relations :

$$\hat{Q} = \sqrt{\frac{\omega}{2K}}(\hat{O}^\dagger + \hat{O}) \tag{2.31}$$

and

$$\hat{P} = i\sqrt{\frac{\omega M}{2}}(\hat{O}^\dagger - \hat{O}) \quad . \tag{2.32}$$

Therefore, the excitation spectrum can be simply built from a ground state $|0\rangle$ by application of the creation operator

$$|GDR\rangle = \hat{O}^\dagger |0\rangle \tag{2.33}$$

2.1.2.6 Sum rules and Energy weighted Sum rule (m_1)

When we will consider excitations or perturbations of the system induced by any operator $\hat{D}$ we will need matrix elements for the induced transitions $\langle 0|\hat{D}|GDR\rangle$. To be more general, we will not only consider one collective state $|GDR\rangle$ but several noted $|i\rangle$. which are supposed to form a complete basis together with the ground state. Then we can introduce various sum rules as

$$m_n = \sum_i (E_i - E_0)^n \left|\langle 0|\hat{D}|i\rangle\right|^2 \tag{2.34}$$

which are nothing but the n^{th} moments of the transition probability distribution usually called strength function

$$S_{\hat{D}}(E) = \sum_i \delta(E - (E_i - E_0)) \left|\langle 0|\hat{D}|i\rangle\right|^2 \tag{2.35}$$

Among all the possible moments m_1 is very particular since the following relation holds

$$m_1 = \frac{1}{2}\langle 0|\left[\hat{D},\left[\hat{H},\hat{D}\right]\right]|0\rangle \tag{2.36}$$

which is easily demonstrated introducing a closure relation $1 = \sum_i |i\rangle\langle i| + |0\rangle\langle 0|$ in the expression of the double commutator and using the fact that the $|i\rangle$ or the $|0\rangle$ are eigen vectors of the Hamiltonian H : $\hat{H}|i\rangle = E_i|i\rangle$. The important property of the relation (2.36) is that the expectation value of the double commutator on the ground state can easily be compute.

For the dipole excitation operator associated with an electric field E in the z direction the operator is $\hat{D} = Ee\sum_{nucl}\frac{z_{nucl}\tau_{nucl}}{2}$ where the fact that we are taking half the sum over protons and neutrons with opposite signs instead of just the sum over protons come from the fact that we have removed the center of mass motion (and we have assumed equal number of protons and neutrons). Then if the interaction does not depend upon the momenta of the particles, the double commutator reduces to a double commutator only with the kinetic part which leads to

$$\left[\hat{D},\left[\hat{H},\hat{D}\right]\right] = \sum_{nucl}\frac{1}{2m}\frac{E^2e^2}{2} \tag{2.37}$$

and the sum rule is nothing but the TRK sum rule

$$m_1 = \frac{A}{4}\frac{E^2e^2}{2m} \tag{2.38}$$

(in the case $N \neq Z$ the factor $A/4$ should be simply replaced by NZ/A).

2.1.2.7 Polarizability sum m_{-1} and adiabatic approaches

Another sum rule plays an important role because it appears in the case a static field A is applied to the system. Indeed, then the system adjust it self (polarized) to this perturbation. In the first order perturbation theory the state of the system is

$$|\Psi\rangle = |0\rangle + \sum_i \frac{\langle i|A|0\rangle}{(E_i - E_0)}|i\rangle \tag{2.39}$$

Therefore, if one measures the expectation value of A, also called polarizability, on the state $|\Psi\rangle$ one gets always at the lowest order

$$\langle\Psi|A|\Psi\rangle - \langle 0|A|0\rangle = \sum_i \frac{|\langle i|A|0\rangle|^2}{(E_i - E_0)} = m_{-1} \tag{2.40}$$

which is nothing but the Polarizability sum m_{-1}.

To apply this method to dipole mode one can polarize the system with an external constant electric field E and measure the induced dipole moment. To compute this moment we can simply minimize the energy of the system in presence of the external field E. Let us introduce the isovector density

$$\rho_{sym} = \rho_p - \rho_n \tag{2.41}$$

Then the energy associated with the external field is given by

$$E_{Coul} = \int d^3r V(r)\frac{e}{2}\rho_{sym} = \frac{e}{2}E\int d^3r z\rho_{sym} \tag{2.42}$$

since the potential associated with E along the z axis is $V = zE$. The symmetry term of the binding energy acts against the separation of protons and neutrons in nuclei. The corresponding energy variation is simply

$$E_{sym} = \frac{1}{2}b_{sym}\int d^3r\frac{\rho_{sym}^2}{\rho_0} \tag{2.43}$$

where b_{sym} is a coefficient with an empirical value about 50 MeV. Then the total energy reads

$$E_{tot} = \int d^3r \left(\frac{1}{2} b_{sym} \frac{1}{2} \frac{\rho_{sym}^2}{\rho_0} + \frac{e}{2} E z \rho_{sym} \right) \tag{2.44}$$

Introducing a small variation of the density ρ_{sym} we get a variation of the total energy

$$\delta E_{tot} = \int d^3r \delta\rho_{sym} \left(b_{sym} \frac{\rho_{sym}}{\rho_0} + \frac{e}{2} E z \right) \tag{2.45}$$

The density which minimize E_{tot} should fullfil this relation for any fluctuation $\delta\rho_{sym}$. Thus we get

$$\rho_{sym} = -\frac{e}{2b_{sym}} E z \rho_0 \tag{2.46}$$

If we now measure the dipole moment D we should compute

$$D = \int d^3r \delta\rho_{sym} \frac{e}{2} z = \frac{e^2 E \rho_0 \langle r^2 \rangle}{12 b_{sym}} \tag{2.47}$$

So that the polarizability α which is nothing but the induced dipole divided by the applied field reads:

$$\alpha = \frac{D}{E} = \frac{e^2 \rho_0 \langle r^2 \rangle}{12 b_{sym}} \tag{2.48}$$

2.1.2.8 GDR energy from sum rules approaches

If we use the relation between the polarizability and the m_{-1} sum rule in the case of a unique collective state we get

$$\alpha = m_{-1} = \frac{\left| \langle GDR | \hat{D} | 0 \rangle \right|^2}{E_{GDR}} \tag{2.49}$$

where A is the dipole operator $A = e \sum_{nucl} \frac{z_{nucl} \tau_{nucl}}{2}$. On the other hand the TRK sum rule was

$$m_1 = E_{GDR} \left| \langle GDR | \hat{D} | 0 \rangle \right|^2 \tag{2.50}$$

Therefore, the GDR energy can be simply obtained from the ration of m_{-1} and m_1

$$E_{GDR} = \sqrt{\frac{m_1}{m_{-1}}} \tag{2.51}$$

Using the derived expressions form_{-1} and m_1 we get

$$E_{GDR}^2 = \frac{3 b_{sym}}{M \langle r^2 \rangle} \tag{2.52}$$

Amazingly this simple model leads to a predicted energy $E_{GDR} \approx 93$ MeV $A^{-1/3}$ which is very close from the actual experimental value.

2.1.2.9 GDR in deformed nuclei

Up to now we have always consider spherical nuclei. If we now study deformed nuclei it is easy to realize that the collective mass (or the TRK sum rule) is independent of the deformation but not the restoring force (or the polarizability sum rule). Indeed, for a deformed system one cannot replace $\langle z^2 \rangle$ by $\langle r^2 \rangle /3$. If we introduce a quadrupole deformation ϵ (this deformation can also be noticed Q_2).

$$\begin{aligned} x &\rightarrow x(1-\epsilon) \\ y &\rightarrow y(1-\epsilon) \\ z &\rightarrow z(1+2\epsilon) \end{aligned} \tag{2.53}$$

we can see that the dipole vibration in the z direction scales like $1/z$

$$E_{GDR_z} = E_{GDR}(1+2\epsilon) \tag{2.54}$$

The two other orthogonal modes have the frequency

$$E_{GDR_x} = E_{GDR_y} = E_{GDR}(1-\epsilon) \tag{2.55}$$

These expressions are rather intuitive since the frequency of the oscillation is slower in the elongated direction. Therefore in prolate nuclei, ϵ is positive therefore the GDR strength presents two components one at a lower energy with half the strength of the other at higher energy which contain the two contributions coming from vibration perpendicular to the symmetry axis.

2.1.3 Microscopic approaches

Microscopically, giant resonances are described as a coherent superposition of 1 particle - 1 hole (1p - 1h) excitations. In a schematic model, the residual particle-hole interaction gives rise to the formation of one strongly collective state which is a coherent superposition of all possible 1p - 1h transitions. Since the residual interaction is attractive for isoscalar and repulsive for isovector states, the corresponding collective states will be shifted up and down with respect to their unperturbed energy which is a multiple of the energy difference between two major shell, $\hbar\omega \approx 41A^{-1/3}$ MeV. One obtain immediately the correct A dependence of the centroid energy. For example, the energy of the GDR which is built with $1\hbar\omega$ particle-hole transition, is shifted up to its observed value of $\sim 2\hbar\omega$ in intermediate and heavy nuclei ($E_{GDR} \approx 80A^{-1/3}$ MeV). This is illustrated in figure 8

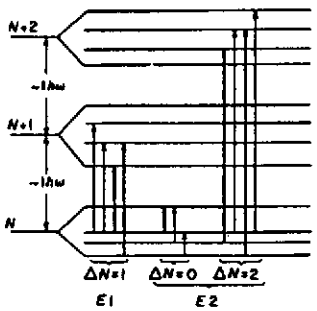

Figure 8 Schematic representation of E1 and E2 transitions between nuclear shell model states.

2.2 Other resonances

Within the same phenomenological liquid drop models with four different fluids protons/neutrons spin-up/spin-down, it is already clear that various other resonances should exist[Ra1877, Bo37, Me39, Bo39, St50, Bo75, Ch76, Ri81, Sp91]. In particular, the surface of the liquid drop can be deformed following different multipolarities giving rise to the so-called surface oscillations. Moreover, the isospin character of a transition with a given multipolarity L is shown to be isovector $\Delta T = 1$ or isoscalar $\Delta T = 0$. Isoscalar transitions correspond to collective nuclear vibrations in which protons and neutrons vibrate in phase and isovector transitions correspond to their vibrations out of phase. In a similar way when all spin components move in phase the vibration is called electric while when spin-up and spin-down are oscillating with opposite phases the mode is called magnetic. With the multipolarity and the spin and isospin character of each mode, this generalization of the Goldhaber-Teller model [Go48] provides a straightforward classification of all collective resonances of different multipolarities

Let us give some specific examples. The electric monopole vibration is for instance interpreted as a compression of the whole nucleus. in the previous sections we have seen that the electric giant dipole is seen as a vibration of the proton fluid against the neutrons (see Fig. 9). An other example of such a surface vibration is given by the giant quadrupole resonance, which corresponds to quadrupole deformation of the nucleus shape (see Fig. 9).

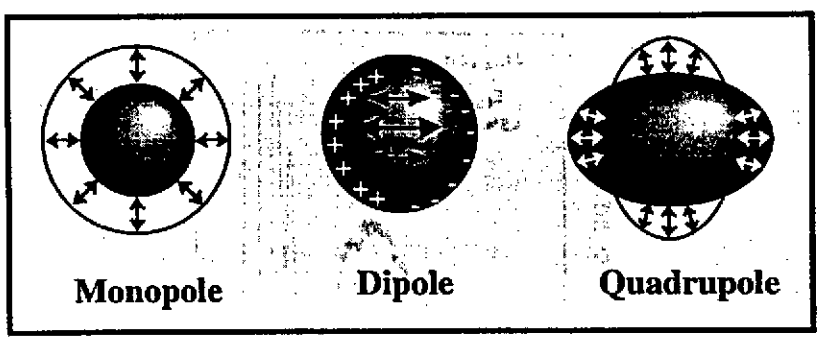

Figure 9 Schematic Representation of Various Giant Resonances : Few giant resonances are illustrated within the liquid drop model: left, the breathing mode, i.e. the isoscalar giant monopole resonance, the oscillation of protons against neutrons; middle, the isovector giant dipole resonance; right, a surface vibration, the isoscalar giant quadrupole resonance.

Microscopically, with the GDR we have seen that giant resonances are described as a coherent superposition of 1 particle - 1 hole (1p - 1h) excitations. Because of the odd-even spin alternation in the shell structure natural parity

(electric) transitions are odd or even multiple of the energy difference between two major shell, $\hbar\omega \approx 41A^{-1/3}$ MeV. Moreover, considering the fact that the in the harmonic oscillator limit an excitation operator with a radial dependence r^L can induce jumps between major shells distant of at maximum L $\hbar\omega$ we get immediately the rule that collective state of spin L and parity $(-1)^L$ should be located around energies $E_L = L\ \hbar\omega$, $(L-2)\ \hbar\omega$, ... Finally because of the opposite signs of the nuclear interaction in the isoscalar and isovector channels, the energy of isovector modes are expected to be higher than the simple rule expressed above while the energy of the isoscalar modes are lowered by the residual interaction. we already discussed the fact that the energy of the GDR which is built with $1\hbar\omega$ particle-hole transition, is shifted up to its observed value of $\sim 2\hbar\omega$ in intermediate and heavy nuclei ($E_{GDR} \approx 80A^{-1/3}$ MeV). We will see that the giant electric quadrupole resonance (GQR) consists of an isoscalar component with a resonance energy $E^{IS}_{GQR} \approx 65A^{-1/3}$MeV and an isovector one with an energy $E^{IV}_{GQR} \approx 130A^{-1/3}$ MeV.

In this section we will concentrate on the electric resonances which are already a very large subject of investigation.. More information and in particular information about the magnetic resonances can be found in review articles [Al96, Be81, Wo87, Sp91]

2.2.1 The giant quadrupole resonance

2.2.1.1 Observations

Only in 1972 was the isoscalar giant quadrupole resonance (GQR) observed for the first time. Today, the properties of the isoscalar GQR are well understood from a large number of different experiments using hadron and electron beams (see for example [Be76a, Wo87]). A schematic illustration of our understanding of this mode is presented in figure 10.

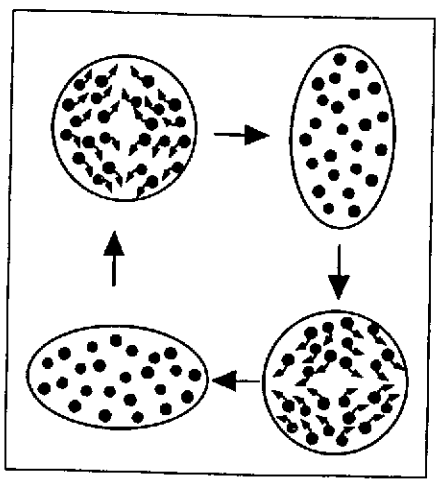

Figure 10 Shematic illustration of the quadrupole resonance in nuclei.

Two examples of experimental data presenting a GQR obtained either with electron scattering or with hadron interaction are shown on figure 11 and 12. In these data the various modes are identified using the fact that excitations of different multipolarities couple in different ways with the waves associated with the projectile. In quantum mechanics the perturbation of the incident projectile waves produces various diffraction patterns. Therefore, the angular distribution associated with excitations of modes of different multipolarities are different. Moreover, depending upon their properties, different modes can be excited with different interactions with different spacial properties. This is for example the case for the isovector electric modes (e.g. the GDR) which are excited by the long range Coulomb excitation while the isoscalar electric modes are also excited by the short range nuclear interaction. Then, the partial waves of the incident projectile participating in the excitation process are different leading to different diffraction pattern.. This is illustrated in figure 13 for an heavy ion reaction.

Figure 14 shows an example experimental results on giant resonances obtained using the heavy ion beams of the GANIL facility together with the high resolution magnetic spectrometer SPEG. The observed peak in the 10-15 MeV region is identified as the excitation of giant resonances in the target [Su89]. The angular distribution of the peak shows that it is composed of several multipolarities essentially L=1 et L=2 [Su89, Su90]. Conversely to the results shown in figure 12 the decomposition in different components was not performed assuming a particular shape for the resonance but by a direct fit of the various energy bin of the inelastic spectra. The extracted cross section for the coulomb excitation of giant dipole resonance (GDR) is in perfect agreement with the photoabsorption data. It should be noticed that because of the time dependence of the Coulomb field the Lorentzan shape should be weighted by a Fourier transform of the force acting on the nuclear dipole. Because of the finite interaction time this Fourier spectrum happen to be strongly decreasing with E. Therefore, in heavy ion reaction at low incident energy, the Lorentzian shape of the GDR appears to be strongly deformed as shown in figure 15 Moreover, the heavy ion reaction results are showing

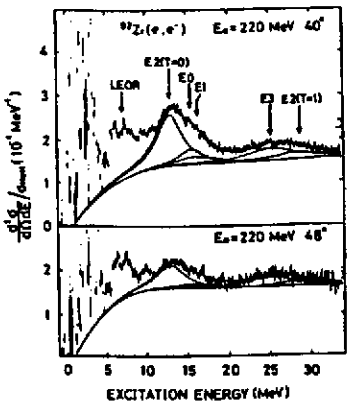

Figure 11 Spectra of inelastically scatered electrons on a Zr target. The lines show the various components of different multipolarities. It should be notice that the various components can be distinguished throught their angular distribution.

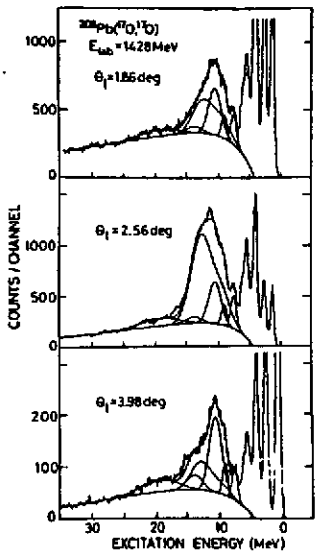

Figure 12 Inelastic spectra from the ^{17}O scattering on a Pb target : The lines coresponds to the various components identified in the analysis of the angular distributions. from ref. [Ba88c].

Another important feature of the heavy ion data is that they present a very strong nuclear excitation of the giant quadrupole resonance (GQR) with a very high peak to background ratio. This is an important characteristic as far as the feasibility of decay studies is concerned. The decay properties of the giant resonances studied using heavy ion probes present very small systematic error due to various contaminations.

The various data reported in Fig.16 coming from proton, α or electron inelastic scattering experiments show that the results obtained using different probes are in good agreement with each other.

For nuclei with A> 40 , 50-100% of the E_2 EWSR has been localized in a peak at about $65A^{-1/3}$MeV. Its width varies from 6 to 2.5 MeV for nuclei from Ca to Pb. For lighter nuclei, the isoscalar GQR is highly fragmented.

2.2.1.2 Microscopic description: a simple diabatic scaling model and its connection with the hydrodynamical picture.

To get a deeper insight into the structure of giant resonances and to be able to make predictions about their properties, one clearly needs a description of these collective states in terms of the underlying fermionic degrees of freedom. At the leading order the description of giant resonances is based on the mean-field approach which can be justify a good starting point because the frequency of the vibration is so high that the nucleons have no time to undergo a collision during one oscillation.

let us first present a simple example of the diabatic motion of a Fermi gas in a deformed container.

We will first recall the intimate connection between hydrodynamics and the Schrödinger equation, showing how the phase of the wave function can be interpreted as a velocity field and its module as a density. These concepts will be helpful to the understanding of approaches such as adiabatic time dependent Hartree-Fock approximation.

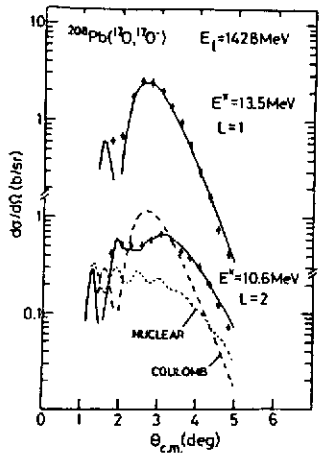

Figure 13 Inelastic angular distribution from the ^{17}O scattering on a Pb target. The dotes are the experimental data for the GDR and GQR. The the lines corespond to the theoretical angular distribution which are only due to the Coulonb interaction for the GDR. In the GQR case the Coulomb and the nuclear interaction can interfere. The observed differences between the expected angular distribution are used in ref. [Ba88c] to disentangle the various contributions associated with these two modes in the inelastic data.

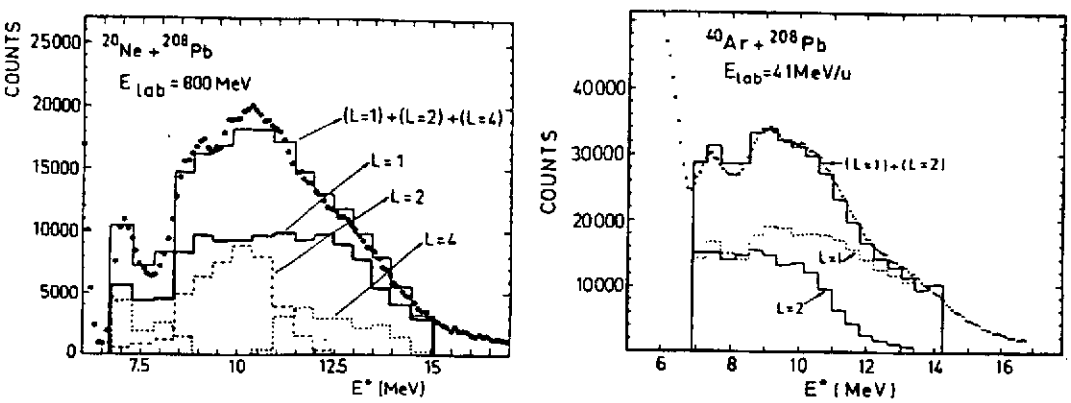

Figure 14 The inelastic Spectra measured for the reactions 20Ne + 208Pb and 40Ar + 208Pb at 40 MeV per nucleon can be decomposed in components of various multipolarities taking advantage of their different multipolarities.

Introducing the motion of collective variables through a simple scaling of the nuclear shape, we will show how the variational formulation of quantum mechanics reduces to the classical action of an oscillator. This simple model illustrates how a quantum many-body system can exhibit collective vibrations.

2.2.1.2.1 Equivalence between Quantum Evolution and Hydrodynamics First, let us make clear the connection between the independent particle picture and the liquid drop model. The Schrödinger equation for a single particle

$$i\frac{\partial\varphi(\mathbf{r},t)}{\partial t} = W\varphi(\mathbf{r},t) = \left(\frac{p^2}{2m} + U(\mathbf{r},t)\right)\varphi(\mathbf{r},t) \tag{2.56}$$

can be viewed as equivalent to the Euler equation for irrotational fluids. Indeed, if we separate the wave function into a modulus and a phase:

$$\varphi(\mathbf{r},t) \equiv \sqrt{\rho(\mathbf{r},t)}e^{-i\chi(\mathbf{r},t)} \quad , \tag{2.57}$$

it is easy to verify that the quantum current $\mathbf{j} \equiv \Im m\ (\varphi^*\nabla\varphi)$ satisfies the relation:

$$\mathbf{j} = \rho\nabla\chi \quad . \tag{2.58}$$

This relation allows to define an irrotational flow $\mathbf{v} \equiv \nabla\chi$.

The equivalence between quantum evolution and hydrodynamics can be easily demonstrated directly from the variational formulation of quantum mechanics. Indeed the wave function $|\varphi(t)>$ solution of the Schrödinger equation (2.56) can be seen as a stationary solution of the action (see appendix A)

$$I[\phi,\phi^*] = \int_{t_0}^{t_1} L(\phi(t),\phi^*(t))dt \quad , \tag{2.59}$$

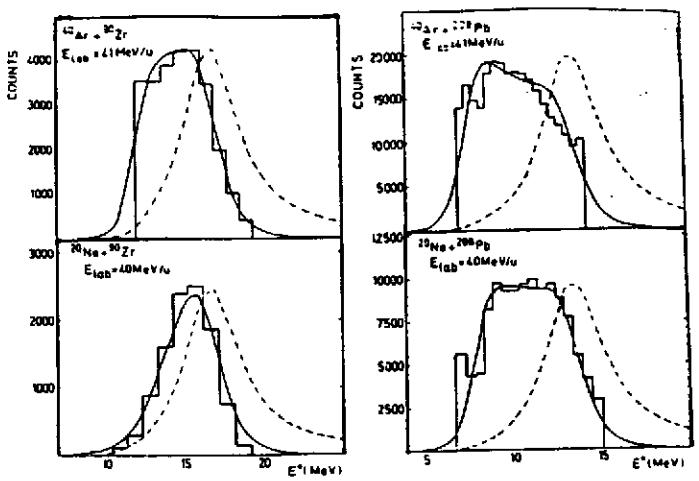

Figure 15 The GDR cross section in various heavy ion reactions (histogram). The dashed lines correspond to the expected photoabsorption spectra while the solid lines corresponds to the Coulomb excitation probability taking into account the energy dependence of the Coulomb field.

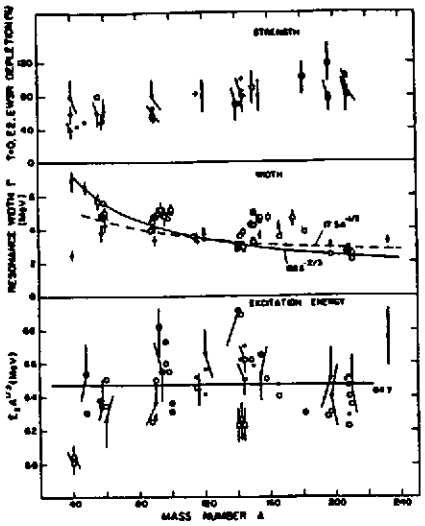

Figure 16 Properties of the GQR : Systematics for the excitation energy E_x, width Γ and fraction of the E_2 energy weighted sum rule strength of the isoscalar giant quadrupole resonance presented as a function of the nucleus mass (see ref. [Be80]).

where the Lagrangian functional is defined as

$$L(\phi(t),\phi^*(t)) =< \phi(t)|i\frac{\partial}{\partial t} - W|\dot{\phi}(t) > \tag{2.60}$$

and where W is nothing but the one-body Hamiltonian: $W = p^2/2m + U$. If we use ρ and χ as variational quantities we get:

$$I[\rho,\chi] = \int dtdr \left(\rho\dot{\chi} - \frac{1}{2m}\left(\rho|\nabla\chi|^2 - \frac{|\nabla\rho|^2}{4\rho}\right) + \rho U\right) \quad . \tag{2.61}$$

The condition of a stationary action in the χ direction leads to the dynamical equations for ρ which are identical to the continuity equation

$$\dot{\rho} + \frac{1}{m}\nabla.\mathbf{j} = 0 \quad , \tag{2.62}$$

where $\mathbf{j}$ is the quantum current $\mathbf{j} = \rho\nabla\chi$. This relation suggests that $\mathbf{v} \equiv \nabla\chi$ can be interpreted as an irrotational flow and indeed the stationarity condition for variations of ρ implies that the velocity field χ evolves according to an Euler-like equation:

$$\dot{\chi} - \frac{1}{2m}\left(|\nabla\chi|^2 - \frac{\Delta\sqrt{\rho}}{\sqrt{\rho}}\right) + U = 0 \quad . \tag{2.63}$$

In conclusion the quantum evolution of a single particle can be equivalent to an irrotational motion in a potential field containing quantum corrections associated with the spacial variation of ρ : $U' = U + \frac{1}{2m}\frac{\Delta\sqrt{\rho}}{\sqrt{\rho}}$.

2.2.1.2.2 A Simple Model: the Diabatic Mean-Field approximation It is interesting to apply and illustrate the previous concept using a simple quadrupole scaling of the whole density assuming the time dependent transformation of the coordinates

$$\begin{aligned} x &\rightarrow x(1+Q) \\ y &\rightarrow y(1+Q) \\ z &\rightarrow z(1-2Q) \end{aligned} \tag{2.64}$$

When Q is time dependent this implies that in each point the matter moves with the velocity

$$\mathbf{v}(x,y,z) = \dot{Q} \begin{pmatrix} x \\ y \\ -2z \end{pmatrix} \tag{2.65}$$

which simply derived from the velocity field

$$\chi = \dot{Q}\left(x^2 + y^2 - 2z^2\right)/2 \tag{2.66}$$

To implement this scheme in quantum mechanics, we can introduce the deformed (but static) single-particle wave functions $\varphi^{(0)}(n,Q,\mathbf{r})$ associated with different quantum numbers (n) through the relation

$$\varphi^{(0)}(n,Q,x,y,z) = \varphi^{(0)}(n,0,x(1-Q),y(1-Q),(1+2Q)z) \tag{2.67}$$

where we have assumed that Q is small. We will create a collective motion by multiplying all the wave functions by an overall phase representing a collective velocity field $\chi(t)$ so that the time dependent single particle wave function reads

$$\varphi(\mathbf{r},t) = e^{i\chi(\mathbf{r},t)}\varphi^{(0)}(n,Q,\mathbf{r}) \ . \tag{2.68}$$

Then we can introduce the one-body density associated with the Slater determinant of A nucleons: $\rho(\mathbf{r}) = \sum_{n\ occ} |\varphi(n,\mathbf{r})|^2$. The occupation numbers are supposed to be "frozen"during the motion, i.e. kept fixed at the ground state, $Q = 0$ (diabatic approximation). With the definition of the scaling of the box size we get a static one body density (for small Q)

$$\rho^{(0)}(Q,\mathbf{r}) = \rho^{(0)}(0,x(1-Q),y(1-Q),(1+2Q)z) \tag{2.69}$$

$$\rho^{(0)}(Q,\mathbf{r}) = \rho^{(0)}(0,\mathbf{r}) - Q\left(x\frac{\partial\rho^{(0)}}{\partial x} + y\frac{\partial\rho^{(0)}}{\partial y} - 2z\frac{\partial\rho^{(0)}}{\partial z}\right) \tag{2.70}$$

while the time dependent one-body density reads

$$\rho(\mathbf{r},t) = e^{i\chi(\mathbf{r},t)}\rho^{(0)}(Q(t),\mathbf{r})e^{-i\chi(\mathbf{r},t)} \ . \tag{2.71}$$

It is easy to see that indeed the potential χ defined in (2.66) corresponds to the minimization of the action (2.59) or (2.61)

$$I = \int_{t_1}^{t_2} \sum_{\mathbf{n}\ occ} L_{\mathbf{n}}(\varphi_{\mathbf{n}},\varphi_{\mathbf{n}}^*)dt \ . \tag{2.72}$$

which in the studied case reads[3]

$$I = \int_{t_1}^{t_2} dt \left(\int d\mathbf{r} \left(\rho\dot{\chi} - \frac{1}{2m}\rho|\nabla\chi|^2 \right) - \sum_{\mathbf{n}\ occ} < \phi_n^{(0)}(Q)\,|W|\phi_n^{(0)}(Q) > \right) \tag{2.73}$$

Indeed, the induced current verify the continuity relation $\dot{\rho} + \frac{1}{m}\nabla.\mathbf{j} = 0$ (2.62).

Then the quantum action,2.73, can be simply expressed as a functional of Q:

$$I = \int_{t_1}^{t_2} dt(-V(Q) + \frac{1}{2}M\dot{Q}^2) \ , \tag{2.74}$$

where

$$M = 2mA < r^2 > \tag{2.75}$$

is the irrotational mass equivalent to that found in the liquid drop model (3.6) and where $V(Q)$ is the diabatic potential:

$$V(Q) = \sum_{\mathbf{n}\ occ} < \phi_n^{(0)}(Q)\,|W|\phi_n^{(0)}(Q) > \ . \tag{2.76}$$

Therefore, one can define a classical Lagrangian, $L(Q,\dot{Q}) = M\dot{Q}^2/2 - V(Q)$, and a classical Hamiltonian:

$$H(Q,P) = P^2/2M + V(Q) \ , \tag{2.77}$$

[3]The diference with the previous case is that the phase $e^{i\chi(\mathbf{r},t)}$ represents only the phase variation and not the total phase.

where the conjugate momentum $P \equiv \partial L/\partial \dot{Q} = M\dot{Q}$. These two terms have a simple interpretation; the first one is the additional kinetic energy due to the collective motion which can be simply obtained by integrating the local kinetic energy $1/2m\rho^{(0)}v^2$ over the space

$$T = \frac{1}{2}M\,\dot{Q}^2 = \frac{1}{2}\int dr m\rho^{(0)}v^2 = \frac{1}{2}\dot{Q}^2\int dr 2m\rho^{(0)}r^2 = \frac{1}{2}\dot{Q}^2 2mA < r^2 > \tag{2.78}$$

while the second one is noting but the total energy associated with the static but deformed Slater state $\Psi(Q)$ built from the $\phi_n^{(0)}(Q)$

$$V(Q) = \quad < \Psi(Q)\,|W|\Psi(Q) > \quad . \tag{2.79}$$

It is important to notice that this energy contain both potential and kinetic terms. This kinetic contribution to $V(Q)$ would not be present in a hydrodynamics approach (since in such a case the matter is supposed to be at the local equilibrium). We will illustrate this point by computing the variation of kinetic energy of a Fermi gas in a deformed box in the next section..

It is easy to demonstrate that the reduction of quantum mechanics to a classical picture is related to the fact that we are studying the time evolution of wave packet. Indeed, the evolution of the parameters of the wave packet is equivalent to the evolution of the mean-value of some observable $< A >$ which is governed by the classical equation $id < A >/dt =< [A, W] >$. Therefore, to obtain the excitation spectrum of the system the classical Hamiltonian (2.77) needs to be requantified.

2.2.1.2.3 Scaling of a Fermi gas in a cubic box Let us consider a Fermi gas in a deformed cubic box of size,

$$L_x = L_y = (1+Q)L^{(0)} \tag{2.80}$$

$$L_z = L^{(0)}/(1+Q)^2 \quad , \tag{2.81}$$

which correspond to the scaling 2.64. In the Fermi gas approximation $V(Q)$ is due only to the deformation of the Fermi sphere (see Fig. 17), and can be expanded as

$$V(Q) = E_F A\frac{3}{5}(1 + 4(Q^2 - \frac{Q^3}{3} + \frac{11}{12}Q^4 + \ldots)) \quad , \tag{2.82}$$

where E_F is the Fermi energy.

At the lowest order in Q the potential (2.82) is equivalent to a harmonic oscillator potential:

$$V(Q) = V^{(0)} + \frac{1}{2}KQ^2 \quad , \tag{2.83}$$

where the restoring parameter K is defined as

$$K = \frac{24}{5}E_F A \quad . \tag{2.84}$$

One recognizes in the expression of the action I (2.74), the classical action of a vibrator. Conserving only the leading term in Q we get a harmonic vibrational spectrum of frequency

$$\omega \equiv \sqrt{\frac{K}{M}} \approx 65A^{-1/3}MeV \quad , \tag{2.85}$$

where we have used the mean square radius of a uniform sphere: $< r^2 >= \frac{3}{5}r_0^2A^{2/3}$.

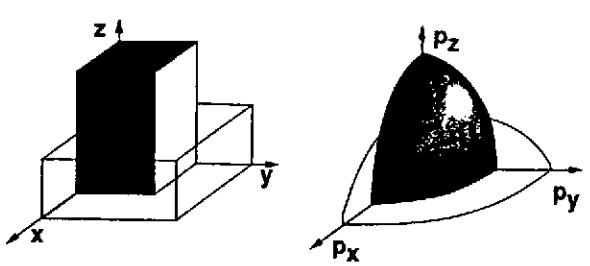

Figure 17 Schematic representation of the quadrupole dformation of a Fermi gas both in r and p -space.

The presented derivation may also yield an estimate of the anharmonicities as can be seen from expression (2.82). In this case, anharmonicities are limited due to the small zero point motion:

$$Q_0 \equiv \sqrt{\frac{1}{M\omega}} \approx 0.36A^{-2/3} \quad , \tag{2.86}$$

so that the potential

$$V(Q) = \frac{\omega}{2}\frac{Q^2}{Q_0^2}\left(1 - \frac{Q_0}{3}\frac{Q}{Q_0} + \frac{11Q_0}{12}\frac{Q^2}{Q_0^2} + \ldots\right) \tag{2.87}$$

$$V(Q) \approx \frac{\omega}{2}\frac{Q^2}{Q_0^2}\left(1 - 0.12A^{-2/3}\frac{Q}{Q_0} + 0.33A^{-4/3}\frac{Q^2}{Q_0^2} + \ldots\right) \tag{2.88}$$

contains only small anharmonic corrections if one considers a large number of nucleons.

In summary, we have shown how a collective deformation of the nucleus follows the equation of motion of a classical oscillator. The above derivation illustrates the extreme importance of the deformation in phase space (diabatic motion) and the fact that a giant vibration cannot be described by an equilibrated evolution as in the hydrodynamical picture. Finally, it may give some hint about the importance of the anharmonicities which appears to be small.

2.2.2 The giant monopole resonance

2.2.2.1 Systematic study

The existence of the electric isoscalar giant monopole resonance (GMR) in medium and heavy nuclei was first established in 1977[Ma76, Ha77, Yo77]. The giant monopole resonance GMR is the L=0 mode and is the only volume oscillation (see fig 18) which has been isolated.

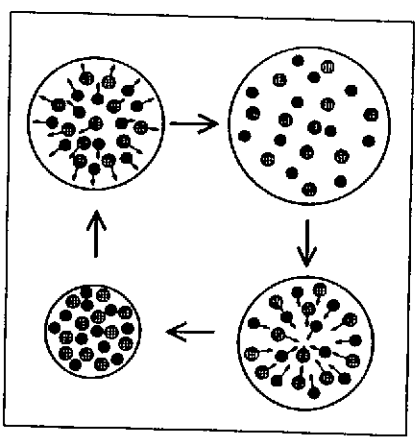

Figure 18 Shematic illustration of the monopole resonance in nuclei.

The frequency of this breathing mode is directly related to the compressibility of the nucleus and the determination of its energy is the most direct way to access to the compressibility modulus of nuclear matter. Indeed, this modulus is simply proportional to the variation of energy density $\varepsilon = E/A$ when the bulk of the nuclear matter is compressed

$$K = 9\rho_0 \frac{d^2\varepsilon}{d\rho_0^2} \tag{2.89}$$

which as the dimension of an energy therefore when a nucleus is compressed the variation of potential energy is directly related to the compressibility modulus. However, nuclei do not resemble to symmetric nuclear matter because of their important surface, of their charge and of the possible neutron-proton asymmetry. This point will be discussed latter on when we will have different models at our disposal.

A large amount of data has been obtained from (α, α') and $(^3He, ^3He')$ reactions[Wo87, Bu84]. The study of the GMR located at nearly $80A^{-1/3}$ MeV which is mixed with other resonances such as the GDR and the ISGQR, required particularly selective measurements. In particular, the contribution of the GDR is strongly inhibited in inelastic scattering of weakly-charged isoscalar projectiles such as α particles. Furthermore, as the GMR is strongly excited in forward angle scattering, 0^0 measurements allow to disentangle the GMR from the other contributions (see Fig.19). Coincidence experiments have complemented successfully our knowledge of this resonance[Br83, Wo87]

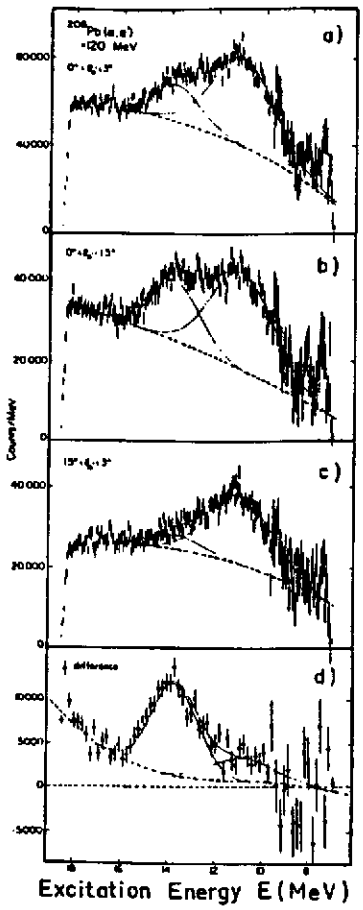

Figure 19 Excitation of the GMR and GQR : Inclusive α spectra for ^{208}Pb at $E_\alpha = 120$ MeV for three different angular range (a,b,c), d) Difference between b and c (for more details see refs. [Br83,Wo87]). Since the GMR cross-section is peaked at 0° while the GQR has a rather flat angular distribution, the difference spectrum d) contains mainly the GMR excitations whereas the large angle spectrum c is dominated by the GQR.

2.2.2.2 A simple scaling model of the GMR

Let us assume that the collective motion corresponds to a global self-similar motion of the nucleus associated with the scaling of the radii:

$$r \rightarrow (1 + Q_0)\, r \tag{2.90}$$

then the associated local velocity is noting but a radial flow:

$$\mathbf{v}\,(\mathbf{r}) = \mathbf{r}\dot{Q}_0 \tag{2.91}$$

With the definition of the scaling (2.90) the static density reads

$$\rho^{(0)}\,(Q_0, r) = \frac{1}{(1+Q_0)^3}\rho^{(0)}\left(0, \frac{r}{(1+Q_0)}\right) = \rho^{(0)}\,(0, r) - Q_0\left(r\frac{\partial\rho^{(0)}}{\partial r} + 3\rho^{(0)}\right) \tag{2.92}$$

where the last equation is obtained retaining only the lowest order in Q_0. Therefore, the density variation takes the form

$$\delta\rho^{(0)} = -Q_0\left(r\frac{\partial\rho^{(0)}}{\partial r} + 3\rho^{(0)}\right) \tag{2.93}$$

which corresponds to the famous Tassie transition density. Using the velocity field (2.91), it is easy to get the kinetic energy variation

$$T = \frac{1}{2}\int d^3r\; m\rho^{(0)}v^2 = \frac{1}{2}\dot{Q}_0^2\int d^3r\; m\rho^{(0)}r^2 = \frac{1}{2}\dot{Q}_0^2 mA < r^2 >= \frac{1}{2}M\,\dot{Q}_0^2 \tag{2.94}$$

defining the mass parameter associated with the monopole vibration

$$M = mA < r^2 > \tag{2.95}$$

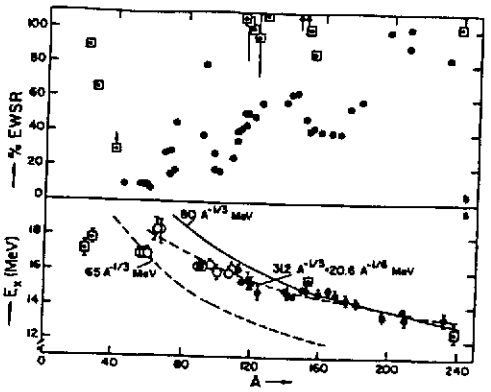

Figure 20 Properties of the GMR : a) the centroid energy as a function of the mass A and b) the fraction of the observed monopolar sum rule. The dashed curve indicated by $\left(31.2A^{-1/3}+20.6A^{-1/6}\right)$ in a) is the GDR energy in order to show that the GDR and the GMR are almost always degenerated. The second dashed line corespond to the GQR energy.

The potential energy can be obtained from the density variation (2.93) as soon as we know the potential energy as a function of the density. If we consider only the volume part of the nucleus, we can use an expansion of the energy around the saturation density

$$\varepsilon\left(\rho^{(0)}\left(Q_0\right)\right)=\varepsilon\left(\rho^{(0)}\left(0\right)\right)+\frac{1}{2}\frac{d^2\varepsilon}{d\rho_0^2}\left(\delta\rho^{(0)}\left(Q_0\right)\right)^2 \tag{2.96}$$

Integrated over the nucleus the energy variation reads leads to the collective potential energy

$$V\left(Q_0\right)=\int d\mathbf{r}\frac{1}{2}\frac{d^2\varepsilon}{d\rho_0^2}\left(\delta\rho^{(0)}\left(Q_0\right)\right)^2=\frac{1}{2}Q_0^2\int d\mathbf{r}K\rho^{(0)}=\frac{1}{2}Q_0^2AK \tag{2.97}$$

Then the total energy variation

$$E=T+V=\frac{1}{2}\dot{Q}_0^2mA<r^2>+\frac{1}{2}Q_0^2AK \tag{2.98}$$

look like an harmonic oscillator Hamiltonian associated with the frequency

$$\omega=\sqrt{\frac{K}{m<r^2>}} \tag{2.99}$$

This frequency has a $A^{-1/3}$ dependence which is close to the experimental data. However, a direct application of this equation to the observed monopolar vibration in Pb would lead to an estimation of the compressibility around $K=140\ MeV$.

2.2.2.3 Discussion of the Link of the GMR frequency with the nuclear compressibility

From the above simple breathing mode model the link between the GMR frequency and the parameters of the nuclear Equation of States (EOS) is clear. However, as we will see in the chapter devoted to results from microscopic calculations this model is by far too simple and neglect many physical effects such as the surface, coulomb potential, nuclear asymmetry effects, ... Therefore the first idea is to replace in the relation (2.99) the infinite nuclear matter compressibility by a compressibility of a finite nucleus, K_A. Then one may think to mimic the liquid drop expansion of the binding energy by introducing volume (K_{Vol}), surface (K_{Surf}), symmetry (K_{Sym}) and Coulomb (K_{Coul}) contributions to this finite system compressibility (K_A)

$$K_A=K_{Vol}+K_{Surf}A^{-1/3}+K_{Sym}\left(\frac{N-Z}{A}\right)^2+K_{Coul}\frac{Z^2}{A^{4/3}}+... \tag{2.100}$$

In the scaling model of a finite nucleus the volume term, K_{Vol} , would simply be identified with the infinite medium compressibility K [Bl80, Bl95]. Then K_A should be extracted from a fit of the available data about the GMR.

Here, we touch the second problem because the simple models are predicting a single resonance frequency while a whole distribution is experimentally observed. Therefore, the single GMR energy which should enter in the fit of the various K should be understood as a well defined average. It can be shown that the mean energy $\sqrt{m_3/m_1}$ where m_n are the n moment of the observed distribution, must be used in order to be able to extrapolate from the compressibility

of the finite nuclei to the compressibility of the nuclear matter. One possibility widely used in the literature is to consider the position (E_0) and the width Γ of the GMR bump and to use the relation

$$\frac{K_A}{m < r^2 >} = E_0^2 + 3\left(\frac{\Gamma}{2.35}\right)^2 \tag{2.101}$$

or even more sophisticated expression [My95, Na95, Sh93].

The first problem of the above method is that the A dependence of K_A appears to be rather weak making difficult and ambiguous the fit procedure [Al96] and in fact rather good fits of the available data can be obtained with a K_{Vol} varying from 100 to 400 MeV. Moreover, the extraction of a single number K_A from the observed strength distribution can be ambiguous especially when only a part of the EWSR has been observed. finally it is discussed in ref. [Ch95a] that even the experimental procedure to extract the GMR strength assumes that the transition density has the Tassie form. Figure 21 present the RPA (solid line) and Tassie (dashed line) transition densities for two strongly excited states of the ^{60}Ni. The normalization factor of Tassie density has been adjusted to match the actual RPA response to the excitation operator r^2.One can notice that, whereas some states are perfectly described by the macroscopic picture other states cannot be reduced to the simple scaling approximation.

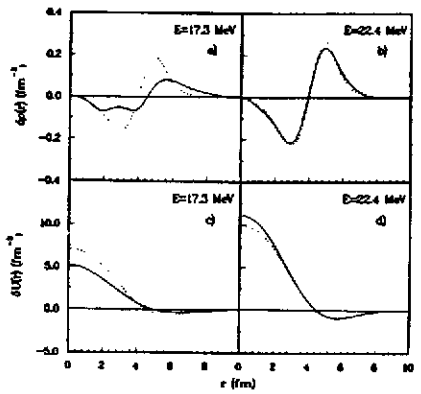

Figure 21 Transition densities (part a and b) and form factors (part c and d) for two monopole states in ^{60}Ni. The solid lines represent the Tassi parametrisation normalized to reproduce the rpa response whereas the dashed lines are obtained from the RPA wave functions.

The figure 22 presents a comparison of the RPA monopole strength functions (hashed histograms) :

$$S(E) = \sum_n \delta(E - \omega_n)| < 0|O|n > |^2 \ , \tag{2.102}$$

with the result of our pseudo-experiment (black histogram in the up-side-down position). The analysis was performed on four different set of pseudo data corresponding to the reactions: α (140 MeV) + ^{40}Ca, ^{60}Ni, ^{90}Zr and ^{208}Pb.

The shapes of these two strength distributions look quite similar especially for the lightest nuclei. However, the experimental analysis overestimates the total strength by some ten to thirty percents. This demonstrates that measuring 100% of a given sum rule do not insure that the whole strength distribution have been observed.

This error on the extracted sum rules can strongly affected the calculation of the compressibility of nuclear matter. It was concluded in ref. [Ch95a] that whereas for the light nuclei (Ca and Ni) the analysis does not induce any sizable bias for the heavy nuclei (Zr and Pb) the difference lies between 300 and 500 KeV making the compressibility smaller and therefore the equation of state softer. This may induce a systematic over estimation of K by at most 10%.

To overcome these difficulties one should directly compare the experimental inelastic spectra with predictions of for example a distorted wave Born approximation (DWBA) using the strength and the form factors coming from a microscopic description of the GMR (c.f.. the RPA) as discussed in ref.[Ch95a]. This analysis was only partially performed in ref. [Bl95]. Indeed, Blaizot et al. have used microscopic approaches to relate the nuclear compressibility of different effective forces to determine the position of GMR in various nuclei. Figure 23 shows their comparison of the experimental GMR position and of the predicted value (C.f. also [Al96] for a review of these points). Taking into account all the available results they get

$$207 < K < 225 \ MeV \tag{2.103}$$

However, this analysis does not take into account the points razed in ref. [Ch95a] concerning the possible systematic errors in the extraction of the monopole strength due to the use of the Tassie form factors in the experimental analysis.

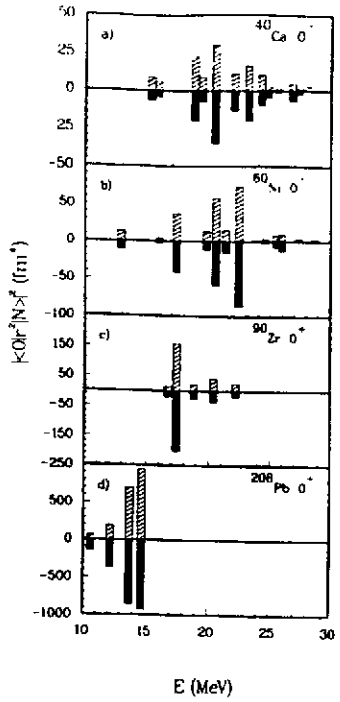

Figure 22 Monopole strength distributions in ^{40}Ca, ^{60}NI, ^{90}Zr and ^{208}Pb nuclei in the giant resonance region: the upper part of each figures is the RPA prediction while the lower (up-side-down) part is the strength as extracted from the pseudo-inelastic cross sections.

2.2.3 Other electric resonances

The isovector monopole resonance has been observed mainly via (π^-, π^0) reactions which are well-adapted to excite isovector giant resonances, but their identification in (π^+, π^0) reaction remains much more difficult. Data are available now on several nuclei[Ba83, Bo84](see Fig.24). Complementary studies are now in progress using heavy-ion charge exchange reactions. For the isovector giant quadrupole experimental evidence is still very scarce.

A reliable and systematic extraction of the characteristics of giant resonances of high multipolarity turns out to be difficult for many reasons. As these resonances are expected to be at higher excitation energy and with a large width which increases with excitation energy, their localization may become somewhat speculative. Furthermore, recent RPA calculations[Lh93] have shown that the strength of high multipolarity giant resonances is spread out and that the amount of collective strength clearly decreases for increasing multipolarities.

2.3 Physical interpretation of angular distribution: diffraction effects.

It is important to understand one of the basic tools to study giant resonances which is the angular distribution. Indeed, in nuclear physics because of the small dimensions of the considered systems the scattering processes have a strong quantal nature. In fact inelastic scatterings are dominated by the wave dynamics. Moreover, because of the short range of the nuclear interaction and because of it strength inelastic interaction are confined in a small region around the surface: Too far there is no interaction, too close the interactions are so violent that the inelastic precesses are destroyed. Therefore, the inelastic scattering look like a surface diffraction effect. Figure 25 shows how a incident wave interact with the motion of the induced vibration.

In fact depending upon the local collective motion the different wavelets associated with the incident projectile are phase shifted. Now depending upon the collective motion these phase shift will be different leading to different interference (diffraction) pattern.

The physics depicted above can be systematically computed using the DWBA and the optical potential concepts. The interested readers can find detailed discussion of this point in the review article [Al96].

2.4 Giant Resonances Built on Excited States

In 1955, D. Brink proposed, that giant resonances can be built on all nuclear states and that their properties should not depend strongly on the details of the considered nuclear state. These giant resonances will have the same characteristics as the giant resonance built on the ground state but their energy will be shifted according to the energy of the state on which they are built. This statement is known as the Brink-Axel hypothesis[Br62]. In this section we will briefly present the actual knowledge about this subject. Some of the presented points especially about hot resonances and

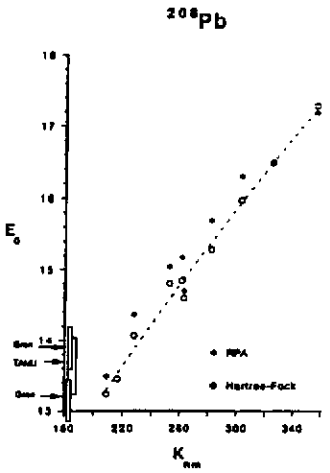

Figure 23 The breathing mode energy computed either using the constrained Hartree-Fock calculation or the RPA using various forces with different compressibility K. The data is shown on the coordinate axis.

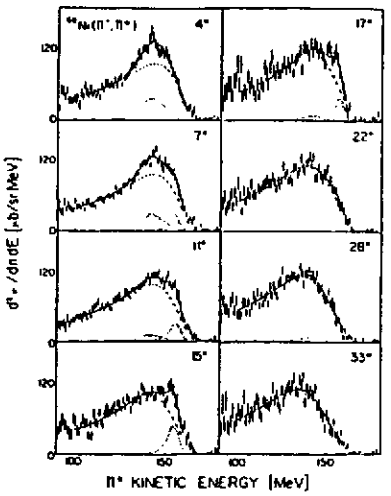

Figure 24 GDR and IVGMR in Charge Exchange Reactions: Doubly differential cross section for the $^{60}Ni(\pi^-,\pi^0)$ reaction at $E_\pi^- = 165$ MeV.(see ref. [Bo84]). The dashed line shows the continuum and the dotted lines the IVGMR (left peak) and the GDR (right peak).

multiphonons will be more developed in the next chapters. However, I believe that in this phenomenological chapter it is important to summarize the actual experimental knowledge about Giant resonances.

2.4.1 GDR built on low lying states

The first observation of a giant resonance built on excited states is reported in the proton capture (p,γ) experiment on ^{11}B performed in 1964 where the GDR built on the first 2^+ state was observed[Ko79].

Since this pioneering work, many experiments have shown that the GDR persists as a collective motion under extreme conditions of excitation energies and angular momentum. We refer the reader to very complete reviews on the subject (see for example [Sn86, Ga88, Ga92]). In the following, we will just mention the main features of these observations.

Since 1980, medium energy (20-80 MeV) (p,γ) experiments in light nuclei (12 <A< 40) have provided new information on the properties of the GDR built on a variety of different states within the same nucleus. These studies demonstrate the existence of γ-decays populating excited final states. The γ-strength function for each excited state can be determine by varying the proton energy giving access to the characteristics of the GDR built on specific states.

The proton capture reaction on ^{27}Al provides a good example of a reaction where the giant dipole resonance built on well separate excited states was observed[Do83]. Figure 28 shows a γ-ray spectrum from this reaction measured at 22 MeV. In the presented spectrum, superimposed on a large bump, one can see many peaks that correspond to known 1p-1h states. These final states are in close correspondence with the states excited in stripping reactions, such as $(^3He, d)$, and a simple proportionality of the strength of the observed resonances to the spectroscopic factors of the

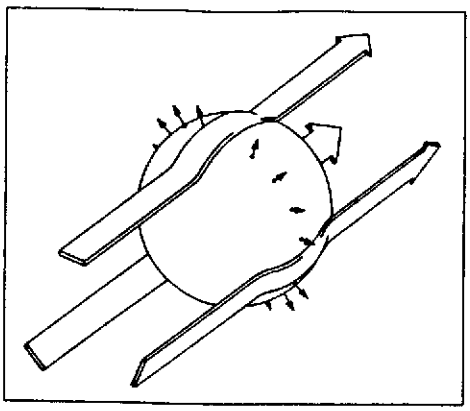

Figure 25 Shematic picture of a projectile as a incident wave, depicted with a broad arrows, envelopping a nucleus. The motion of the latter is represented by small arrows.

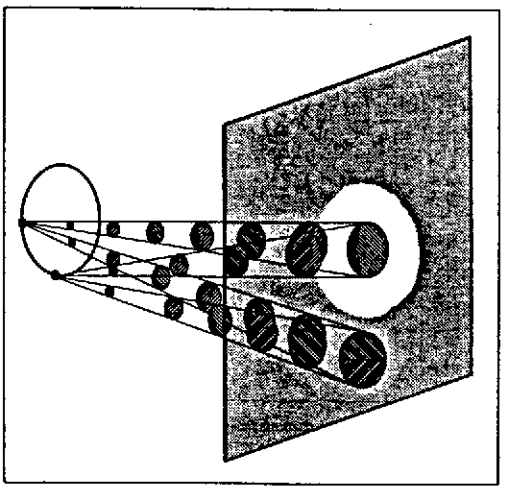

Figure 26 Shematic picture of the diffraction of different wavelets at the peripherie of a nucleus performing a monopole vibration. because of the sperical symmetry the differents wavelats receives the same phase shift and therefore they always interfere positively in the forward direction..

populated final states (see ref. [Do83]) is observed. Thus, the (p,γ) reactions appear to be a good tool for studying single proton strength in light nuclei.

A cross section for the excitation of every final state can be obtained from the line-shape decomposition of the γ-ray spectrum (see Fig. 28). Performing this analysis for different incident proton energies yield an excitation function for all the final states. The excitation function for various final states is displayed in Fig. 29 as a function of the emitted-γ energy, E_γ, i.e. the proton-capture excitation energy minus the excitation energy of the final state. In Fig. 29, resonances are observed all peaked at $E_\gamma \approx 20$ MeV which correspond to the energy of the GDR built on the ground state. These results clearly show that the observed resonances are due to giant dipole excitations built on various states as expected from the Brink-Axel hypothesis. However, the width of these resonances (see Fig. 29) strongly increases with the increasing excitation energy of the excited states.

2.4.2 GDR in hot nuclei

Studies at higher bombarding energies on the same nucleus have been performed and show that, when the incident energy is high enough, the spectrum of single particle strength in the final nucleus is washed out, leaving only an enhancement peaked at the γ energy expected for the GDR. This transition can be interpreted as the transition from the excitation of a giant resonance built on well defined single particle states toward the excitation of a giant resonance built on a compound nucleus. Indeed, at high excitation energy the single particle states form a dense continuum strongly coupled to more complex states. Therefore, they can be identified with compound nucleus states.

These collectives modes of a compound nucleus can also be studied by measuring the γ decay from a hot equilibrated system formed in heavy ion collisions. The presence of GDR excitations in the composite systems is now clearly demonstrated from a variety of recent experiments. The hot GDR was first observed in the γ-ray spectra from the statistical decay of compound nuclei formed in ^{40}Ar induced fusion reactions at 170 MeV[Ne83]. In Fig. 30, the

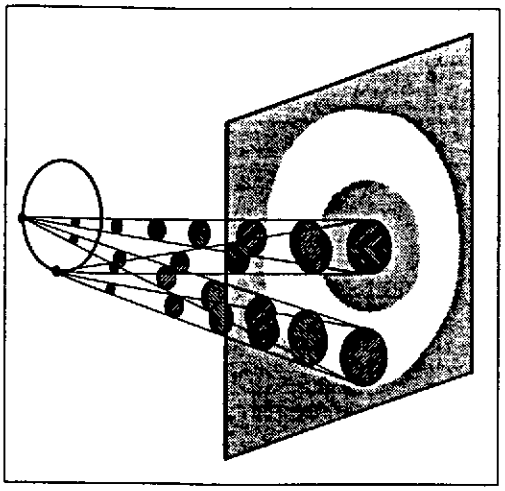

Figure 27 Shematic picture of the diffraction of different Wavelets at the peripherie of a nucleus performing a quadrupole vibration. depending about the phase of the local vibration of the surface the differents wavelets receive different phase shif. In particular, the wavelets at the maximum elongation and the others at the minimum elongation have oposite phases. Therefore they interfere negatively in the forward direction leading to a minimum in this direction. However, at an other angle they may interfere positively and so a maximum cross section can be expected at a finite angle.

γ-ray spectrum obtained in such reactions shows an enhancement for a value E_γ corresponding to the average energy of the GDR. Indeed, the fact that the GDR is observed in the decay of compound nuclei can be understood as the reverse process of the statistical decay of a GDR built on excited states. As a matter of fact, the existence of such a coupling between the resonance and the compound nucleus states allows to consider that the phonon gas is in thermal equilibrium with the nucleus and the observed photons are the signature of the presence of these phonon excitations.

The main features of the GDR decay which emerge from the available data can be summarized as follow [Sn86, Ga92].

At low temperature (T $\leq$ 2-3 MeV), the statistical description of the GDR decay gives a good account of the measured spectra. The GDR strength and mean energy of the resonance follow the ground state GDR systematics over a wide range of masses. The extracted E_1 strength is in general in good agreement with the energy weighted sum rule suggesting that the high collectivity of the vibration is not affected by the temperature. The width and shape of the GDR is sensitive to the shape deformation and fluctuation of the excited nucleus. This, in general, results in a broadening of the observed resonance. The coupling of the GDR to the quadrupole shape degrees of freedom is important and allows to study nuclear structure effects as a function of temperature. In particular, the importance of the nuclear shell structures appears to diminish strongly for temperature about 1.5 MeV as shown in studies of the nuclear shapes as a function of temperature and spin. At higher temperature (T $\geq$ 3 MeV), the position and the strength of the GDR remain constant at its ground state values but contradictory results on the width of the GDR have been published. However, some observations indicate that the width does not increase as fast as in the lower excitation energy domain because of the saturation of the spin transferred during the fusion process. At T > 5-6 MeV, experimental results are more fragmentary but have yielded indications for a saturation of the γ-multiplicity in the GDR region. The interesting new physics lies in the way in which the properties of the GDR are modified in highly excited nuclei. This study may provide new insight into the mechanisms of thermal equilibration and into the properties of hot nuclear matter.

In all the discussed experiments, because real photons are observed, E_1 transition dominates. Relatively little is known about giant resonances of other multipolarity built on excited states. In particular, it would be extremely interesting to investigate properties of the giant monopole resonance in a hot nucleus and to obtain informations about the compressibility of nuclear matter at high temperature. Indeed, the compressibility is a key ingredient of the equation of state of the nuclear matter. This equation governs the behavior of hot nuclear system and is of great interest for astrophysics as well as for nuclear physics. Recent experiments on the dilepton decay of the giant monopole resonance are in progress[Bu94] but no results are available today.

2.4.3 Giant resonances built on top of other giant resonances: The multiphonons

We have discussed in the previous chapters that the giant resonances were understood as a first quantum of vibration. However, until recently, the higher quanta were escaping from the experimental observation. This fact was a puzzle for our understanding of these collective modes. The observation of different multiphonon states in various types of reactions is a strong confirmation that these modes are the first states of vibrational band (for more details see ref. [Ch95a]).

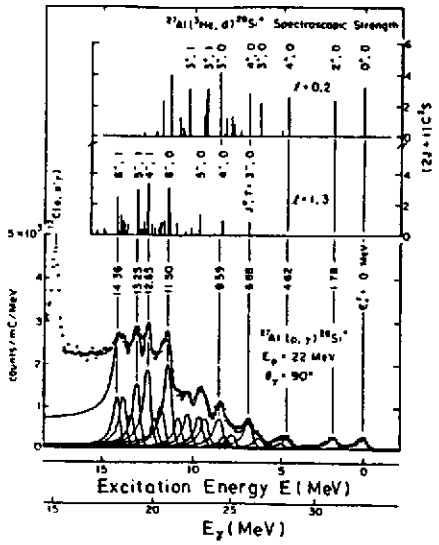

Figure 28 γ-ray spectrum from the proton capture reaction on ^{27}Al measured at 22 MeV showing the preferential population of particular final states (see ref. [Do83]).

2.4.3.1 Excitation of multiphonons in heavy ion reactions.

The first observations of structures in the inelastic spectra of heavy ion reactions that could be interpreted as multiphonon back traces back to 1977 [Fr77, Fr80]. In 1984, new data were showing high-energy structures that could be interpreted as multipole excitations of giant resonances [Ch84c, Ch84b, Ch84a, Ch84] (see figure 31). Since our theoretical predictions [Ch86b] were showing that the excitation of multiphonon states built with the giant quadrupole resonance is optimum around 50 MeV per nucleons, experiments have been performed at the GANIL [Fr87] (see figure 32).

However, the unambiguous signatures of the multiphonon nature of the observed resonances have been found only recently with the study of their decay modes in particle coincidence experiments.

The idea is simple, when the target nucleus is excited above its particle emission threshold it decays by emitting particles. The observation of these particles is therefore a signature of target excitations. This is exactly what is done in ref. [Sc91, Sc93]. Figure 303 shows the inelastic spectrum of the 40Ca + 40Ca reaction at 50 MeV per nucleon gated by the requirement that a proton is detected in the backward hemisphere. According to the previous discussion, this spectrum corresponds to target excitations. On this figure one can see the a structure at twice the giant quadrupole resonance in 40Ca that is interpreted as the excitation of two GQR phonons in the target nucleus.

However, this observation is not sufficient to sign unambiguously the excitation of a two- phonon state. To demonstrate that these states correspond to a two-phonon state, we will take advantage of the existence of a direct decay channel (the escape width) which can be used as a fingerprint of the excitation of a given mode. Indeed, in the case of the GQR in 40Ca, we have seen that it was decaying directly toward the ground state and the first hole state of 39K (as recall schematically on figure 34).

If we now look at the missing energy spectrum associated with the emission of one proton from the structure situated at twice the GQR energy, we can see sharp peaks on top of large background coming from the statistical decay of a compound nucleus. These peaks are the signature that the decay cascade went through well defined states. These peaks can be associated with the excitation of two GQR in the target which directly decay independently just as the GQR does, going to well-defined hole states. The simulation of this independent decay gives a good reproduction of the positions of the observed peaks as seen on figure 35 (see references [Sc93, Ch95a] for more details).

This demonstrates that the structures, observed around 34 MeV excitation energy, are indeed due to the excitation of two GQR Phonons. This state appears to correspond to a very harmonic vibration since the observed energy of the peak is very close to twice the GQR energy which centroid energy is around 17 MeV.

The observed width of the two-phonon state is very close to 1.5 the width of the GQR itself. This is also pleading in favor of an independent phonon picture. Indeed, the multiphonon theory predicts that the width of an N-phonon state should vary in [Ch84c, Ya85, Ch92, Ch95a]

Finally, the two-phonon state appears to decay directly as two non-interacting modes. All these properties show that giant resonances are behaving as weakly interacting excitations.

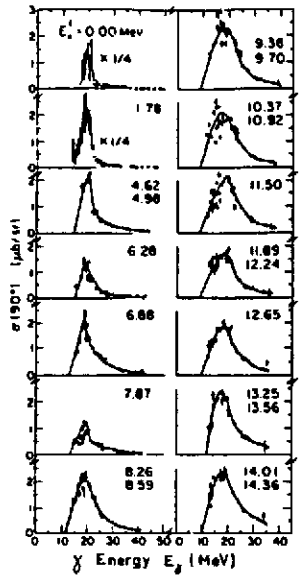

Figure 29 Excitation of the GDR on Top of Various States : Excitation function of the population of well defined final states in a (p,γ) reaction obtained by varying the incident proton energy. This cross section is plotted as a function of γ-energy, $E_\gamma = E_p^{cm} + Q - E_x$. (for more details see ref. [Do83]).

2.4.3.2 Observations of two-phonon states.

During the past 5 years the multiphonon studies have been widely extended using not only heavy ion beams from 10 to 14 000 MeV per nucleon [Ri93, La93, Au93] but also pion beams [Mo88, Mo91]. Figures 36 and 37 give two illustrations of these results while figure 38 summarized the essential properties observed experimentally (for a complete experimental and theoretical review see ref. [Ch95a]).

From these studies, it appears that the two-phonon states are very harmonic. Their energy is within 10deduced from the independent phonon picture. Only their cross-section seems always underestimated by the theoretical calculation based on a harmonic approximation. Let us now discuss all these properties.

2.4.3.3 Width.

In the previous sections we have shown that the giant resonances are good vibrators giving, some foundation to the widely-used picture of independent phonons. The anharmonicities are small: they induce a splitting of the strength smaller than 1 MeV, which will result in a small increase of the multiphonon width. Therefore the multiphonon width can be discussed within the independent phonon picture. Since this model predicts that the multiphonon response involves a folding of the one-phonon strength function (see eq. (3.60)) one may conclude that the widths are added quadratically as the variances of statistically independent processes [Ya85, Ch88]. However, as far as the interpretation of the width in terms of the inverse of a life-time is concerned, one would predict that the widths are simply additive.

This apparent contradiction is in fact solved in ref. [Ch92], using the relation between the life-time and the strength function. A phonon state at an energy ω which is decaying exponentially with a life-time $\tau = 1/\Gamma$, is associated by Fourier transform with a Lorentzian response :

$$S(E) = \frac{S_0}{(E-\omega)^2 + \Gamma^2/4} \quad , \tag{2.104}$$

where S_0 is a normalization. If the Lorentzian shape (2.104) is introduced in equation 3.60 to compute the two-phonon strength function one can show easily, using Fourier transform for example, that the line shape of the two-phonon state is again a Lorentzian with a width

$$\Gamma_2 = 2\Gamma \quad , \tag{2.105}$$

because the inverses of the life-times are additive. In this case the argument about the variances does not hold because the variances diverge.

However, as soon as the variance can be defined (for example when the strength function appears to be more like a normal distribution) the width appears to be quadratically additive

$$\Gamma_2 = \sqrt{2}\Gamma \quad , \tag{2.106}$$

because the variances are additive and proportional to the square of the widths [Ch84a].

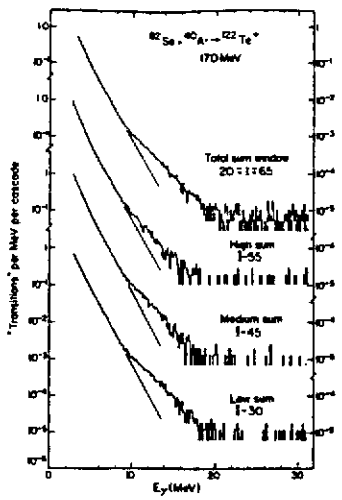

Figure 30 GDR Excitation in Hot Nuclei : γ-ray spectra from the decay of compound nuclei formed in fusion reactions using an ^{40}Ar beam at an energy of 170 MeV (see ref. [Ne83]). The observed shoulder can be associated with the statistical excitation of a GDR in the compound system.

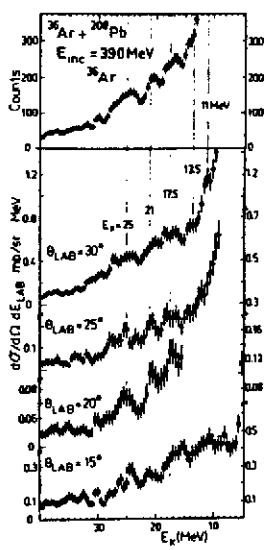

Figure 31 Inelastic spectrum showing high energy structures which are candidates for multiphonon excitations [Ch84, Ch84a, Ch84b, Ch84c].

This is not a violation of the Heisenberg relation $\Delta E\ \Delta t \geq 1$ because in the case of a distribution which is not of a Lorentzian type the width cannot be directly related to a life-time except through the inequality $\Gamma > 1/\tau$. For example we discussed in section 3.2.3 that the Landau spreading of the strength cannot be related to a life-time[Ya85, Ch87, Gi87, Ch88, La90] .

Both the Lorentzian and the Gaussian line shapes correspond to idealized pictures which are found neither in realistic models nor in nature. For instance, the resonance damping due to the coupling to more complicated states[Be83] leads to a Lorentzian shape only in an oversimplified model. In detailed calculations, strength distributions are predicted to be neither Lorentzian nor Gaussian[Co92]. The Landau broadening itself gives line shapes which can be somewhat complicated. The possibility to obtain normal distribution in the case of nearly chaotic spreading dynamics is discussed in ref. [Ze93]. Therefore, the concept of width is not well defined, either theoretically or experimentally. Moreover, concerning the folding procedure, one is always dealing with truncated strength distributions since there is no strength at negative energies whereas physical conservation laws impose an upper energy limit. All the moments of the strength are finite allowing us to use the variance as a measure of the width. So, as far as the independent excitation picture is valid, the multiple excitation spectrum is predicted to be the folding of the single excitation spectrum and the variance of the multiphonon spectrum is the sum of the variances associated with each individual phonon.

For instance, we have already discussed that the strength of the giant dipole resonance (GDR), which is one of the best examples of a Lorentzian, must be multiplied by a Gaussian cut-off in order to fit the data on the low energy

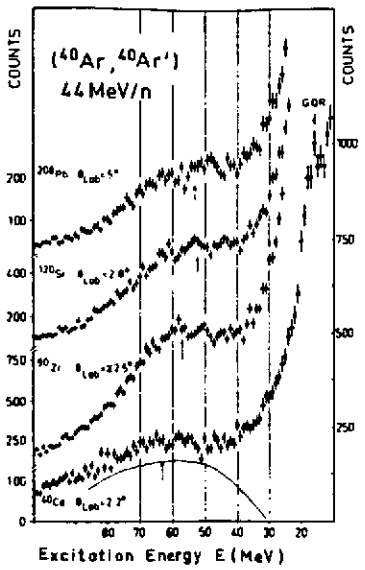

Figure 32 Inelastic spectra showing high energy structures excited in different target nuclei by a heavy ion projectile at about 50 MeV per nucleon.

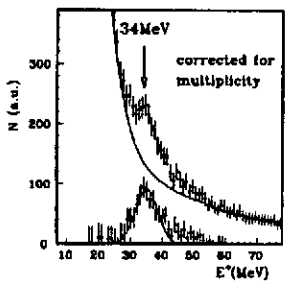

Figure 33 Inelastic spectrum measured in the 40Ca + 40Ca reaction at 50 MeV per nucleons in coincidence with backward emitted protons. This spectrum corresponds to target excitation. The structured observed at high excitation energy is interpreted as the excitation of two GQR phonons.

side and that in actual experiments; the GDR strength is weighted by the virtual photon spectrum which decreases exponentially up to a maximum energy given by energy- and momentum-conservation. Also in this case, the relation (2.106) is expected to hold. Another way to compute the anharmonicities is to consider that the first phonon is already damped when the second phonon is excited. Therefore, the second phonon is built on a hot system. Since the temperature effects on giant resonances are relatively small, one may conclude that the anharmonicities are very small [Sn86].

In conclusion, the life-time of a multiphonon state is inversely additive whereas the variance of a multiphonon cross-section is predicted to be always defined and additive. One generally expects relation (2.106) to hold in the limit of an independent-phonon picture. The introduction of anharmonicities induces a small increase of the two phonon width of about 1 MeV [Ca89, Be92] if the different components are not resolved. Consequently, one can estimate that the width of the two-phonon states will be $\sqrt{2}$ times that of the single phonon plus 0.5-1 MeV due to the anharmonicity. This simple law, originally predicted in reference [Ch84a] and later on rederived by many authors [Ba92, Ll92, Ze93], is in very good agreement with all the present multiphonon measurements [Ya85, Mo88a, Fr88, Mo90, Ku92, Em94] .

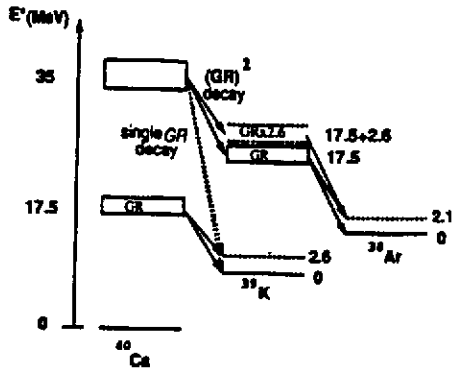

Figure 34 Schematic diagram of the direct decay of a giant resonance and of a two-phonon state

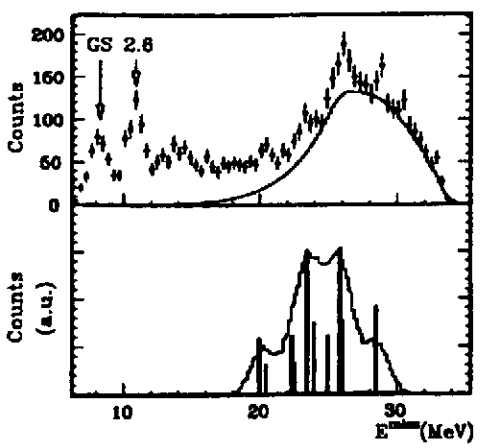

Figure 35 Missing energy spectra b) associated with the structure observed at twice the energy of the GQR. c) same spectrum simulated assuming an independent decay of two GQR as shown on previous figure.

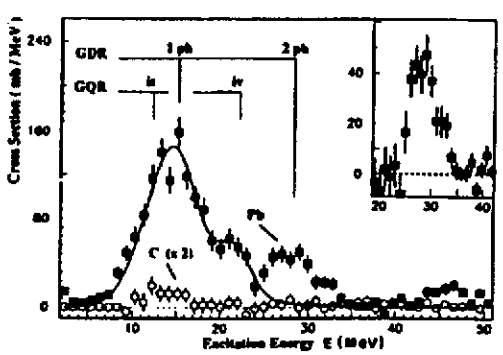

Figure 36 Spectrum of the Coulomb excitations of 136Xe arrizing from its collision with a Pb target at 700 MeV per nucleons. The first peak corresponds to the GDR while the second one is attributed to the two GDR phonon states (see ref. [La93])

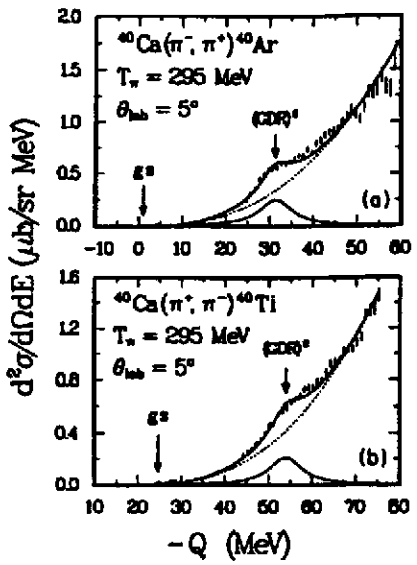

Figure 37 Double charge exchange spectrum measured on a 40Ca target with a pion beam. The shoulder indicated by (GDR)2 correspond to the isospin flip 2 member of the GDR multiplet (see ref. [Mo91]).

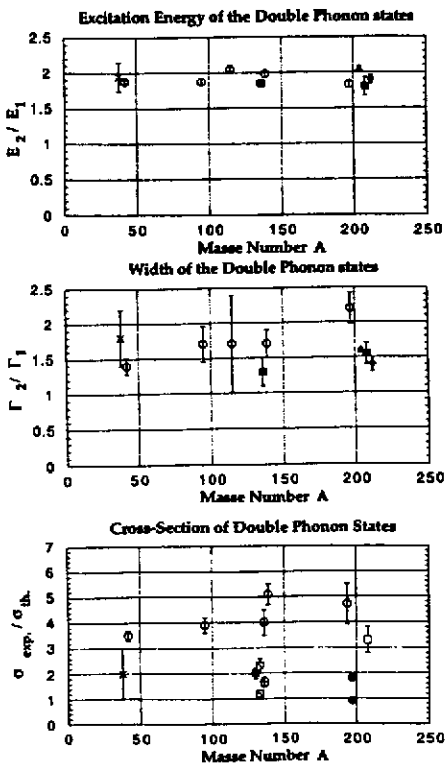

Figure 38 Synthetic presentation of the various experimental results concerning two phonon states (see ref. [Ch95a] for more details).

Chapter 3 Theoretical descriptions

In this chapter we present an overview of the different approaches which have been applied to the descrition of collective vibrations.

3.1 Macroscopic Models of Surface Vibrations

We will use the surface vibration model as an illustration of these macroscopic models based on the liquid drop approach[Bo75, Br81]. These surface modes are analogous to the ripples on the interface of two fluid as shown on figure 1. The inertia comes from the fluid motion while the restoring force is due to the surface tension..

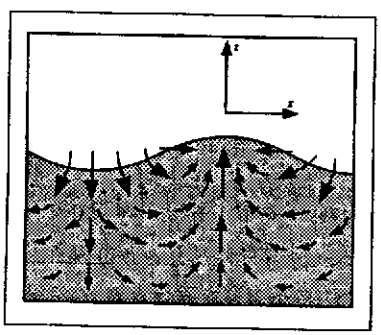

Figure 1 Shematic ilustration of the vibration of the surface of a fluid.

Let us consider a spherical incompressible liquid drop. The excitation of the shape can be described by expanding the surface coordinate on the spherical harmonic basis

$$R(\theta,\phi) = R_0\left(1+\sum_{\lambda\mu} Q_{\lambda\mu}Y^*_{\lambda\mu}(\theta,\phi)\right) \quad . \tag{3.1}$$

We will show in this section that the motion of the collective deformation parameters $Q_{\lambda\mu}$ can be associated with a harmonic oscillator Hamiltonian (3.7).[1] This fact justifies the introduction of the concept of vibrations and phonons. We will describe how the surface-vibration model can be used in a phenomenological manner (see section 3.1.4) and we will discuss how it is possible to go beyond the harmonic picture (see section 3.1.5). In particular, we will introduce the so-called nuclear field theory (see Fig. 2) which is a powerful tool to study phonon properties such as anharmonicities (see Fig. 2).

3.1.1 Potential Energy of a Deformed Liquid Drop

In the surface oscillation model, the restoring force arises from two opposite effects: the surface tension which favors the spherical configuration, and the Coulomb force which tends to deform the nucleus. The increase of surface energy is proportional to the increase of the surface $\Delta E_S = \sigma\Delta S$,where σ is the surface tension parameter. The increase of the surface due to the deformation Q can easily be obtained at the first order in Q [Bo75]:

$$\Delta E_S = \frac{\sigma}{2}\sum_{\lambda\mu}(\lambda-1)(\lambda+2)|Q_{\lambda\mu}|^2 \quad . \tag{3.2}$$

The Coulomb energy variations of a deformed uniformly-charged drop is given by (at the lowest order in Q):

$$\Delta E_{Coul} = -\frac{3}{4\pi}\frac{Z^2e^2}{R_0}\sum_{\lambda\mu}\frac{\lambda-1}{2\lambda+1}|Q_{\lambda\mu}|^2 \quad . \tag{3.3}$$

Therefore, the total energy variation can be approximated by a harmonic potential V:

$$V = \Delta E_S + \Delta E_{Coul} = \frac{1}{2}\sum_{\lambda\mu} K_\lambda |Q_{\lambda\mu}|^2 \quad . \tag{3.4}$$

[1] Except for Q_{00} which is constrained by the volume conservation and $Q_{1\mu}$ which corrects for the center of mass motion.

3.1.2 Kinetic Energy

In order to get a complete description of the considered excitation, one still needs to derive the kinetic energy associated with the surface motion. This quantity depends on the flow associated with the collective motion. If an irrotational flow is assumed, a simple expression of the mass of the collective motion can be derived. Indeed, one can introduce a velocity $\mathbf{v} = -\nabla\chi$, where velocity potential χ fulfills the condition $\Delta\chi = 0$ when the fluid is incompressible. Using the boundary condition at the surface which, for small values of Q, reads $v_r(R_o) = \dot{R}$ one gets $\chi = -\sum_{\lambda\mu} \lambda^{-1} R_0^{2-\lambda} \dot{Q}_{\lambda\mu} Y^*_{\lambda\mu}$. In this case, the total kinetic energy becomes

$$T = \sum_{\lambda\mu} \frac{M_\lambda}{2} |\dot{Q}_{\lambda\mu}|^2 \quad , \tag{3.5}$$

where the parameter

$$M_\lambda = (3/4\pi) M A R_0^2/\lambda \tag{3.6}$$

can be interpreted as the mass of the vibration.

3.1.3 Quantization of the vibrations

The total Hamiltonian,

$$H = \sum_{\lambda\mu} \frac{1}{2M_\lambda} |P_{\lambda\mu}|^2 + \frac{K_\lambda}{2} |Q_{\lambda\mu}|^2 \quad , \tag{3.7}$$

in which $P_{\lambda\mu} = M_\lambda \dot{Q}^*_{\lambda\mu}$ is the momentum conjugated of the coordinate $Q_{\lambda\mu}$, can now be quantified as a harmonic oscillator with the frequency:

$$\omega_\lambda = \sqrt{\frac{K_\lambda}{M_\lambda}} \quad . \tag{3.8}$$

Therefore, the excitation spectrum exhibits single and multiple phonon excitations. We can introduce the creation and annihilation operators for the phonons, $O^\dagger$ and O, defined by the relations :

$$Q = \sqrt{\frac{\omega}{2K}} (O^\dagger + O) \tag{3.9}$$

and

$$P = i\sqrt{\frac{\omega M}{2}} (O^\dagger - O) \quad . \tag{3.10}$$

The Hamiltonian (3.7) gives a good framework to describe giant resonances. However, the liquid drop parameters for the potential energy do not always give the correct energy for the resonance. For example, for the quadrupole resonance, one gets $\omega \approx 38 A^{-1/2} MeV$ which is far from the experimental value $E \approx 64 A^{-1/3} MeV$.

The reason why the liquid-drop picture fails to reproduce some giant resonances is due to the fact that the motions described by the hydrodynamical model must be slow in comparison with the characteristic equilibration time. Indeed, we suppose that all the internal degrees of freedom are equilibrated when we assume that only the surface modification is contributing to the energy increase (adiabatic approximation). However, the equilibration time can be computed by investigating the time between two collisions undergone by one nucleon. At low excitation energy, this time is very long because many collisions are blocked by the Pauli exclusion principle. If the mean free path of the nucleon is found to be larger than the nuclear size, the equilibration time is greater than 10^{-22}s. Therefore fluid dynamics can be applied only to slow processes(slower than 10^{-22}s), such as fission, but not to giant resonances which have a period of oscillation of the order of 10^{-22}s.

The correct picture is to assume that the nucleons do not have the time to readjust their distribution to the variations of the mean-field (diabatic approximation) and that they still move on the same orbital (see chapter on TDHF approximation). Therefore, not only is the surface deformed but rather the whole nucleus is out of equilibrium. In this case the restoring force becomes a volume force generating the correct $A^{1/3}$ behavior..

In conclusion, the liquid drop model helps in understanding the vibrational nature of giant resonance but cannot be used to quantitatively derive their properties. Therefore, this model must be considered as phenomenological, the parameters K and M being derived from experiment [Br81].

3.1.4 Phenomenological approach

In the phenomenological approach the mass M and the restoring force K are considered as free parameters which are fitted in order to reproduce the resonance frequency and the electric multiple moments $B(E_{\lambda\mu})$. Indeed, the transition between the ground state $|0>$ and the first phonon state $|1_\lambda>$ is related to the amplitude of the vibration. In particular, assuming a sharp uniform charge distribution one gets [Br81]:

$$B(E_\lambda) \equiv |<1_\lambda|\mathcal{M}_\lambda|0>|^2 = \sqrt{\frac{\omega_\lambda}{2K_\lambda}} \frac{3Ze}{4\pi} R_c^\lambda \sqrt{2\lambda+1} \quad , \tag{3.11}$$

where $\mathcal{M}$ are the electric multiple moments ($\mathcal{M}_\lambda \equiv er^\lambda Y_{\lambda,0}$). The actual strength associated with a given mode can be measured experimentally through inelastic collisions.

The $B(E_\lambda)$ value together with the excitation energy ω uniquely define the two parameters K and M of the vibration.

3.1.5 Anharmonicities and Phonon Couplings

The surface vibration model have been widely used for the study of low-lying states such as the low frequency quadrupole mode. In the fifties, the experimental observation that low-lying quadrupole states are the basis of a vibrational band with a large anharmonicity [Go59, Bo65, Bo75] stimulated many theoretical efforts. Some studies were simply based on a phenomenological expression for the Hamiltonian describing the interaction between phonons [Br65, Bo75]. Others were based on a general expansion of the deformation potential (3.4) and of the kinetic energy (3.5) in terms of the deformation parameters Q and velocities $\dot{Q}$ [Be61, Ke62, Be62, Ch64]. However, the properties of the phonons such as the anharmonicity were derived from phenomenological analyses of experimental observations [Bo75]. None of these developments have been applied to multiple excitation of giant resonances because of the lack of experimental data to fit the phenomenological parameters of the models.

To avoid this difficulty, an alternative route is to consider the particle-vibration coupling model (or the nuclear field theory)[Bo75]. Since this model opens the possibility of predicting properties of multiple phonon states built with giant resonances, we will discuss it in some detail[2].

The basic idea is that the leading order of the particle-vibration coupling is identical to the excitation of a phonon during the scattering of a particle. Therefore, the coupling interaction can be written as

$$H_{Coupl} = \mathbf{F}.\mathbf{Q} = \sum_\lambda F_\lambda(r) \sum_\mu Y^*_{\lambda\mu} Q_{\lambda\mu} \quad , \tag{3.12}$$

where Q is the deformation operator and F is a one-body operator. The operator F can either be obtained phenomenologically or can be derived from the microscopic models (see section 3.2.3). In equation (3.12) the collective coordinate Q can be quantified as a harmonic oscillator

$$Q = \sqrt{\frac{\omega}{2K}}(O^\dagger + O) \quad , \tag{3.13}$$

where $O^\dagger$ and O are creation and annihilation operators for phonons and the one body operator F can be expressed as

$$F = \sum_{ij} F_{ij} a^\dagger_j a_i \quad , \tag{3.14}$$

where $a^\dagger_i$ (resp. a_i) creates (resp. annihilates) a particle in the orbital i. Therefore,the interaction between particle and phonons, H_{coupl}, can be graphically represented as in Fig. 2. Higher order terms require computing variety of

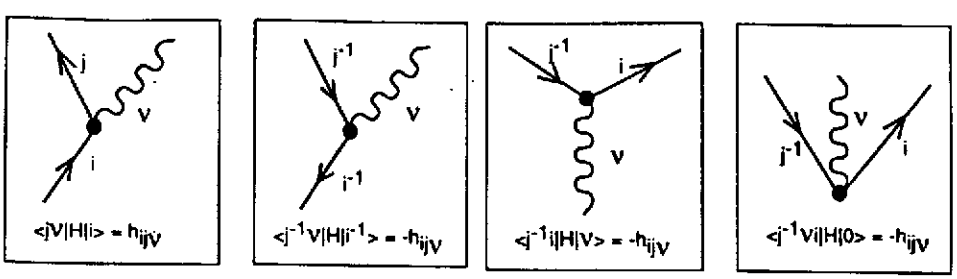

Figure 2 Graphic Representation of the Coupling Hamiltonian : In this figure the straight lines represent particle states noted i or j, (lines going upward) or hole states, noted i^{-1} or j^{-1}, (lines going downward). The heavy lines symbolize phonon excitations labelled by ν. The different point represents vertices associated with a given matrix element.

interactions. For example, the coupling between one- and two-phonon states can be estimated computing the three diagrams shown in Fig. 3 and the additional diagrams obtained by interchanging the direction of the particle arrow (in fact, interchanging particles and holes) and the two final phonons.

The four-phonon interaction requires the estimate of more diagrams which are obtained by attaching the four phonon lines to the four possible fermion vertices shown in Fig. 4 and by inverting the direction of the fermion line.

By generalizing this approach it is, in principle, possible to compute all matrix elements between multiphonon states and to infer properties such as anharmonicities or mixing between one and two phonon states.

[2]Some preliminary results obtained within the nuclear field theory are contained in ref. [Ce89] but no extensive study of the multiple giant resonance excitations have been yet published.

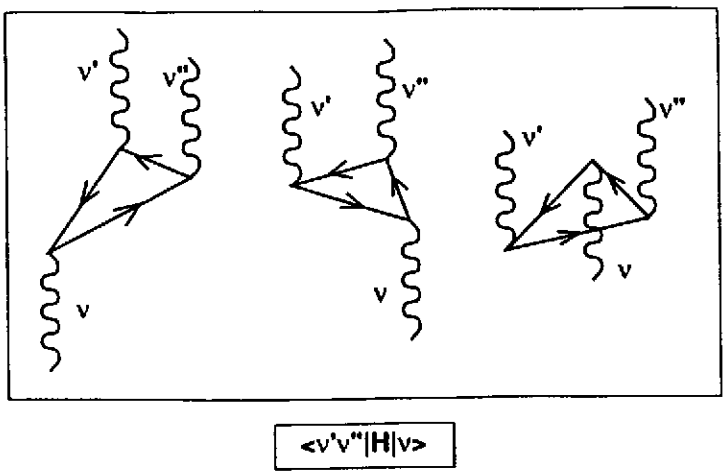

Figure 3 Interactions between one and two Phonons: Different graphs contributing to the coupling between one- and two-phonon states.

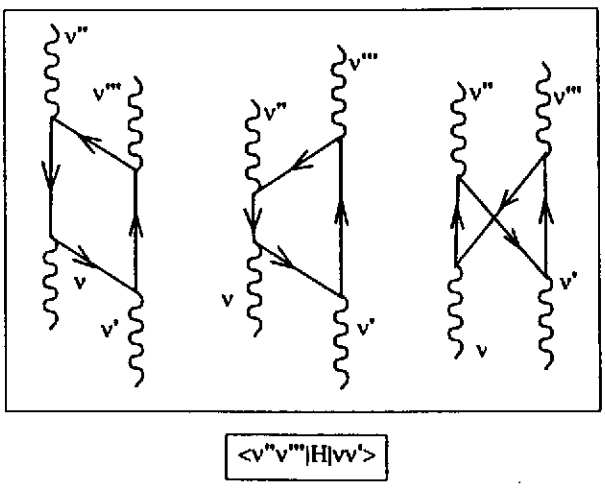

Figure 4 Two-Phonon Interactions: Different graphs containing four phonons in interaction, two in the intial state and two in the final state.

3.1.6 Discussion

The macroscopic model is a useful phenomenological approach which provides a simple representation of the collective excitations of the nucleus. The general concepts such as the small amplitude vibrations of the nuclear density or the quantization of the motions in terms of harmonic oscillations are in common with the microscopic approaches presented in the following section. However, the macroscopic model must be considered with some caution because it basically ignores the microscopic content of the collective excitations. In particular, the macroscopic model provides only a rough estimate of the transition densities associated with the collective modes, i.e. the variation of density observed during the vibration of the nucleus. This may be an important drawback of the method when macroscopic and microscopic form factors are compared. In conclusion, a quantum microscopic description of giant resonances and multiphonons is called for.

3.2 Mean Field Approximation and Beyond

Since the discovery of magic numbers and their interpretation in terms of shell effects (see textbooks such as [Bo69, Ri81]), the idea that nuclei can be described in terms of independent particle motion is well established. The main justifications of such a picture are related to the quantal and fermionic nature of the nucleons: on the one hand, their zero-point motion ($\approx$ 5 fm) is large in comparison with the strong interaction range ($\approx$ 1 fm) and the radius of the hard repulsive core ($\approx$ 0.4 fm); on the other hand, in the interior of the nucleus, most of the collisions are Pauli blocked so that the nucleon mean-free path is long in comparison with the nuclear dimensions. Therefore, the nucleons can be described in a first approximation as interaction-free particles moving in the mean-field created by all the other particles.

The mean-field approximation is the starting point of elaborated descriptions of the nucleus. When looking at static properties of a system, the mean- field treatment leads to the Hartree-Fock approximation (HF) which has been very successful in describing static properties of nuclei (see textbooks such as [Ri81] or recent reviews such as [Ab90] and ref. therein). The time-dependent generalization of this approximation, the time-dependent Hartree-Fock (TDHF) approximation [Di30, Fe57, Fa59, Bo76, Ri81], has also been very successful in describing the dynamical properties of nuclei and low energy heavy-ion reactions. Recently, the semi-classical version of TDHF, the Vlasov equation, has proven to yield a valid description of nuclear properties and reactions, especially in its extended version which includes a Pauli-blocked collision term, the so-called Boltzmann-Uehling-Uhlenbeck (BUU) equation[Be88].

In this section we will first recall a modern derivation of the TDHF approximation where we will define the notations used in the following. In particular we will introduce the Liouville formalism and we will define a natural metric in the Liouville space. Then, we will present the concept of collective vibrations through the linearization of the TDHF equation leading to the Random Phase Approximation (RPA). This introduction will lead to the presentation of various extensions of the mean-field approach. We will start by discussing the so-called Adiabatic TDHF approximation and its predictions for multiphonon anharmonicities. We will then present the Generator Coordinate Method which can be seen as one of the possible bridges towards the Boson mapping method developed in the last section of this chapter. Finally, we will describe the different attempts to use quantified periodic orbits of TDHF in order to go beyond the RPA.

3.2.1 Link between structure calculation and time dependent approximation

The fact that time dependent approaches are general tools to get information on the eigenenergies and eigenstates of the time independent Schrödinger equation is an important concept in physics which deserves some detailed explanations..

From the general point of view time dependent approximations are espoused to provide good approximations for the evolution of quantum systems. In fact, these approximations are often restricted to the prediction of few observations on the system. For example, the time-dependent mean-field approaches are optimized to predict the evolution of the observations of one-body observables $< \hat{D} >$. To understand the link between these approximations and the exact quantum problem one should first introduce the exact eigenstates of the Hamiltonian

$$\hat{H} \left| n \right\rangle = \omega_n \left| n \right\rangle \tag{3.15}$$

Then any initial states

$$\left| \Psi \right\rangle = \sum_n A_n \left| n \right\rangle \tag{3.16}$$

evolve according to the Schrödinger equation

$$\left| \Psi \left(t \right) \right\rangle = \sum_n A_n e^{-i\omega_n t} \left| n \right\rangle \tag{3.17}$$

Therefore, the result of the observation of any observable $\hat{D}$ happens to be

$$< \hat{D} > (t) = \left\langle \Psi \left(t \right) \right| \hat{D} \left| \Psi \left(t \right) \right\rangle = \sum_{nm} A_n e^{-i(\omega_n - \omega_m)t} \left\langle m \right| \hat{D} \left| n \right\rangle \tag{3.18}$$

This means that the Fourier transform of the quantity $< \hat{D} > (t)$ implicitly contains both the energy difference $(\omega_n - \omega_m)$ and the transition amplitude $\left\langle m \right| \hat{D} \left| n \right\rangle$. A case of particular interest correspond to the measure of an observable $\hat{D}$ on a slightly perturbed ground state (as the suddent application of an operator $\hat{B}$). In such a case, at the first order of the perturbation theory we can write

$$\left| \Psi \left(t \right) \right\rangle = \left| 0 \right\rangle + \sum_{n \neq 0} \left\langle n \right| \hat{B} \left| 0 \right\rangle \ e^{-i\omega_n t} \left| n \right\rangle \tag{3.19}$$

and so we get

$$< \hat{D} > (t) = \sum_{n \neq 0} e^{-i(\omega_n - \omega_0)t} \left\langle n \right| \hat{B} \left| 0 \right\rangle \left\langle 0 \right| \hat{D} \left| n \right\rangle + h.c. \tag{3.20}$$

Therefore, the Fourier transform of the predictions of time dependent approximations may give information on the eigen energies and transitions amplitudes of states correctly connected through the corresponding observable. For example, time-dependent mean field approaches are known to be built to predict evolutions of one-body observables therefore the Fourier analysis of the TDHF dynamics may give information on the excitation energy and transition amplitude of states strongly connected to the ground state through one body operators. This means that only the frequencies and amplitude of transition should be interpreted and not other predictions of the approximation such as the wave-function. We will come back to this point when we will discuss periodic orbits of TDHF or correlated ground states of the quasi-boson approximation.

3.2.2 Time-Dependent Hartree-Fock Approximation

Let us consider the Hamiltonian H_f of a fermionic system (e.g. a nucleus) with a two-body interaction V:

$$H = \sum_{ij} t_{ij} a_i^\dagger a_j + \frac{1}{4} \sum V_{ij,kl} a_i^\dagger a_j^\dagger a_l a_k \ , \quad , \tag{3.21}$$

where $a_i^\dagger$ is the creation operator of a particle in the orbital i.

The TDHF approximation reads (see appendix 5.2):

$$i\dot{\rho} = [W(\rho), \rho] \ , \tag{3.22}$$

where ρ is the one-body density matrix, $\rho_{ij} \equiv < a_j^\dagger a_i > \equiv \mathrm{Tr} D a_j^\dagger a_i$ and where the mean-field Hamiltonian is:

$$W = \frac{\partial E(\rho)}{\partial \rho^*} \ , \tag{3.23}$$

with E being the total energy $E(\rho) \equiv < H > \equiv \mathrm{Tr} HD$. In these definitions D is the many-body density matrix of the system supposed to be of independent-particle type (see eq. 5.8).

Diagonalizing the one-body density matrix ,

$$\rho = \sum_i |\varphi_i > n_i < \varphi_i| \tag{3.24}$$

we can define single-particle orbitals φ_i and occupation numbers $\rho_{ij} = \delta_{ij} n_i$. The occupation numbers are constants of the motion and the TDHF equation corresponds, for each orbital φ_i, to a single-particle Schroedinger evolution generated by the self-consistent one-body (HF) Hamiltonian W:

$$i \frac{\partial \varphi_i}{\partial t} = W \varphi_i \ . \tag{3.25}$$

An important application is to consider the evolution of Slater determinants (i.e. $n_i = 0$ or 1). However, the derivation presented in appendix 5.2, was performed in a general framework so that one can consider mixing of independent particle states in which $0 \leq n_i \leq 1$. This is, in particular, the case when one considers a hot system.

In the following, we will use the Liouville formalism [Zw60, Fa64] in the single-particle space. The one-body density matrices, ρ, are considered as super-kets, noted $\|\rho \gg$[3], with elements ρ_α where the index α labels the pair of single particle indices (i, j). The super-operators acting on the Liouville space will be noted by calligraphic letters. In particular, we can write the TDHF equation (5.10):

$$i\|\dot{\rho} \gg = \mathcal{W}\|\rho \gg \ , \tag{3.26}$$

where we have introduced the super matrix $\mathcal{W}$ defined by $\mathcal{W}\|. \gg \equiv \|[W, .] \gg$. The dual of the single-particle Liouville space is the space of the one-body observables, A, (i.e. of the Hermitian one-body operators) and the result of a measurement is given by :

$$\ll A\|\rho \gg \equiv \sum_\alpha A_\alpha^* \rho_\alpha \equiv \mathrm{tr} A\rho \equiv < A > \ , \tag{3.27}$$

This relation provides a scalar product in the Liouville space

$$\ll \sigma\|\rho \gg \equiv \sum_\alpha \sigma_\alpha^* \rho_\alpha \equiv \mathrm{tr}\sigma\rho \ , \tag{3.28}$$

if we define the super-bra $\ll \rho\|$ as being the Hermitian one-body operator associated with ρ. It should be noticed that the conjugate of a super-matrix, $\mathcal{L}$, is $\mathcal{L}^\dagger_{ij,kl} = \mathcal{L}^*_{lk,ji}$ since it is defined by $\ll \rho\|\mathcal{L}^\dagger\|\sigma \gg \equiv \ll \sigma\|\mathcal{L}\|\rho \gg^*$

The TDHF equation (3.26) and the scalar product (3.28) will be the building-blocks of the following developments.

3.2.3 Random Phase Approximation

In this section we will present the linearization of the TDHF equation which leads to the so-called RPA.. Considering the discussion about the link between time dependent approaches and eigen-energies and transition amplitudes we can directly understood that a Fourier analysis of the linearized TDHF should directly give access to excitation energies of states which can be excited from the ground state through a one-body operator.

[3] We will sometimes omit the super-ket symbols $\| \ldots \gg$ when no confusions are possible

3.2.3.1 Small Amplitude Vibrations

Let us consider the case of small amplitude motion around a given density $\rho^{(0)}$[Ri81]. In this case if we expand the TDHF equation (3.26) to the first order assuming that

$$\rho = \rho^{(0)} + \rho^{(1)} + \cdots \quad , \tag{3.29}$$

we get

$$i\|\dot{\rho}^{(1)} \gg = \mathcal{K}\|\rho^{(1)} \gg \quad . \tag{3.30}$$

In this equation we have introduced the RPA matrix defined by

$$\mathcal{K}_{\alpha\beta} \equiv \frac{\partial [W,\rho]_\alpha}{\partial \rho_\beta} \quad , \tag{3.31}$$

or equivalently by

$$\mathcal{K} = \mathcal{E} + \mathcal{F}\mathcal{L} \quad , \tag{3.32}$$

where the super matrices $\mathcal{E}, \mathcal{F}, \mathcal{L}$ are defined by:

$$\begin{array}{lcl} \mathcal{E}\|\sigma \gg & = & \|[W^{(0)},\sigma] \gg \\ \mathcal{F}\|\sigma \gg & = & -\|[\rho^{(0)},\sigma] \gg \\ \mathcal{L} & = & \frac{\partial W}{\partial \rho} = \frac{\partial^2 E}{\partial \rho^* \partial \rho} \quad . \end{array} \tag{3.33}$$

In order to solve equation 3.30, we introduce the eigenmodes, $\mathcal{X}^\nu$, of the RPA matrix $\mathcal{K}$:

$$\mathcal{K}\|\mathcal{X}^\nu \gg = \omega_\nu \|\mathcal{X}^\nu \gg \quad . \tag{3.34}$$

Realizing that the operator $\mathcal{F}^{-1}\mathcal{K}$ is Hermitian according to the scalar product $\ll \| \gg$ of the Liouville space (i.e. $\mathcal{K}^\dagger \mathcal{F}^{-1} = (\mathcal{F}^{-1}\mathcal{K})^\dagger = \mathcal{F}^{-1}\mathcal{K}$) we can easily show that the linear evolution, 3.30, preserves the simplectic RPA form $\ll \|\mathcal{F}^{-1}\| \gg$:

$$\frac{d}{dt} \ll \rho^{(1)}(t)\|\mathcal{F}^{-1}\|\sigma^{(1)}(t) \gg = 0 \quad , \tag{3.35}$$

where $\rho^{(1)}$ and $\sigma^{(1)}$ are any linear perturbations of $\rho^{(0)}$. Therefore, according to this simplectic structure of $\mathcal{K}$, each eigenmode $\|\mathcal{X}^\nu \gg$ with an energy ω_ν can be associated with the eigenmode $\|\mathcal{X}^{\nu'} \gg$ with an energy $-\omega_\nu$. Moreover, the different modes are orthonormalized according to the RPA simplectic form:

$$\ll \mathcal{X}^\nu \|\mathcal{F}^{-1}\| \mathcal{X}^\mu \gg = \delta_{\nu\mu} sgn(\omega_\nu) \quad , \tag{3.36}$$

and the closure relation reads:

$$\sum_\nu sgn(\omega_\nu) \|\mathcal{X}^\nu \gg \ll \mathcal{X}^\nu \|\mathcal{F}^{-1} = 1 \quad . \tag{3.37}$$

Eq. (3.34) is the most general RPA equation valid for time dependent problems with occupation numbers different from 0 or 1. It is also built to accommodate density dependent interactions or three body forces.

3.2.3.2 Linearization in a moving frame

Let us generalize a little the above presentation by considering the case of a small amplitude motion around a TDHF trajectory. In the mean-field approximation, the single-particle density matrix ρ of the system is determined by the time-dependent Hartree-Fock (TDHF) equation,

$$i\hbar \frac{\partial \hat{\rho}(t)}{\partial t} = [\hat{W}[\rho],\ \hat{\rho}(t)], \tag{3.38}$$

where $\hat{W}[\rho] = \hat{\mathbf{p}}^2/2m + \hat{U}[\rho]$ denotes the mean-field Hamiltonian, and $\hat{U}[\rho]$ is the density dependent self-consistent mean-field potential. Let us assume that the system is represented at the initial time $t = 0$ by a density matrix $\hat{\rho}_0 = \hat{\rho}(0)$ determined by the constraint Hartree-Fock equation $[\hat{W}[\rho_0] - \lambda\hat{Q},\ \hat{\rho}_0] = 0$, where $\hat{W}[\hat{\rho}_0]$ is the mean-field Hamiltonian at the initial state, $\hat{Q}$ is a suitable constraining operator for preparing the system and λ is the associated Lagrange multiplier. To study the propagation of small perturbations around the trajectory defined by the initial constrained state $\hat{\rho}_0$ it is more convenient to consider the density matrix $\hat{\varrho}(t)$ in the "moving frame", $\hat{\varrho}(t) = exp[\frac{i}{\hbar}\lambda t\hat{Q}]\ \hat{\rho}(t)\ exp[-\frac{i}{\hbar}\lambda t\hat{Q}]$, and transform the TDHF equation into the moving frame,

$$i\hbar \frac{\partial \hat{\varrho}(t)}{\partial t} = [\hat{W}(t) - \lambda\hat{Q},\ \hat{\varrho}(t)], \tag{3.39}$$

where the mean-field Hamiltonian in the moving frame is given by,

$$\hat{W}(t) = exp[i\lambda t\hat{Q}]\ \hat{W}(t)\ exp[-i\lambda t\hat{Q}]. \tag{3.40}$$

In order to investigate the early evolution of instabilities, we linearize this equation around $\hat{\varrho}_0(t)$, $\hat{\varrho}(t) = \hat{\varrho}_0(t) + \delta\hat{\varrho}(t)$, where $\hat{\varrho}_0(t)$ is the solution of the TDHF eq.(2) with the initial condition $\hat{\varrho}_0$ determined by the constraint Hartree-Fock equation. The small fluctuation $\delta\hat{\varrho}(t)$ is determined by the linearized TDHF equation in the moving frame,

$$i\hbar\frac{\partial\delta\hat{\varrho}}{\partial t} = [\hat{W}_0(t) - \lambda\hat{Q},\ \delta\hat{\varrho}] + [\delta\hat{U}(t),\ \hat{\varrho}_0(t)] = \mathcal{M}(t)\cdot\delta\hat{\varrho}(t), \tag{3.41}$$

where the mean-field Hamiltonian $\hat{W}_0(t)$ and the fluctuations of the mean-field potential $\delta\hat{U}(t)$ in the moving frame are defined in a manner similar to eq.(3), and $\mathcal{M}(t)$ denotes the instantaneous RPA matrix. The formal solution of this equation can be expressed as

$$\delta\hat{\varrho}(t) = \mathcal{U}(t)\cdot\delta\hat{\varrho}(0), \tag{3.42}$$

where

$$\mathcal{U}(t) = \mathcal{T}(exp[-\frac{i}{\hbar}\int_0^t ds\mathcal{M}(s)]) \tag{3.43}$$

denotes the linearized evolution operator with $\mathcal{T}$ as the time ordering operator. The eigenvalues of the evolution operator $\mathcal{U}(t)$ determine the stability of the TDHF trajectories as a function of time. However the construction of $\mathcal{U}(t)$ is, in general, a very difficult task. Therefore, we consider the early evolution of the instabilities in the vicinity of the initial state $\hat{\varrho}_0$ and solve the RPA problem associated with $\mathcal{M}(0) = \mathcal{M}$. Introducing the eigenmodes $\delta\hat{\varrho}(\omega)$ associated with the eigenvalue $\hbar\omega$ and incorporating the representation $|i>$, which diagonalizes $\hat{W}_0 - \lambda\hat{Q}$ and $\hat{\varrho}_0$, the RPA equation $\mathcal{M}\ \delta\hat{\varrho}(\omega) = \hbar\omega\ \delta\hat{\varrho}(\omega)$ for the collective modes becomes

$$(\hbar\omega - \epsilon_i + \epsilon_j)\ <i|\delta\hat{\varrho}(\omega)|j> \ = \ <i|\delta U(\omega)|j>\ (\rho_j - \rho_i), \tag{3.44}$$

where ρ_i and ϵ_i are the occupation number and the energy associated with the constraint Hartree-Fock state $|i>$, respectively. The temperature dependence may enters into the calculations through the occupation number $\rho_i$if it is given by the Fermi-Dirac function in terms of the single-particle energies ϵ_i.

3.2.3.3 Dispersion relation method

The RPA eq.(3.44) can be solved using standard techniques [Ri81]. However, we can consider a simplified approach, and parametrize the transition density associated with an isoscalar collective mode in terms of a known operator $\hat{F}$ such as a multipole operator,

$$\delta\hat{\varrho}(\omega) = \alpha(\omega)\ \hat{F} \tag{3.45}$$

where $\alpha(\omega)$ is the amplitude associated with the collective mode. This relation can be inverted using any observable $\hat{D}$

$$\alpha(\omega) = K\ \mathrm{tr}\hat{D}\delta\hat{\varrho}(\omega), \tag{3.46}$$

where the normalization factor K_L is given by

$$\frac{1}{K} = \mathrm{tr}\hat{D}\hat{F} \tag{3.47}$$

Such a density variation induces a variation of the mean-field

$$\delta U(\omega) = \alpha(\omega)\partial U/\partial\alpha \tag{3.48}$$

A dispersion relation for the frequencies of the collective modes can be deduced from the self-consistency condition that is obtained by inserting the solution of the RPA equation for $\delta\hat{\varrho}(\omega)$ into the right hand side of eq..(3.44). This gives

$$\frac{\alpha(\omega)}{K} = \sum_{i,j}\frac{\alpha(\omega)\ <i|\partial U/\partial\alpha|j><j|\hat{D}|i>}{\hbar\omega - \epsilon_i + \epsilon_j}\ (\rho_j - \rho_i), \tag{3.49}$$

This dispersion relation is valid, in principle, for any choice of $\hat{D}$, provided that the parametrization (3.45) is a good approximation for the density fluctuations in a multipole mode. In fact, the dispersion relation is not very sensitive to the specific form of $\hat{D}$ so we can take $\hat{D} = \partial U/\partial\alpha$. This gives rise to a symmetric dispersion relation,

$$\frac{1}{K} = \sum_{i,j}\frac{\left|<j|\hat{D}|i>\right|^2}{\hbar\omega - \epsilon_i + \epsilon_j}\ (\rho_j - \rho_i), \tag{3.50}$$

which is equivalent to the RPA problem with a separable interaction of the form,

$$V(1,2) = \frac{1}{2}\ K\ \hat{D}(1)\hat{D}(2), \tag{3.51}$$

with the coupling constant K given by the normalization factor in eq.(3.47).

The dispersion relation (3.50) allows to determine frequencies ω associated with the collective modes. This dispersion relation can be solve graphically outing the intersection of the curve

$$y = \sum_{i,j} \frac{\left| < j|\hat{D}|i > \right|^2}{\hbar\omega - \epsilon_i + \epsilon_j}\ (\rho_j - \rho_i), \tag{3.52}$$

with the line

$$y = \frac{1}{K} \tag{3.53}$$

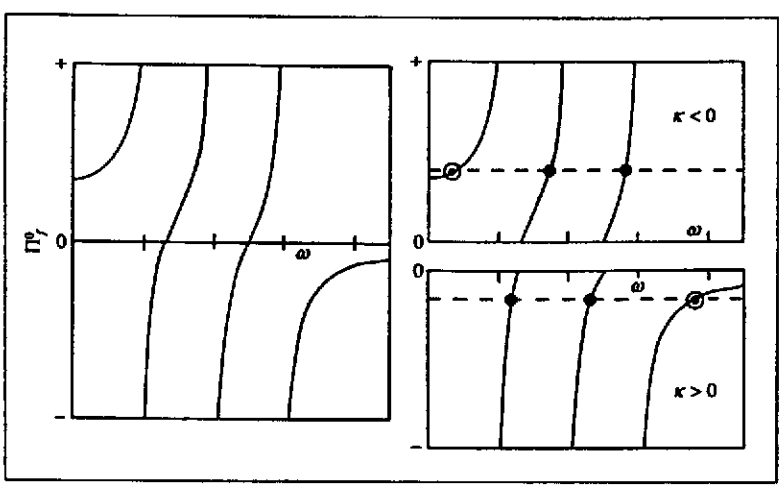

Figure 5 Shematic picture of the graphic resolution of the dispesion relation.

3.2.3.4 Zero-Temperature RPA

At zero-temperature the ground state is described by a single Slater determinant. The occupied states are usually called holes (h) while the unoccupied orbitals are named particles (p). In this case the RPA Eq. (3.34) reduces to the zero-temperature RPA equation :

$$i \begin{pmatrix} \dot{\rho}^{(1)}_{ph} \\ \dot{\rho}^{(1)}_{hp} \end{pmatrix} = \begin{pmatrix} A & B \\ -B^* & -A^* \end{pmatrix} \begin{pmatrix} \rho^{(1)}_{ph} \\ \rho^{(1)}_{hp} \end{pmatrix} \ . \tag{3.54}$$

In this equation, we have introduced the matrices A and B which are given by:

$$\begin{aligned} A_{ph,p'h'} &\equiv \mathcal{K}_{ph,p'h'} \\ B_{ph,p'h'} &\equiv \mathcal{K}_{ph,h'p'} \ . \end{aligned} \tag{3.55}$$

Solving the RPA equation (3.54), we must introduce the eigenenergy and eigenvalues of the RPA matrix :

$$\begin{pmatrix} A & B \\ B^* & A^* \end{pmatrix} \begin{pmatrix} X^\nu \\ Y^\nu \end{pmatrix} = \omega_\nu \begin{pmatrix} X^\nu \\ -Y^\nu \end{pmatrix} \ . \tag{3.56}$$

The positive frequencies define the eigenmodes of the nucleus and X and Y , the transition from the ground state to the excited state $\mid \nu >$ induced by the one-body operator F (see appendix 5.3):

$$< o|F|\nu >= \sum_{ph} F_{hp} X^\nu_{ph} + F_{ph} Y^\nu_{ph} = \ll F \| \mathcal{X}^\nu \gg \ . \tag{3.57}$$

We can therefore compute the strength function associated with the operator F

$$S(E) \equiv \sum_\nu | < o|F|\nu > |^2 \delta(E - \omega_\nu) = \sum_\nu | \ll F \| \rho^{(1)}_\nu \gg |^2 \delta(E - \omega_\nu) \ . \tag{3.58}$$

Since the introduction of the RPA[Bo53] in nuclear physics [Gl59, Fa59a, Go59a, Ta59, Ik59, Ar60, Ba60, Ka60, Ma60, Th61a] numerous applications have been worked-out and it is beyond the scope of the present article to review them all. We will only discuss some important points and refer the reader to the existing articles and textbooks (for example see refs. [Ri81, Sp91]) for a more complete status report on this subject. We will in particular concentrate the discussion on the self-consistent RPA approaches which are fully microscopic [Be75, Be74, Li76, Bl76, Kr77, Bl77, Li76a].

Two avenues have been investigated up to now. The first approach consists in the diagonalization of the H.F.

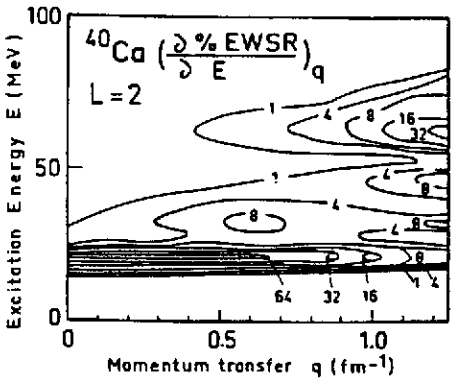

Figure 6 Quadrupole Strength : From ref. [De82] and [Bl88] . Bidimensional contour plot of the L=2 response of ^{40}Ca to the $j_L(qr)$ operator as a function of the momentum transfer q and of excitation energy E.

mean-field on a discrete basis followed by a diagonalization of the RPA matrix. Figure 6 presents the quadrupole strength obtained from a self consistent RPA calculation using a finite range effective force, the Gogny force D1[De82]. The giant quadrupole resonance is clearly observed around 20MeV. This figure also illustrates the extreme sensitivity of the shape of the strength to the excitation operator F.

The second possibility is to compute directly the strength function in the continuum. This approach is based on the Green's function methods. The RPA Green's function can be directly computed from equation (5.21). For finite-range nuclear forces, this method presents enormous numerical difficulties. However, the problems become much simpler for zero-range effective interactions such as Skyrme forces [Be73, Sh75, Be75, Li76a, Ts78] because one can solve the Bethe-Salpeter equation (5.21) directly in coordinate space (see appendix 5.2).

An example of such a calculation is shown in Fig. 7 from [Ch88]. Only the continuum part of the strength is represented. It can be seen that this calculation predicts a width for the peaks and giant resonances. This width

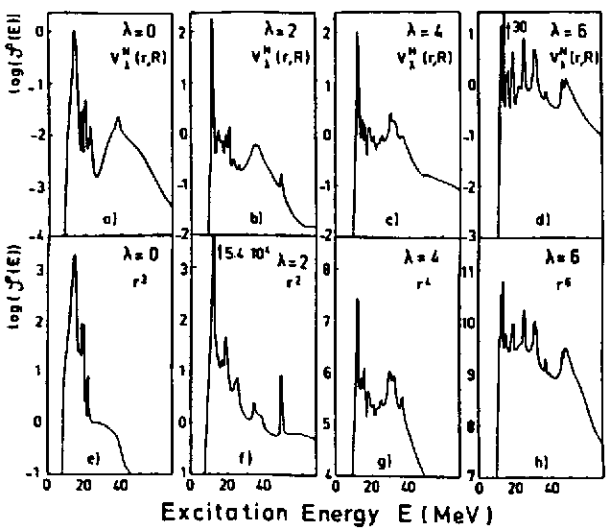

Figure 7 Multipole Strength : From ref. [Ch88] : RPA strength distributions in ^{208}Pb induced by an ^{36}Ar projectile calculated with : (1) the excitation operator corresponding to the Ar at a distance R = 11.35fm, (parts(a)-(d) in MeV) ; (2) $r^{\lambda'}Y_{\lambda 0}(\hat{r})$ with $\lambda' = \lambda$ if $\lambda > 1$ or $\lambda' = \lambda + 2$ if $\lambda \leq 1$, (parts(e)-(h) in fm$^{2\lambda'}$ MeV-1)

includes both the Landau spreading and the escape width.

3.2.3.5 Multiphonon Strength

The RPA approximation is an harmonic approximation therefore we can define a multiple excitation strength as

$$S(E,n) = \sum_{\nu_1,\ldots,\nu_n} | < o|F|\nu_1 > |^2 \ldots | < o|F|\nu_n > |^2 \delta(E - (\omega_{\nu_1} + \ldots + \omega_{\nu_n})) \quad , \tag{3.59}$$

which reduces to the usual strength function S(E) (3.58) for n=1. This multiple excitation strength can be also expressed as a folding of the strength function

$$S(E,n) = \frac{1}{n!} \int dE_1 \ldots \int dE_n S(E1) \ldots S(E_n) \delta(E - (E_1 + \ldots + E_n)) \quad . \tag{3.60}$$

This expression is also valid in the case of a continuous spectrum. The folding product (3.60) is intimately related to the assumption that phonons are purely harmonic vibrations. This is clearly a very crude approximation which needs to be carefully investigated. To get a handle on the magnitude of the anharmonic effects one clearly needs to go beyond the RPA. This will be the subject of the next paragraphs.

3.2.4 Adiabatic TDHF approximation

The adiabatic TDHF (ATDHF) approximation is intended to describe slow collective motion of large amplitude. However, from the previous discussions, it appears that giant resonances are akin to the diabatic motion of the nucleons in a rapidly vibrating mean-field. So, it may seem surprising to use the ATDHF formalism to study giant resonances. This apparent contradiction can be resolved by recalling that the adiabaticity condition is in fact defined by comparing the collective velocity measured by the collective kinetic energy with the single-particle energy times the number of nucleons involved in the motion [Ba72, Vi72, Vi75, Br76, Vi77, Ba78, Ri81]. Therefore it can be valid for the description of collective modes in which many nucleons are participating. This is precisely the case of giant resonances.

In this section we will show how the approximation leads to the definition of collective potentials and masses which give direct access to the anharmonicity of the phonons (a more detailed discussion can be found in appendix 5.4). Indeed, we will show that the problem reduces to the quantization of the collective degrees of freedom in this collective potential.

The basic idea is to decompose ρ in order to extract a velocity field and a set of collective coordinates. Since the coordinates are usually time reversal invariant quantities, Baranger and Véneroni [Ba78] proposed to decompose the density using two time-even Hermitian matrices, a density $\rho^{(0)}(t)$ and a velocity field $\chi(t)$:

$$\rho(t) = e^{i\chi(t)} \rho^{(0)}(t) e^{-i\chi(t)} \quad . \tag{3.61}$$

They also proposed the adiabatic approximation assuming that $\rho(t)$ is very close to $\rho^{(0)}(t)$, i.e. that the velocity field is small enough to be treated perturbatively. Using the density (5.35) the Hartree-Fock energy can be expanded as :

$$E(\rho) = E(\rho^{(0)}) + \frac{1}{2} \ll \chi \| \mathcal{M}^{-1} \| \chi \gg \quad , \tag{3.62}$$

where we have introduced the mass tensor which reads using the RPA notation:

$$\mathcal{M} = (\mathcal{K}\mathcal{F})^{-1} \quad . \tag{3.63}$$

The first term in equation (3.62) can be interpreted as a potential energy $V(\rho^{(0)})$ whereas the second one corresponds to a kinetic energy term $T(\chi, \rho(0))$. The energy E plays the role of a classical Hamiltonian for which $\rho^{(0)}$ and χ appear as conjugate variables. Therefore, the dynamical equations for $\dot{\rho}^{(0)}$ and $\dot{\chi}$ can be derived from the Hamiltonian equations: $\|\dot{\rho}^{(0)} \gg \equiv \|\partial E/\partial \chi^* \gg$ and $-\|\dot{\chi} \gg \equiv \|\partial E/\partial \rho^{(0)^*} \gg$. However, they are often too difficult to solve without further approximations. In fact this approach is really useful if we can assume that the density $\rho^{(0)}(t)$ is driven by an ensemble of collective coordinates $Q(t)$

$$\|\rho^{(0)}(t) \gg = \|\rho^{(0)}(Q(t)) \gg \quad . \tag{3.64}$$

In such a case, we can write the kinetic energy as $T = \frac{1}{2}\dot{Q}M\dot{Q}$ where the mass tensor is defined in appendix 5.4. Therefore, if we define the momentum $P = M\dot{Q}$, equation (3.62) yields the collective Hamiltonian

$$E(\rho) \equiv H(P,Q) = \frac{1}{2} PMP + V(Q) \quad , \tag{3.65}$$

where the potential is the mean value of the energy associated with $\rho^{(0)}$: $V(Q) \equiv E(\rho^{(0)})$. Therefore, the ATDHF approximation leads to a classical Hamiltonian similar to the one of the macroscopic approaches.

The last step of the ATDHF approximation is to requantify the classical collective Hamiltonian (3.65) in order to define the ground state and the excited states of the system. If the anharmonicity is weak the lowest excited states can be associated with the single phonon whereas the higher states can be interpreted as multiple excitations.

However before studying the spectrum of predicted excitations one must discuss the validity of the ATDHF treatment as far as the giant resonances are concerned.

The adiabaticity approximation implies that the time-odd component of any single particle wave function is small. This condition can be shown to be equivalent to the requirement that the collective kinetic energy is small in comparison with the typical particle-hole energy times the number of states participating in the collective mode. Therefore, it can be applied to the description of giant resonances.

In principle, the ATDHF treatment also gives access to the anharmonicities of the modes because the Hamiltonian (3.62) or (3.65) do not imply an harmonic approximation. Realistic calculations have been carried out with Skyrme forces [En75, Va75, Gi76, Go77, Gi80]. They all have to face the problem of defining the collective variable i.e. the collective path $\rho^{(0)}(Q)$. Two possibilities are often explored, either performing a constrained Hartree-Fock calculation or simply scaling the ground state density. Fig 8 shows the potential energy V(Q) computed in ref. [Gi80] using the scaling approach and Fig.9 presents the associated mass parameter.

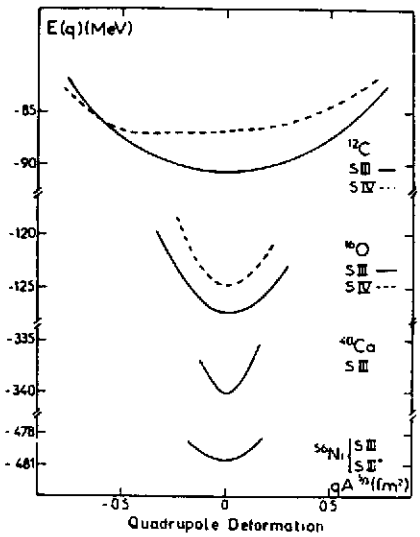

Figure 8 ATDHF Potential.: From ref. [Gi80] , Potential energy $V(\alpha)$as a function of the quadrupole deformation parameter Q for ^{12}C,^{16}O,^{40}Ca and ^{57}Ni. The dashed line were obtained using the Skyrme interaction SIV while the solid curve represents the results obtained using the SIII interaction.

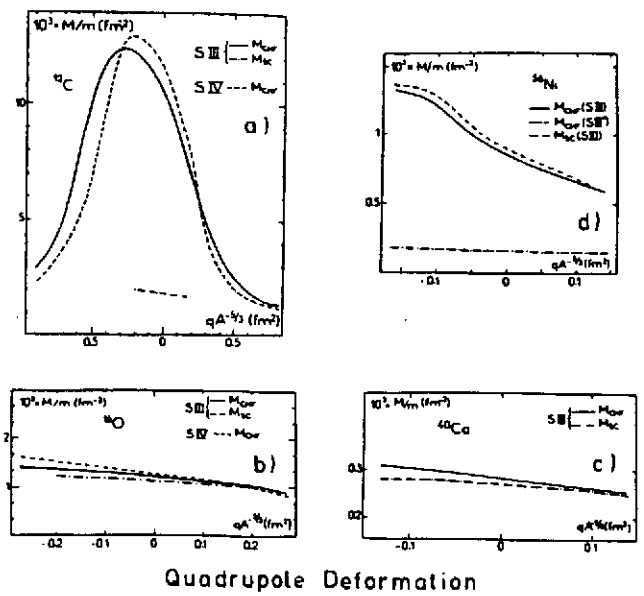

Figure 9 ATDHF Masses. : From ref.[Gi80], adiabatic mass parameters, M_{CHF}, associated with the quadrupole modes in various nuclei ^{12}C,^{16}O,^{40}Ca,^{56}Ni obtained from a constrained HF calculation with the quadrupole operator Q_{20} of the static HF solution

It can be seen that open shell nuclei such as ^{12}C present strong anharmonicities whereas closed-shell nuclei can be considered as good harmonic vibrators. For example in the case of the quadrupole deformation , $Q =< x^2+y^2-2z^2 >$,

of the ^{40}Ca nucleus we can parametrize the potential energy and the mass as [Tr81]

$$V(Q) = \frac{1}{2}M_0\omega^2Q^2 + V_3Q^3 \quad (3.66)$$

$$M(Q) = M_0 + M_1Q \ , \quad (3.67)$$

where $M_0/m_n = 0.285\ \ 10^{-3}$ (m_n being the nucleon mass) $M_1/m_n = -0.28\ \ 10^{-6}$ fm^{-4}, $\omega = 17.5$ MeV and $V_3 = -0.14\ \ 10^{-5}$ MeV fm^{-6}.

The relative anharmonicity can be estimated from the ratio between the harmonic and the anharmonic parts of the potential computed at a typical deformation. If we introduce the zero point motion $Q_0^2 = 1/M\omega$ as a typical deformation we get a relative anharmonicity $(2V_3Q_0)/M_0\omega^2$ of the order of -0.1. This is a rather small value which is however larger than the simple estimate (2.87) which gives around -0.02 for the ^{40}Ca.

The ATDHF method can be useful for the computation of non linearities and anharmonicities. However, a systematic study remains necessary to realistically extract the properties of multiphonon states. One difficulty lies in the fact that for such calculations, many degrees of freedom need to be taken into account, such as the different angular momenta $\lambda\mu$. Moreover, the ambiguities in the definition of the collective variable complicate the problem. In particular, one may think of using several collective variables for the same angular momentum, or even a complete set of collective operators such as in equations (5.41) and (5.42). But then the method becomes intractable. A way to construct the "good" collective variables is to introduce the RPA eigenstates and to use the ATDHF treatment to compute corrections to the RPA. In the next section we will discuss two other ways to requantify TDHF and we will discuss their predictions concerning in particular the anharmonicities. However, as far as the ATDHF approach is concerned, we have seen that the anharmonicity of the giant resonances in closed-shell nuclei is predicted to be around 10 % .

3.2.5 Generator Coordinate Method

In the previous section we have discussed the ATDHF approximation and have shown how this method leads to the definition of a classical Hamiltonian in terms of $\rho^{(0)}$ and χ (see eq. (3.61)) or in terms of some collective variables Q and P (see eq. (5.35)). These results were derived within the mean-field approximation. However, requantifying the ATDHF Hamiltonian goes beyond the mean-field approximation. Indeed, an eigenstate will correspond to a wave function f in the collective coordinate Q so that the many-body wave function can be viewed as a superposition of Slater determinants which cannot be considered as an independent particle wave function.

This idea to coherently mix several generating many-body wave functions such as Slater determinants is in fact the starting point of the method called GCM, Generator Coordinate Method [Hi53, Gr57, La74, Mo76, La76, To77, To78, Ri81]. Let us consider a continuous set of generating many-body wave functions $\mid \Phi(Q) >$ which are labelled by an ensemble of coordinates (Q_μ) and let us construct a many-body wave function $\mid \Psi >$ as a linear superposition of the $\mid \Phi(Q) >$:

$$\mid \Psi >= \int dQ f(Q) \mid \Phi(Q) > \ , \quad (3.68)$$

where f is a weight function. The $\mid \Psi >$'s form a trial set which can be used to variationally determine the eigenstates of the exact many body problem. It should be noticed that the trial set may possibly contain all the Hilbert space. This is for example the case if Q is the one-body density itself because the Slater determinants are a basis of the Hilbert space.

Determining the extremum of $< \Psi \mid H \mid \Psi > -E < \Psi \mid \Psi >$, where E is a Lagrange multiplier associated with the normalization of the wave functions, yields the equation

$$\int dQ' < \Phi(Q') \mid H \mid \Phi(Q) > f(Q) = E \int dQ < \Phi(Q') \mid \Phi(Q) > f(Q) \ , \quad (3.69)$$

when variations of f^* are considered.

The equation (3.69) can be viewed as a generalized eigenvalue problem for the weight function f, the so-called Hill-Wheller equation [Hi53] :

$$\mathcal{H}f = E\mathcal{N}f \ , \quad (3.70)$$

where $\mathcal{H}(Q,Q') =< \Phi(Q) \mid H \mid \Phi(Q') >$ and where $\mathcal{N}(Q,Q') =< \Phi(Q) \mid \Phi(Q') >$ is an overlap metrics.

The equation (3.70) can be solved directly in some cases by discretization of the variable Q. This method was used in different calculations of monopole and quadrupole phonon spectra [Ca73, Ab75, Gi75, Fl75, Kr76, Fl76].

One can see on table 3.1 that the CGM method predicts rather small anharmonicities.

In addition to the direct solutions of the Hill-Wheeler equation, numerous approximations have been developed to transform it into a Schrödinger equation in the collective variable Q [Fe72, Ha73, Ba73, Ho73, Gi75, Re76].

For example, assuming that the overlap metrics is Gaussian, one gets a collective Hamiltonian which is close to the ATDHF Hamiltonian except for the mass parameter [Hi53, Pe62, Ja64, Ka68, Vi75], which is generally not as good. Moreover, it should be noticed that, as far as the ambiguity in the definition of the collective variable is concerned, the CGM method faces the same problems as the ATDHF approach.

	^{16}O	^{40}Ca
E_0	−140.3	−403.3
E_1	−108.7	−374.9
E_2	−81.8	−347.0

Table 3.1 GCM Results. From ref. [Fl76], energies of the three first solution of the Hill-Wheeler equation for the isoscalar monopole resonance calculated using the SIII Skyrme force.

Two other avenues have been followed in the literature. The first one is to use the CGM to deduce a mapping of the fermion dynamics into a dynamics of bosons. This will be the subject of the section on boson expansions. The second avenue is to introduce schematic models. In particular the Lipkin model or other two level models can be explicitly solved [Be92]. Another classical example is given by the deformed oscillator model [Dr88] in which the single particle wave functions are simply boosted harmonic oscillator eigenfunctions. However these simple models must be considered as tests for more elaborated approximations or treatments. In particular the above models have been used to test the description of eigenstates in terms of TDHF periodic orbits as we will discuss in the next section.

3.2.6 Periodic orbits of TDHF

The TDHF approximation assumes that at each time t the nucleus is described by a Slater determinants or more generally a density matrix which is the exponential of a one body operator. Therefore, the TDHF equation can be considered as the evolution equation of mean values of one-body observables.. In this sense, it is a classical approximation and it needs to be quantified in order to yield energy levels of the system. One standard approach is the semiclassical quantization of periodic orbits.

In fact, the importance of periodic orbits has been recognized in classical mechanics [Po1892] for more than a hundred years. The idea of obtaining the energy levels of a microscopic system by quantifying its action along periodic orbits proposed by Bohr for the description of the hydrogen atoms, was a key step towards the elaboration of quantum mechanics

In the 70's, a well-founded relation between the periodic orbits of a classical system and the energy levels of the associated quantum problem has been developed by Gutzwiller [Gu67, Gu69, Gu70, Gu71]. In particular, this author showed how to approximate the quantum Green's function (or the level density) as a sum over all possible periodic trajectories. These studies were pursued and extended by many authors [Ba72, Ba74, Be76, Bc77, Pe77]. As far as the periodic orbits of mean field approximations are concerned, their connections with the energy spectrum were elucidated in several references [Ka79, Le80, Le80a, Bl81, Ne82, Za84, Dr86a].

In particular, using functional integral techniques and saddle point approximations, the role of periodic orbits was made explicit and the condition of quantization derived. The result can be qualitatively understood by noting that the Green's function in its spectral representation involves a Fourier transform in the time coordinate. Periodic orbits will dominate because they provide an equal contribution at each period. However, the phase of this contribution over a period must be a multiple of 2π otherwise the different terms do cancel out. This condition yields the desired quantization procedure.

Then the general problem of finding exact periodic trajectories of a given Hamiltonian arises. For a classical system with few degrees of freedom this problem has already been widely discussed (see for example ref. [Za84]). In the nuclear context, similar methods were tested. For example, the method proposed in ref. [Ca85] is based on an iterative construction of a family of periodic orbits. From a periodic orbit at an energy E one can build another trajectory at an energy $E + \delta E$ using the linear response theory. The new trajectory can be adjusted in order to be periodic through the Newton method. However, this method was only applied to schematic cases because of its intrinsic complexity when many degrees of freedom are coupled.

The method proposed in ref. [Ch86] is an iterative method based on the existence of a distance in the Liouville space constructed from the scalar product (3.28)

$$\ell(\rho, \varrho) = \ll \rho - \varrho \| \rho - \varrho \gg \quad . \tag{3.71}$$

Therefore, if one starts with an arbitrary solution $\rho(0)$, one can first find the period T for which the distance, $\ell(\rho(0), \rho(T))$, is minimum. One can thus look for the small variation $\delta\rho(0)$ which will reduce the distance $\ell(\rho(0), \rho(T))$. It is explained in appendix 5.5 how using a linear approximation for the evolution of $\delta\rho$ it is possible to iteratively reduce the distance ℓ.

This method was successfully applied in ref. [Ch86] to the monopole vibration. However, an exhaustive study of different vibrations remains to be done. The main difficulties associated with this method is that it requires important numerical effort. Moreover, this method faces some difficulties when considering unbound states which cannot be periodic due to their decay except if an external gas of nucleons is added which will however perturb the response.

The problem of finding periodic trajectories was recently revisited by A. Abada and D. Vautherin [Ab91, Ab92, Ab92a], who proposed an elegant method, a perturbative expansion in the amplitude of the collective vibrations, to find periodic orbits. This method is in fact a standard technique used in celestial mechanics [Po1892] or in the theory of non linear oscillators [La69].

The basic idea is to expand the density in powers of a small number, the amplitude of the oscillations ε

$$\rho(t) = \rho^{(0)} + \varepsilon\rho^{(1)}(\frac{\omega t}{\omega^{(0)}}) + \varepsilon^2\rho^{(2)}(\frac{\omega t}{\omega^{(0)}}) + \varepsilon^3\rho^{(3)}(\frac{\omega t}{\omega^{(0)}}) + \cdots \quad , \tag{3.72}$$

where the frequency is also expanded in a power series of ε :

$$\omega = \omega^{(0)} + \varepsilon\omega^{(1)} + \varepsilon^2\omega^{(2)} + \varepsilon^3\omega^{(3)} + \cdots \quad . \tag{3.73}$$

The dynamical equations for $\rho^{(n)}$ are obtained from the expansion of the TDHF equations (3.26) at the n'th order in ε (see appendix 5.5).

The equation for $\rho^{(1)}$ is the RPA equation which implies that $\delta\rho$ can be expended on to the RPA eigenstates as follows

$$\|\rho^{(1)}(t) \gg = \sum_\nu a_\nu \left(\|\mathcal{X}^\nu \gg e^{-i\omega_\nu^{(0)}t} + \|\mathcal{X}^{\nu\dagger} \gg e^{i\omega_\nu^{(0)}t} \right) \quad , \tag{3.74}$$

where the a_ν are free parameters. If we are looking for periodic solutions we can only mix commensurable frequencies. The equations for $\rho^{(n)}$ are RPA equations containing source terms generated by products of lower order terms which might be resonant. The requirement that no resonance are present in the source terms leads to the equations for the $\omega^{(n-1)}$. When this condition is fulfilled the equations for $\rho^{(n)}$ can be solved. The above procedure can be iterated in order to find all the the frequencies $\omega^{(n)}$ requiring that no resonant terms appear in the equation of evolution of $\rho^{(n+1)}$. The last step is to calculate the action on a given trajectory and to apply a quantization rule in order to define the deformation parameter ε.(see appendix 5.5) This procedure gives corrections to the one phonon state frequency ω_1 and also to the two phonon states ω_2. In realistic calculations, one needs to introduce the angular momentum. In refs. [Ab91, Ab92, Ab92] an ansatz is proposed in analogy with the idea of the projection onto a good angular momentum.

^{16}O				^{40}Ca			
J^π	$\omega^{(2)}$	E^*	δE	J^π	$\omega^{(2)}$	E^*	δE
0^+	362.4	13.793	1.683	0^+	421.2	10.134	2.134
2^+	260.7	13.251	1.141	2^+	121.2	8.516	0.516
4^+	−19.9	12.031	−.079	4^+	−16.1	7.936	−.064
6^+	−63.5	11.861	−.249	6^+	20.9	8.085	0.085

Table 3.2 Periodic TDHF Results. From ref. [Ab92], two-octupole-phonon states in ^{16}O and ^{40}Ca. For each state are reported its spin and parity, $\omega^{(2)}$ in keV, the excitation energy E^* in MeV and the shift δE (in MeV) with respect to the unperturbed energy $\omega^{(0)}$.

Table (3.2) gives the excitation energies of the two-phonon states built with the octupole low-lying collective states in ^{16}O and ^{40}Ca. For ^{16}O, $\hbar\omega_{3^-}^{(2)} = 0.547MeV$ and the quantization gives $E_1^* = 6.666MeV$ and $E_2^* = 14.78$. The anharmonicity defined by $A_n = \varepsilon_n^2\omega^{(2)}/\omega$, is equal to 9% for the first state and 18% for the second state when the angular momentum is not introduced and a splitting of 2 MeV is predicted using the projection ansatz. For the ^{40}Ca, $\hbar\omega^{(2)} = 0.547MeV$ so that $E_1^* = 4.63MeV$ and $E_2^* = 11MeV$ when no projection is applied.

Ref. [Ab92] also presents results for the quadrupole state in ^{40}Ca . In this case, it appears that a non-collective state is very close to the excitation energy of the two-phonon state. This case can be included in the formalism by introducing the resonant state in $\rho^{(1)}$. This coupling gives a first-order correction to ω which yields a very small splitting of the two phonon states of about 1 MeV.

To conclude on the use of periodic orbits, we may say that it is a very promising and powerful method. However, many questions remain open and so there is still a lot of work to be done. In particular, the projection onto a good angular momentum is not justified: there is no reason to associate the order of the perturbative expansion to the number of phonons n. Indeed, if we are interested in 3-phonon states, the angular momenta can be coupled to λ_3 between 0 and 3λ. We expect that the second order $\omega^{(2)}$ will give corrections to all the 3-phonon states, but if we use the projection assumption we realize that $\omega^{(2)}$ does not contribute for the 3-phonon states of λ_3 greater than 2λ. For these states, only the third order will contribute, which is somewhat peculiar. This remark is related to the problem of coupling different states, which has not yet been studied . The last question arises from the fact that the presented methods are based on the mean-field approach. This may induce specific features or limitations which have not yet been investigated. In particular, one may want to investigate the dynamics of density matrices containing correlations, e.g. $D = \exp(0^{(1)} + 0^{(2)})$, where $0^{(1)}$ is a one-body operator and $0^{(2)}$ is a two-body operator. This approach will yield some extended TDHF approximation which will exhibit a variety of periodic orbits which can be different from the trajectories found in the mean-field approach.

The present method naturally extends previously described approaches such as the RPA and it correctly treats the Pauli exclusion principle. In the next section, we will present the boson expansion method which is supposed to be a fully quantum approach. However, the present classical approach raises questions about the dynamics of the nucleus vibrations described as non-linear oscillators. For example, it is known in classical mechanics that the response of an

anharmonic oscillator exhibits new phenomena. In particular, around a resonance ω_0, the response is different from the linear case because it depends on the strength of the external perturbation [La69].

For example, let us consider the classical non linear damped oscillation of an oscillator with an equation of motion

$$\ddot{x} + 2\lambda\dot{x} + \omega^{(0)^2}x = -\alpha x^2 - \beta x^3 + \frac{f}{m}\cos\omega_f t \quad . \tag{3.75}$$

We can see that the resonance frequency is given by $\omega(b) = \omega^{(0)} + \omega^{(2)}b^2$, where b^2 is the amplitude of the oscillation and $\omega^{(2)}$ is given by $\omega^{(2)} = (3\beta/\delta\omega_{(0)} - 5\alpha^2/12\omega^{(0)^3})$. The amplitude of the forced motion is given by the equation

$$b^2\left((\omega_f - \omega(b))^2 + \lambda^2\right) = \frac{f^2}{4m^2\omega^{(0)^2}} \quad , \tag{3.76}$$

so that the resonance looks like the schematic picture shown on Fig.(10) For a very small perturbation f we recover

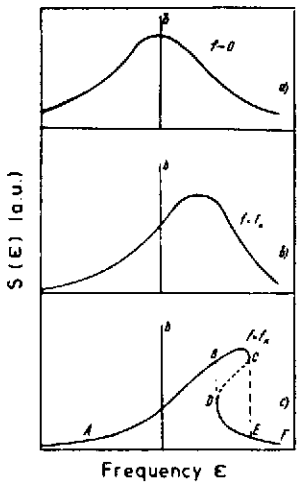

Figure 10 Classical Response : Schematic drawing of the non-linear response for increasing perturbation strength f showing a transition from a linear regime ($f \longrightarrow 0$) to a critical behavior $f > f_k$, (from top to bottom).

the usual response but when f increases the response is deformed up to a critical value

$$f_k^2 = \frac{32m^2\omega^{(0)^2}\lambda^3}{3\sqrt{3}|\omega^{(2)}|} \quad , \tag{3.77}$$

after which the strength exhibits regions with two stable and one unstable solutions. In the nuclear case we get a critical perturbation :

$$|\ll \mathcal{X}^{\nu}||F_k \gg|^2 = \frac{8\Gamma^3}{3\sqrt{3}|\omega^{(2)}|} \quad , \tag{3.78}$$

where Γ is the width of the state ν and $\omega^{(2)}$ the quadratic correction to the frequency.

In conclusion, strong fields may generate a critical behavior for the response function. Other resonances, critical or not critical, can be observed for frequencies around $n\omega_0/m$. These non-linear features may also be important because we may excite a resonance at the energy ω with an external field which does not contain components at this frequency but only components at lower frequencies $\omega_0/2$ or $\omega_0/3$. This may, for example, be the case for Coulomb excitation at low incident energy, which presents a cut off at high energy response. However, the anharmonic oscillation need to be studied further. In particular the discussed properties are observed in classical mechanics and may be different when quantum mechanics is applied.

3.2.7 An Example the Lipkin model

Let me first illustrate this method on a simple model: the Lipkin model. In this model two levels containing states labelled by the quantum number , can be occupied by particles. [?]

3.2.7.1 The Hamiltonian

The energy difference between the two levels is ϵ. The operator $a^{\dagger}_{\sigma,n}$ ($a_{\sigma,n}$) creates (annihilates) a particle on the level with the energy $E = \sigma\epsilon/2$ with $\sigma = \mp 1$ at the position n. Since each particle n can only occupied two levels we can

describe it in analogy with the spin 1/2 which is called pseudo-spin. The algebra

$$\begin{aligned} K_0 &= \frac{1}{2}\sum_{m=1}^{\Omega}(a^\dagger_{+,m}a_{+,m} - a^\dagger_{-,m}a_{-,m}) \\ K_+ &= \sum_{m=1}^{\Omega} a^\dagger_{+,m}a_{-,m} \\ K_- &= (K_+)^\dagger = \sum_{m=1}^{\Omega} a^\dagger_{-,m}a_{+,m} \end{aligned} \tag{3.79}$$

does correspond to pseudo-spin operators which fulfils the standard SU(2) commutation algebra

$$[K_+, K_-] = 2K_0 \;\; [K_0, K_\pm] = \pm K_\pm \tag{3.80}$$

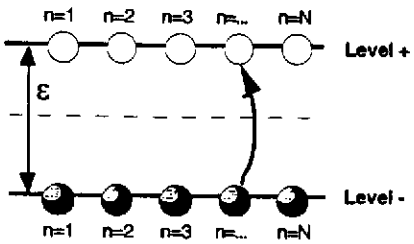

Figure 11 Schematic representation of the Lipkin model in which two levels with N available cites can be occupied by N particles. is the energy distance between the two levels.

We introduce a residual interaction between the various particles in such a way that the Hamiltonian reads

$$H_{LMG} = \epsilon K_0 + V_1 K_x^2 \tag{3.81}$$

where

$$K_x = \frac{K_+ + K_-}{2} \tag{3.82}$$

Looking at the form of the residual interaction we can see that it can only generate jumps from the lower level to the upper one or vis versa without changing the quantum number.

3.2.7.2 The Hilbert space

The model we are considering thus reduces to the known problem of N coupled spin. Therefore the Hilbert space can be decomposed into irreducible subspaces with a good total pseudo-spin. The state in which all the particles occupied the lower level pertain to the unique subspace associated with the maximum pseudo-spin $J = N/2$.We note this state $|J, -J\rangle$ while the other members of the considered multiplet are $|J, M\rangle$. It should be noticed that since the Hamiltonian is completely written in terms of the pseudo-spin operators the Hamiltonian does not couple subspace with different total pseudo-spin.

In each subspace all the operators can be computed using the pseudo-spin properties

$$\begin{aligned} K_\pm |J, M\rangle &= \sqrt{J(J+1) \pm M(M+1)}\,|J, M \pm 1\rangle \\ K_0 |J, M\rangle &= M\,|J, M\rangle \end{aligned} \tag{3.83}$$

Therefore this model can be easily exactly solved.

If we neglect the residual interaction, the ground state of the system is naturally $|J, -J\rangle$ which energy is nothing but $-\epsilon N/2$. In this state all the particles are occupying the lowest accessible orbital. This is the analogous of the Hartree-Fock ground state. In the following we will use this state to construct the TDHF coherent states.

3.2.7.3 Coherent states of SU(2)

For this model the coherent states are naturally provided by the application of a SU(2) unitary transformation on the Hartree-Fock ground state which is equivalent to the rotation group. Therefore the parameters are nothing but the

rotation angles. In the present case using the Euler angles we can define the Slater $|\psi(t)>$, through a rotation of the HF groundstate par rotation de ,

$$|\psi(Z(t))) = \hat{R}(Z(t))\,|0\rangle = e^{-i\alpha(t)K_0}e^{-i\beta(t)K_y}e^{-i\gamma(t)K_0}\,|0\rangle \tag{3.84}$$

where $Z = (\alpha, \beta, \gamma)$ are the Euler angles and $K_y = (K_+ + K_-)/2i$. If we assume that $|0\rangle = |J, -J)$ then the rotation of the angle γ only modify the phase and so can be omitted. Then the parameters of the coherent state are only the two Euler angles $Z = (\alpha, \beta)$

To evaluate expectation values over the state $|\psi(Z(t)))} = \hat{R}(Z(t))\,|0\rangle$ of any operator $\hat{D}$ it is often convenient to introduce the inverse transformation of $\hat{D}$:

$$\hat{D}(Z(t)) = \hat{R}^{\dagger}(Z(t))\;\hat{D}\;\hat{R}(Z(t)) \tag{3.85}$$

so that the relation

$$< \hat{D} > (t) = \langle\psi(Z(t))|\,\hat{D}\,|\psi(Z(t))\rangle = \langle 0|\,\hat{D}(Z(t))\,|0\rangle \tag{3.86}$$

In particular we only need to transform the operators $\hat{K}$. Since $\hat{K}$ is a vector a simple geometrical analysis shows that

$$\left\{\begin{pmatrix} K_x(Z) \\ K_y(Z) \\ K_z(Z) \end{pmatrix} = \begin{pmatrix} \cos\alpha\cos\beta & -\sin\alpha & \cos\alpha\sin\beta \\ \sin\alpha\cos\beta & \cos\alpha & \sin\alpha\sin\beta \\ -\sin\beta & 0 & \cos\beta \end{pmatrix}\begin{pmatrix} K_x \\ K_y \\ K_z \end{pmatrix}\right. \tag{3.87}$$

Therefore it is easy to compute as

$$\left\{\begin{pmatrix} < K_x > \\ < K_y > \\ < K_z > \end{pmatrix} = \begin{pmatrix} \langle 0|\,K_x(Z)\,|0\rangle \\ \langle 0|\,K_y(Z)\,|0\rangle \\ \langle 0|\,K_z(Z)\,|0\rangle \end{pmatrix} = -J\begin{pmatrix} \cos\alpha\sin\beta \\ \sin\alpha\sin\beta \\ \cos\beta \end{pmatrix}\right. \tag{3.88}$$

These three relations gives the correspondence between $< K >$ and the Euler parameters $Z = (\alpha, \beta)$. It should be noticed that the $< K >$ is a vector of norm J therefore only two angles are needed to define it completely.

3.2.7.4 Mean- eldsolution

Now we can study the dynamics of the system assuming that the wave functions are restricted to coherent states $|\psi(Z(t)))$. The evolution of the $Z = (\alpha, \beta)$ or of the averaged value $< K >$ are obtained using the generalized Ehrenfest equation

$$i\frac{\partial}{\partial t} < A >= - < [H, A] > \tag{3.89}$$

where all the averages are evaluated over the coherent state$|\psi(Z(t)))$

$$\left\{\begin{pmatrix} i\frac{\partial}{\partial t} < K_x > \\ i\frac{\partial}{\partial t} < K_y > \\ i\frac{\partial}{\partial t} < K_z > \end{pmatrix} = \begin{pmatrix} \langle [K_x, H]\rangle \\ \langle [K_y, H]\rangle \\ \langle [K_z, H]\rangle \end{pmatrix} = i\begin{pmatrix} \epsilon < K_y > \\ \epsilon < K_x > -V < K_xK_z + K_zK_x > \\ V < K_xK_y + K_yK_x > \end{pmatrix}\right. \tag{3.90}$$

Using the transformation 3.85 we can evaluate the contributions due to the residual interaction using the relations

$$< \quad K_xK_z + K_zK_x >= \left(2 - \frac{1}{J}\right) < K_x >< K_z > \tag{3.91}$$

$$< \quad K_xK_y + K_yK_x >= \left(2 - \frac{1}{J}\right) < K_x >< K_y > \tag{3.92}$$

which leads to the following mean field equations

$$\left\{\begin{pmatrix} \frac{\partial}{\partial t} < K_x > \\ \frac{\partial}{\partial t} < K_y > \\ \frac{\partial}{\partial t} < K_z > \end{pmatrix} = \begin{pmatrix} \epsilon < K_y > \\ \epsilon < K_x > -V\left(2 - \frac{1}{J}\right) < K_x >< K_z > \\ V\left(2 - \frac{1}{J}\right) < K_x >< K_y > \end{pmatrix}\right. \tag{3.93}$$

These equations are highly non linear because the expectation values of two-body terms coming from the residual two-body interaction have been approximated by products of average values of one-body operators (i.e. $< K >$). We can try to analyze the small amplitude oscillations around the HF ground state ($< K >= (0, 0, -J)$) but in principle the corresponding dynamics could present characteristic behaviors of non-linear systems such as chaos. However, in the simple case studied here if the Hamiltonian is not time dependent the system possesses two constants of motion (the energy and the norm $|< K >|^2$) and only three degrees of freedom .Therefore in this special case the mean-field equation of motion are integrable and so the mean-field dynamics will always be regular and will present oscillations with a basic frequency and all its multiples.

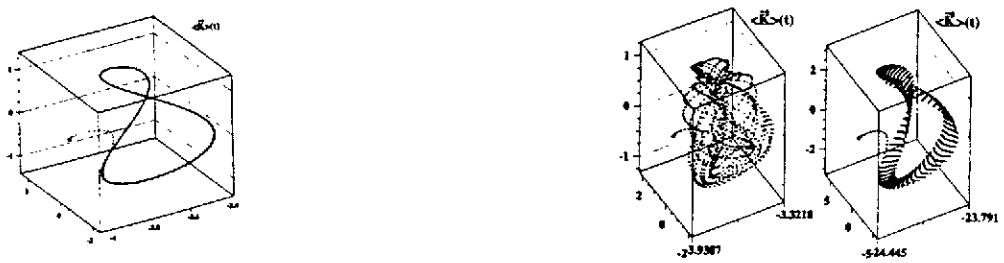

Figure 12 This figure presents the time evolution of the vector $< K >$ after a short excitation with an operator $W(t)K_x$. The left part corresponds to the mean field solution while the two diagrams on the right correspond to the exact dynamics with two different total number N.

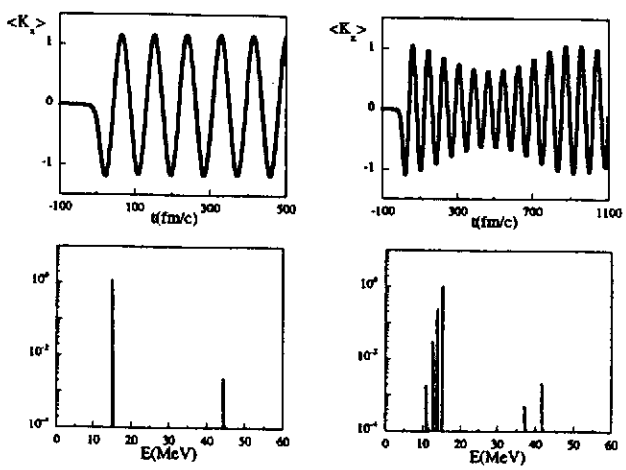

Figure 13 Time evolution of $< K_x >$ and its Fourier analysis after a time greater then the excitation time. The left part is the TDHF result while the right part is the exact dynamics.

3.2.7.5 Small amplitude response

In figure 12 and 13 we present the evolution of the Lipkin model after a short excitation with an operator $W(t)\,K_x$. One can see that, after the transient period when a time dependent external field $W(t)$ is applied, the mean-field approach is rather smooth (it is in fact regular) and present oscillations which resemble the exact dynamics. Indeed, the frequency of the collective mode appears to be close from the exact frequencies directly related to the diagonalization of the Schrödinger equation.

However, TDHF approach fails to reproduce the details of the exact trajectory. Indeed, when going from the quantum mechanics to the mean field approach we have replace the average value of two body operators such as by essentially the simple product of two average values. This means that we have disregarded the quantum fluctuations and correlations. In the complete dynamics these quantum terms are introducing fluctuations around the mean field trajectory in such a way that the mean-field trajectory remains close to the exact one only during a finite time.

This illustrates the fact that in mean field approaches we always have only a partial knowledge of the system. Indeed except for some algebraic models the complete description of the system would require an enormous ensemble of expectation values while we have seen that the system is often described through a small subensemble of expectation values of few operators (in the present case the $\hat{K}'s$). Therefore, in general we are forced to go beyond mean-field.

3.2.8 Discussion

In this section we have presented various microscopic many body theories based on extensions of the mean-field concepts. We have shown that these theories provide well-founded approaches to describe the properties of giant resonances and multiphonons. The RPA can be considered as a first step in our understanding of collective vibrations. However, the RPA is by essence a harmonic approximation and therefore we have discussed more elaborate approaches to study the properties of multiphonon states. Formally, the method presented may yield a very accurate description of the collective vibrations. In particular, the Generator Coordinate Method may in principle give an exact solution of the many-body problem. However, the general solutions of the presented extensions of the mean-field are untractable because they require the coupling of too many degrees of freedom. In fact all the results presented have been obtained considering very few collective coordinates. This fact can be considered as a general drawback of the methods presented

because not only is the choice of the collective coordinates somewhat arbitrary but very few collective degrees of freedom can be actually coupled.

We have presented the results of several calculations in which few collective vibrations are considered. Despite the diversity of the methods and approximations all the different results advocate a quasi-harmonic picture of giant resonances.

3.3 Boson Expansion Methods

We have discussed in the beginning of the present chapter that the collective motions of the nucleus associated with the excitation of giant resonances can be understood in terms of vibrations. This promotes the idea that the excitations of a many-fermion system can be described in terms of boson degrees of freedom. In fact, this idea is underlying numerous approximations such as phonons in solids or in nuclei, plasmons, Cooper pairs, ^4He atoms ..... Indeed the excitations of an even number of fermions carry the quantum numbers of a boson. As an example we will recall how the RPA can be recovered starting from a quasi-boson approximation for the particle-hole excitations. We will use these new concepts to extend the formalism to include the 2particle-2hole states and we will see that this so-called second-RPA allows to predict the width of giant resonances.

As far as the multiple excitations are concerned we clearly need to go beyond the RPA and the quasi boson approximation [Dy56, Us60, Be62, Ma64, Pr68, Ma71, Ha72, Sc73, Ma74, Bo75, Ma76, Bl78, Ma80, Ma80a, Ri81, Ia87, Bo88, Ca89, Be92, Ca94]. This problem finds a natural solution in the boson mapping methods which are mathematical connections between fermion pairs and bosons.

In this section, we will present different methods involving boson representations and indicate how they can be used to study the properties of multiphonon states. In particular, we will show how a harmonic approximation to the excitation spectrum of the many fermion system can be variationally defined. Treating the residual interaction between phonons will allow to predict anharmonicities. We will also discuss how the transition amplitudes can be obtained and how they may exhibit non-linear features.

3.3.1 Quasi Boson Approximation

Let us first recall how the RPA approximation discussed in the previous sections is equivalent to the simple approximation that a fermion pair can be considered as a boson. Let us consider the Hamiltonian H_f of a fermionic system (e.g. a nucleus) with a two-body interaction V (c.f. Eq. (3.21)):

$$H_f = \sum_{ij} \epsilon_i a_i^\dagger a_i + \frac{1}{4} \sum V_{ij,k\ell} a_i^\dagger a_j^\dagger a_\ell a_k \ , \tag{3.94}$$

This Hamiltonian can be expressed in the particle-hole representation defined by the static Hartree-Fock solution [Ri81].

The RPA equations can be obtained assuming that the fermion pair operators behave as bosons. Therefore we can introduce boson degrees of freedom through the mapping:

$$a_p^\dagger a_h \longrightarrow b_{ph}^\dagger \ . \tag{3.95}$$

It can be seen that the Hamiltonian is expressed as a quadratic form in the boson field:

$$H_b = E_{HF} + \sum_{\alpha,\alpha'} \left(A_{\alpha,\alpha'} b_\alpha^\dagger b_{\alpha'} + \frac{1}{2} (B_{\alpha,\alpha'} b_\alpha^\dagger b_{\alpha'}^\dagger + h.c.) \right) \tag{3.96}$$

$$H_b = E_{HF} + \frac{1}{2} \sum_{\alpha,\alpha'} A_{\alpha,\alpha'} + \frac{1}{2} \begin{pmatrix} b^\dagger & b \end{pmatrix} \begin{pmatrix} A & B \\ B^* & A^* \end{pmatrix} \begin{pmatrix} b \\ b^\dagger \end{pmatrix} \ , \tag{3.97}$$

where we have used the label α instead of the pair indices (p,h). The coefficients A and B can be easily obtained from the calculations of the commutators of b and H:

$$A_{\alpha\alpha'} = < 0 | [b_\alpha, [H_b, b_{\alpha'}^\dagger]] | 0 > = < HF | [a_h^\dagger a_p, [H_f, a_{p'}^\dagger a_{h'}]] | HF > \tag{3.98}$$

$$-B_{\alpha\alpha'} = < 0 | [b_\alpha, [H_b, b_{\alpha'}]] | 0 > = < HF | [a_h^\dagger a_p, [H_f, a_{h'}^\dagger a_{p'}]] | HF > \ . \tag{3.99}$$

The Hamiltonian (3.96) is nothing but the Hamiltonian of coupled harmonic oscillators which can be diagonalized as

$$H_b = E_{RPA} + \sum_\nu \omega_\nu O_\nu^\dagger O_\nu \ , \tag{3.100}$$

by introducing new bosons O_ν defined by the Bogoliubov transformation::

$$O_\nu^\dagger = \sum_\alpha X_\alpha^\nu b_\alpha^\dagger - Y_\alpha^\nu b_\alpha \ . \tag{3.101}$$

The coefficients of the transformation, X^ν and Y^ν, and the energy, ω_ν. are obtained by solving the RPA equations (equivalent to Eq. (3.56)):

$$\begin{pmatrix} A & B \\ B^* & A^* \end{pmatrix} \begin{pmatrix} X^\nu \\ Y^\nu \end{pmatrix} = \omega_\nu \begin{pmatrix} X^\nu \\ -Y^\nu \end{pmatrix} \quad . \tag{3.102}$$

The above derivation of the RPA demonstrates that this approximation is deeply connected with a description of the considered fermion system in terms of independent bosons. Therefore, it predicts a harmonic vibration spectrum with regularly spaced multiphonon states. As stated in the previous sections, the study of anharmonicities, non-linearities and interactions between phonons implies going beyond the RPA, i.e. beyond the quasi-boson approximation. In the next section we will mainly discuss two different methods which have been followed in the literature to achieve this goal. The first one is to extend the configuration space to two-particle two-hole excitations. This approach, called the second-RPA, should in principle describe one- and two- phonon states. Indeed, it is equivalent to the diagonalization of the total Hamiltonian in the subspace containing one and two phonon states. The second method is in principle more general because it uses a mathematical correspondence between fermion and boson dynamics. Therefore, its only limitation should be given by our ability to solve the eigenvalue problem in the boson space. However we will see that in practical calculation one must face the problem of truncating the infinite boson expansion and of the resulting possible contamination from spurious states, the boson states which does not pertain to the image of the fermion space induced by its boson mapping.

3.3.2 Second RPA Equation

An interesting extension of the RPA formalism is to include more complicated states in the boson definition (3.101). In particular one may consider the coupling with 2p-2h states.

Considering the 1p-1h and 2p-2h excitation as bosons and performing the Bogoliubov transformation

$$\begin{aligned} O^\dagger_\nu &= \textstyle\sum_{ph} X^\nu_{ph} a^\dagger_p a_h - Y^\nu_{ph} a^\dagger_h a_p \\ &+ \textstyle\sum_{p<p',h<h} X^\nu_{pp'hh'} a^\dagger_p a^\dagger_{p'} a_{h'} a_h - Y^\nu_{ph} a^\dagger_h a^\dagger_{h'} a_{p'} a_p \end{aligned} \tag{3.103}$$

yield the so- called second RPA equations [Su61, Pr65, Sa62, La64, Ya83, Dr86, Sp91]:

$$\begin{pmatrix} \mathcal{A} & \mathcal{B} \\ \mathcal{B}^* & \mathcal{A}^* \end{pmatrix} \begin{pmatrix} \mathcal{X}^\nu \\ \mathcal{Y}^\nu \end{pmatrix} = \omega_\nu \begin{pmatrix} \mathcal{X}^\nu \\ -\mathcal{Y}^\nu \end{pmatrix} \quad , \tag{3.104}$$

where the $\mathcal{X}$ and $\mathcal{Y}$ are the vectors containing the 1p-1h and 2p-2h components while the $\mathcal{A}$ and $\mathcal{B}$ are generalization of the A and B RPA matrices. These matrices couple 1p-1h and 2p-2h bosons. Their elements are obtained as the expectation value of double commutators analogous to the definitions (3.98) and (3.98) extended to include also the 2p-2h bosons.

It is often assumed that the coupling with the 2p-2h states is weak so that 1p-1h phonons can be seen as doorway states which decay into more complicated excitations. In this way the RPA (single) phonons get a spreading width when they are computed in the second RPA scheme. This width can be obtained by projecting out the 2p-2h states from the second-RPA equation (3.104). Since the $\mathcal{B}$ matrix does not couple to the 2p-2h bosons either to the 1p-1h or to the 2p-2h ones, the only effect of the projection is that the RPA matrix A becomes a complex, energy-dependent, matrix. Therefore, the RPA energies get an imaginary part, a spreading width. This width physically represents the decay of the phonons into 2p-2h configurations.

Figure 14 presents an example of such second-RPA calculations. It can be seen that the main effect of the

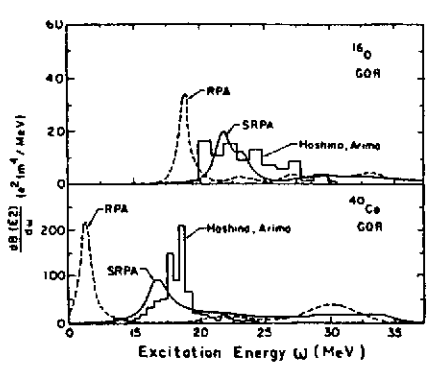

Figure 14 Second-RPA GQR Strength Function : The $B(E_2)$-strength distributions in ^{16}O and ^{40}Ca nuclei obtained solving the exact second-RPA equations (histograms) from ref. [Ho76] are compared with the RPA (dashed lines) and uncorrelated 2p-2h second-RPA (Solid lines) calculations of ref [Dr86]. This figure is extracted from ref. [Sp91].

introduction of the 2p-2h configurations is to shift the giant resonance peak and to introduce a width which is comparable to the experimental spreading width.

It should be noticed that the second-RPA can be still considered as a quasi-boson approximation and so the eigenstates can be viewed as independent bosons. Therefore the multiple excitation strength is given by the same equations (3.59) or (3.60) as in the RPA case [Ya85] .

If a complete diagonalization of Eq. 3.104 is performed in the full 1p-1h and 2p-2h configuration space one can, in principle, describe one and two phonon states. Unfortunately, no systematic study of this type has been performed yet. However, one may worry about the fact that the above approach is implicitly built on a quasi-boson approximation and may, therefore, lead to some violation of the Pauli principle. Moreover, in second-RPA approach the two phonon states can be obtained in two different manners, either as a double excitation of a 1p-1h phonon or as a single excitation of a 2p-2h vibration. This may also lead to double counting and to violations of the Pauli principle.

3.3.3 Boson Mapping

As just mentioned, the quasi-boson approaches give rise to several questions concerning the violation of the Pauli principle and the residual interaction between phonons. These questions have found natural answers, at least in principle, in the mathematical developments of exact mapping $\mathcal{M}$ between fermion and boson systems [Dy56, Us60, Be62, Ma64, Pr68, Ma71, Ha72, Sc73, Ma74, Bo75, Ma76, Bl78, Ma80, Ma80a, Ri81, Ia87, Bo88, Ca89, Be92, Ca94].

Indeed, using a boson mapping, the problem reduces to the diagonalization of a Hamiltonian of bosons which can explicitly be achieved using a multiphonon basis. Moreover, the boson mapping approaches are supposed to correctly treat the Pauli blocking effects and allows the derivation of a residual interaction between phonons.

The explicit construction of $\mathcal{M}$ can be done in many ways, either conserving the commutation properties of the mapped observables (Beliaev-Zelevinsky type [Be62, Ma71, Ma74, Ma76, Ma80, Ma80a, Ri81]), or mapping first the states and then deriving the operators through the conservation of their matrix elements (Marumori type [Ma64, Ma71, Ma74, Ma76, Ot78, Ma80, Ma80a, Ri81]) or using the Generator Coordinate Method (Lambert type [Ha72, Ri81, Be92]).

Let us take the latter type as an example since the Generator Coordinate Method can be also used to discuss multiphonon excitations and anharmonicities. In the GCM method the wave functions of the fermionic system are expanded on the basis of Slater determinants $|\Phi(Q)>$ associated with a value Q of some generating coordinate:

$$|\Psi>=\int dQ f(Q)|\Phi(Q)> \quad . \tag{3.105}$$

Therefore, the many-fermion dynamics are mapped onto the evolution of the complex function f which is equivalent to the Bargmann representation of a boson field problem[Ba62]. In ref. [Ha72], this analogy is used to derive a mapping of the p-h degrees of freedom:

$$a_h^\dagger a_p \xrightarrow{\mathcal{M}} (a_h^\dagger a_p)_b = b_{ph} + (1-\sqrt{2})\sum_{p'h'} b^\dagger_{p'h'} b_{p'h} b_{ph'} + \ldots \tag{3.106}$$

and

$$\begin{aligned} a_p^\dagger a_{p'} &\xrightarrow{\mathcal{M}} (a_p^\dagger a_{p'})_b = \textstyle\sum_h b^\dagger_{ph} b_{p'h} \\ a_h a_{h'}^\dagger &\xrightarrow{\mathcal{M}} (a_h a_{h'}^\dagger)_b = \textstyle\sum_p b^\dagger_{ph} b_{ph'} \end{aligned} \quad . \tag{3.107}$$

We can see that the quasi-boson approximation corresponds to the first terms of theses expansions, namely, the first term of eq. (3.107). The remaining terms in the infinite expansion (3.107) are due to the Pauli principle.

An example of the corresponding Hamiltonian in the boson space can be found in appendix 5.6. In the following we will use the short hand notation[4]:

$$H_f \xrightarrow{\mathcal{M}} H_b = \sum_{\substack{m \\ n}} :^m_n H^{\alpha_1 \ldots \alpha_m}_{\alpha'_1 \ldots \alpha'_n} b^\dagger_{\alpha_1} \ldots b^\dagger_{\alpha_m} \ldots b_{\alpha'_1} \ldots b_{\alpha'_n} \quad . \tag{3.108}$$

These mappings connect the fermion Hilbert space to a boson space which can be built from its vacuum $|\phi_b\succ$ by applying the boson creation operators so that any fermion state is associated with a boson state:

$$|\nu_f> \xrightarrow{\mathcal{M}} |\nu_b\succ \quad . \tag{3.109}$$

where the curved brackets represent states in the boson space. However it should be noted that, because of the antisymmetrization principle of the fermion states, the fermion space is mapped onto a subspace of the boson space. The image of the fermion world is called the physical space because all the computed quantities are meaningful only inside this space, the remaining part of the boson space being spurious. The existence of these spurious states may yield some difficulties and we refer the reader to the literature for a further discussion of this problem [Ma71, Ma74, Ma76, Ma80, Ma80a, Ri81, Bo88, Be92].

[4] In this equation the Hamiltonian is written in normal order with respect to the boson vacuum. However, all the discussed applications can be easily generalized to handle expansions which are not normally ordered.

3.3.4 A Non-Linear RPA

The boson mapping methods were used by several authors to extend the RPA. Here, we will present one of these approaches, which has been recently applied to the description of the multiple excitation of giant resonances. In ref. [Ca89, Be92, Ca94], it is proposed to use a variational principle in order to determine a harmonic approximation of H_b . This harmonic approximation will define a natural basis of the boson Fock space on which it will be convenient to compute the excitation spectrum and to derive properties such as anharmonicities.

Let us first introduce a set of bosons O by means of the generalized Bogoliubov transformation defined by [Ri81]:

$$\begin{pmatrix} b_\alpha \\ b^\dagger_\alpha \end{pmatrix} = \begin{pmatrix} X^\nu_\alpha & Y^{\nu^*}_\alpha \\ Y^\nu_\alpha & X^{\nu^*}_\alpha \end{pmatrix} \begin{pmatrix} O_\nu \\ O^\dagger_\nu \end{pmatrix} + \begin{pmatrix} \gamma^*_\alpha \\ \gamma_\alpha \end{pmatrix} \quad . \tag{3.110}$$

The vacuum $|\phi_O \succ$ belonging to the new bosons O (defined by $O|\phi_O \succ = 0$) can be related to the vacuum $|\phi_b \succ$ of the b bosons by the Thouless theorem for bosons (see appendix E of ref. [Ri81] for more details)[5]:

$$|\phi_O \succ = \exp\left(\sum_\alpha {}^1Z_\alpha b^\dagger_\alpha + \sum_{\alpha \le \alpha'} {}^2Z_{\alpha\alpha'} b^\dagger_\alpha b^\dagger_{\alpha'} \right) |\phi_b \succ \quad . \tag{3.111}$$

By assuming that the vacuum $|\phi_O \succ$ minimizes the energy $\prec \phi_0|H_b|\phi_0 \succ$ (with respect to the variational parameters ${}^1Z$ and ${}^2Z$) and by considering small variations around this vacuum we can easily demonstrate [Be92] that the minimum energy condition implies:

$${}^1_0H_\nu \equiv \prec \phi_O| \ [O_\nu, H_b] \ |\phi_O \succ = 0 \tag{3.112}$$

$${}^2_0H^{\nu\nu'} \equiv - \prec \phi_O| \ [O_\nu, [H_b, O_{\nu'}]] \ |\phi_O \succ = 0 \quad , \tag{3.113}$$

Moreover we can simultaneously impose:

$${}^1_1H^\nu_{\nu'} \equiv \prec \phi_O| \ [O_\nu, [H_b, O^\dagger_{\nu'}]] \ |\phi_O \succ = \omega_\nu \delta_{\nu\nu'} \quad . \tag{3.114}$$

Equations (3.113-3.114) reduce to an RPA-like problem. Indeed, using the Bogoliubov transformation (3.110) these equations become:

$$\begin{pmatrix} A(\varrho,\kappa,\gamma) & B(\varrho,\kappa,\gamma) \\ B(\varrho,\kappa,\gamma)^* & A(\varrho,\kappa,\gamma)^* \end{pmatrix} \begin{pmatrix} X^\nu \\ Y^\nu \end{pmatrix} = \omega_\nu \begin{pmatrix} X^\nu \\ -Y^\nu \end{pmatrix} \quad , \tag{3.115}$$

where the matrices A and B are given by

$$\begin{aligned} A(\varrho,\kappa,\gamma)_{\alpha\alpha'} &= \prec \phi_O|[b_\alpha, [H_b, b^\dagger_{\alpha'}]]|\phi_O \succ \\ B(\varrho,\kappa,\gamma)_{\alpha\alpha'} &= - \prec \phi_O|[b_\alpha, [H_b, b_{\alpha'}]]|\phi_O \succ \end{aligned} \tag{3.116}$$

The A and B matrices can be expressed in terms of the mean field, γ, the normal boson density, ϱ and the anomalous boson density, κ, which are defined by:

$$\gamma_\alpha \equiv \prec b^\dagger_\alpha \succ \quad , \tag{3.117}$$

$$\varrho_{\alpha\alpha'} \equiv \prec T^\dagger_{\alpha'} T_\alpha \succ = \sum_\nu X^{\nu^*}_{\alpha'} X^\nu_\alpha \quad , \tag{3.118}$$

$$\kappa_{\alpha\alpha'} \equiv \prec T_{\alpha'} T_\alpha \succ = \sum_\nu Y^{\nu^*}_{\alpha'} X^\nu_\alpha \quad , \tag{3.119}$$

where T_α is the boson operator $T_\alpha = b_\alpha - \gamma^*_\alpha$.

The extended RPA equation, (3.115) is non-linear and is associated with a subsidiary condition for determining the shift γ, namely:

$$C_\alpha(\varrho,\kappa,\gamma) = \prec \phi_O|[H, b^\dagger_\alpha]|\phi_O \succ = 0 \quad . \tag{3.120}$$

Equation (3.120) corresponds to the minimization of the energy under the variations of γ: $C_\alpha(\varrho,\kappa,\gamma) = \partial \prec H \succ / \partial \gamma^*_\alpha = 0$. Since $\gamma_\alpha = \prec b^\dagger_\alpha \succ$ is related through the mapping to the one-body density $\prec a^\dagger_\mu a_\mu \succ$ in the fermion space Eq. (3.120) can be interpreted as a Hartree-Fock approximation for fermions. Therefore Eqs. (3.115) and (3.120) correspond to a non-linear RPA coupled to a self-consistent mean field approximation for fermions. When γ is non zero, the solution of Eq. (3.120) corresponds to a redefinition of the HF basis and in particular of the particle or hole states. In this case a better approximation would be to consider the mapping of quasi-particle (fermion) excitations defined within a Hartree-Fock-Bogoliubov calculation (for fermions).

[5] *It should be notice that the considered vacuum might contained a mixing of the physical and spurious states. Formally, since the boson Hamiltonian can be correctly projected on the physical subspace this is not a problem. Indeed, it is equivalent to consider a projected vacuum. However, if the Hamiltonian is not correctly projected on the physical subspace as it might be, for instance, the case when truncations of the infinite boson expansions are introduced, pollutions coming from the spurious components of the vacuum might be expected and must be controlled.*

Using the solution of Eqs. (3.115)and (3.120) H_b reads:

$$H_b = \prec H_b \succ + \sum_\nu \omega_\nu O^\dagger_\nu O_\nu + H_{res} \quad , \tag{3.121}$$

where H_{res} contains only terms of order higher than 3 in the bosons O. The two first terms of Eq.(3.121) define the Hamiltonian H_h corresponding to a variationally-defined harmonic approximation" i.e. $H_h = \prec H_b \succ + \sum_\nu \omega_\nu O^\dagger_\nu O_\nu$ The Hamiltonian H_{res} can be interpreted as a residual anharmonic coupling between phonons. The interaction between phonons originates in the terms of the fermionic force not included in the RPA treatment. It also contains terms which allow, in principle, to preserve the Pauli exclusion principle. The harmonic part of the Hamiltonian defines a multiphonon basis of the Fock space. This basis may be used to study the effects of the residual interaction between phonons, as discussed in the following.

For example, the residual interaction in the two phonon space can be obtained from:

$$\begin{aligned} &\prec \phi_O | O_{\nu_1} O_{\nu_2} : H_{res} : O^\dagger_{\nu_3} O^\dagger_{\nu_4} | \phi_O \succ \\ &\quad = \sum_{\alpha_1\alpha_2\alpha_3\alpha_4} {}^2_2 H^{\alpha_1\alpha_2}_{\alpha_3\alpha_4} \prec \phi_O | O_{\nu_1} O_{\nu_2} : T^\dagger_{\alpha_1} T^\dagger_{\alpha_2} T_{\alpha_3} T_{\alpha_4} : O^\dagger_{\nu_3} O^\dagger_{\nu_4} | \phi_O \succ \\ &\quad + \quad ({}^3_1 H^{\alpha_1\alpha_2\alpha_3}_{\alpha_4} \prec \phi_O | O_{\nu_1} O_{\nu_2} : T^\dagger_{\alpha_1} T^\dagger_{\alpha_2} T^\dagger_{\alpha_3} T_{\alpha_4} : O^\dagger_{\nu_3} O^\dagger_{\nu_4} | \phi_O \succ + h.c.) \\ &\qquad + \quad \ldots \end{aligned} \tag{3.122}$$

The strength of this interaction can be obtained using the Wick theorem and the contractions:

$$\prec \phi_O | T^\dagger_\alpha O^\dagger_\nu | \phi_O \succ = Y^\nu_\alpha \quad , \tag{3.123}$$

$$\prec \phi_O | T_\alpha O^\dagger_\nu | \phi_O \succ = X^\nu_\alpha \quad . \tag{3.124}$$

Eq.(3.122) can be used in realistic calculations to predict the anharmonicities in the two phonon space [Ca89].

3.3.5 Anharmonicities of two-phonon states

The above formalism has been used in realistic calculations to study the anharmonicities of the two phonon states in ^{40}Ca [Ca89]. The phonons were obtained solving the standard RPA equations. The calculation was performed using the Skyrme interaction SGII [Gi81]. The dominant RPA one-phonon states are given in table 3.3.

State	$J^\pi T$	$E(MeV)$	$\%EWSR$
GD_1	1^-1	16.978	12
GD_2	1^-1	19.569	18
GD_3	1^-1	23.105	12
GQ_1	2^+0	17.438	59
GQ_2	2^+0	18.321	18
LEO	3^-0	5.600	12
HEO	3^-0	34.251	13

Table 3.3 RPA Single Phonons : From ref. [Ca89], energies of the most collective dipole, quadrupole and octupole states in ^{40}Ca. In the last column the percentage of the energy-weighted sum rule is given.

The anharmonicities were computed by diagonalizing the residual interaction in a two-phonon subspace. Table 3.4 presents the results obtained for the positive parity states lying between 30 and 50 MeV of excitation energy.

From this study one can see that, as expected [Bo75], the giant resonances are good vibrators. The anharmonicities are found to be of the order of less than 1 MeV while the splitting of the different angular momenta never exceed 200 keV.

It should be noticed that the presented calculation does not include the giant dipole resonance in the charge-exchange channels. Indeed, as far as the isospin is a good quantum number, one expects to observe two multiplets of isospin T=0,2 split in 2 different spins $\lambda = 0$ or 2 and a (double) triplet of isospin and spin 1 as a result of the coupling of two T=1 S=1 bosons[6]. The fact that charge-exchange phonons may contribute to the wave function in the inelastic channel is illustrated in Fig. 15. This possibility is now under study, the previous formalism being valid for particles and holes of different charge [Ca94].

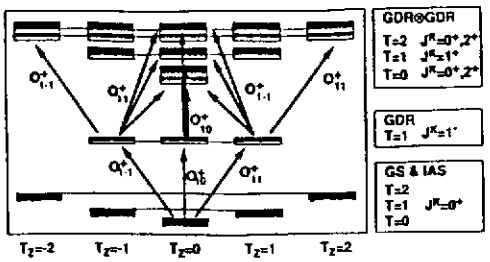

Figure 15 Coupling of Isovector Dipole Phonons : Pictorial representation of the possible coupling of phonons of isospin 1 and spin 1 (such as the GDR) in an N=Z nucleus. The figure shows that these couplings result in the creation of various spin and isospin multiplets.

3.3.7 Summary and discussion

In this section we have shown that the use of boson mapping methods allows a rather convenient description of multiphonon excitations. In particular, it gives a systematic approach to study the properties of phonons built from excitations of fermions. It provides a way to address general problems such as the effects of non-linear excitations or the effects of the Pauli principle. From the practical point of view it allows to study the coupling of a large number of collective vibrations. However, one must keep in mind that as soon as the infinite boson expansion is truncated there is no guarantee about the possible effects of the spurious states. Therefore, any numerical results must be considered with some caution and must be carefully checked. One possible check discussed in the literature is to compare the approximate solutions provided by the boson method with the exact solutions of solvable schematic models. It is shown in ref. [Be92] that the boson method discussed above gives a good description of the one- and two- phonon states. Another possibility is to estimate the corrections induced by the truncated terms of the boson expansion (introducing for example the next order terms in the boson expansion) as discussed in ref. [Be92].

In this section, we have discussed the first applications of the boson method. It has been demonstrated that multiple excitations of nuclear giant resonances are nearly harmonic. Anharmonicities and non-linearities are of the order of a few per-cent. It should be noticed that the same methods have been recently applied to study the multiple excitation of plasmons in metallic clusters. In that case the anharmonicities have been found to be strong, reaching one hundred percent[Ca93].

As far as the nuclear multiphonons are concerned, many studies remain to be done, such as the coupling of the double inelastic ($T_Z = 0$) isovector degrees of freedom with the double charge exchange channels in order to understand the various multiplets associated with the double excitation of the giant dipole resonance.

State	E_0(MeV)	J^π	ΔE	ΔE_0(keV)
$GD_1 * GD_1$	33.956	0^+	−60.0	−16.0
		2^+	−191.0	−175.0
$GQ_1 * GQ_1$	34.877	0^+	4.0	74.0
		2^+	136.0	230.0
		4^+	257.0	330.0
$GQ_1 * GQ_2$	35.761	0^+	268.0	518.0
		1^+	117.0	117.0
		2^+	315.0	569.0
		3^+	73.0	73.0
		4^+	351.0	570.0
$GD_1 * GD_2$	36.547	0^+	−373.0	−382.0
		1^+	−304.0	−298.0
		2^+	−228.0	−231.0
$GQ_2 * GQ_2$	36.644	0^+	431.0	114.0
		2^+	614.0	266.0
		4^+	649.0	358.0
$GD_2 * GD_2$	39.138	0^+	−9.0	130.0
		2^+	10.0	80.0
$LEO * HEO$	39.911	0^+	37.0	38.0
		1^+	85.0	84.0
		2^+	76.0	75.0
		3^+	96.0	96.0
		4^+	85.0	85.0
		5^+	124.0	124.0
		6^+	208.0	208.0
$GD_1 * GD_3$	40.084	0^+	−79.0	−179.0
		1^+	−231.0	−231.0
		2^+	−306.0	−334.0
$GD_2 * GD_3$	42.674	0^+	−421.0	−496.0
		1^+	−500.0	−506.0
		2^+	−358.0	−409.0
$GD_3 * GD_3$	46.211	0^+	−71.0	−74.0
		2^+	−76.0	−80.0

Table 3.4 Anharmonicity Calculations : From ref. [Ca89], for the positive parity two-phonon states between 30 and 50 MeV, the energy, in MeV and the anharmonicity in keV for all the possible total spin. The unperturbed (harmonic) energy, E_0, is presented together with the perturbative estimate of the anharmonicity, E_0, and the full diagonalization of the truncated residual interaction in the two phonon sub-space, E.

3.3.6 Non Linear Coupling

Another important feature of the boson mapping methods is the possibility to compute non-linearities in the excitation or deexcitation processes. The physical idea is that the particle-particle or hole-hole component of the external one-body perturbation will be mapped into the product of two boson operators (c.f. eq. (3.107)). These non-linear components in the external field may, for instance, induce direct transitions from the ground state to a two-phonon state. However, it should be noticed that these transitions are possible only via the correlated part (related to the Y amplitude) of the RPA phonons.

The study of the non-linear effects has been recently performed for the electromagnetic decay from high-lying two-phonon states in ^{40}Ca [Ca92]. The authors have found that the decay rate of the 1^- two- phonon states built with the GQR and the GDR is only 30 times smaller than the decay rate of the GDR itself (see table 3.5). Therefore, it might be observed experimentally.

The presented calculation, however, does not include the coupling between the one- and two- phonon states which may affect the results and therefore this investigation needs to be completed [Ca94].

Transitions	Decay	Transition rate (s^{-1})
dipole	GDR → g.s.	0.65×10^{18}
	GDR ⊗ GQR → g.s.	0.16×10^{17}
quadrupole	GQR → g.s.	0.60×10^{16}
	GDR ⊗ GDR → g.s.	0.90×10^{14}
	GQR ⊗ GQR → g.s.	0.26×10^{15}

Table 3.5 Transition Rates : From ref. [Ca92], dipole and quadrupole transition rates (in sec^{-1}) from one- and two-phonon states to the ground state.

Chapter 4 Conclusions and perspectives.

The properties of the nucleus cannot be reduced to the properties of its constituents: it is a complex system. The fact that many properties of the nucleus are consequences of the existence of mean-field potential is a manifestation of this complexity. In particular the nucleons can thus self-organize in collective motions such as giant resonances. Therefore the study of these collective motions is a very good tool to understand the properties of the nucleus itself. The purpose of this article was to stress some aspects of these collective vibrations.

In particular we have studied how an ensemble of fermions as the nucleus can self-organize in collective vibrations which are behaving like a gas of bosons in weak interaction. The understanding of these phenomena remains one of the important subjects of actuality in the context of quantal systems in strong interaction. In particular the study of the states with one or two vibration quanta provides a direct information on the structure if nuclei close to their ground states.

Moreover, some collective states appear to be very robust against the onset of chaos. This is the case of the hot giant dipole built on top of a hot nucleus which seems to survive up to rather high temperatures. Their sudden disappearance is still a subject of controversy. It may be that the mean-field and the associated collective states are playing a crucial role also in catastrophic processes such as the phase-transitions. Indeed, when the system is diluted the collective vibrations may become unstable and it seems that these unstable modes provide a natural explanation to the self organization of the system in drops. Finally, considering the diversity of the different structures of exotic nuclei one may expect new vibrations types.

All these studies are showing the diversity of the collective motions of strongly correlated quantum systems such as the nucleus but many open questions remain to be solved.

Chapter 5 Appendix

5.1 Variational formulation of Shrödinger equation.

If we now want to address the problem of the evolution of the system we will rather introduce a variational formulation of the Schrödinger equation

$$i\frac{\partial|\varphi\rangle}{\partial t} = W|\varphi\rangle \tag{5.1}$$

using an integral along a given trajectory $|\varphi(t)\rangle$

$$I[\phi,\phi^*] = \int_{t_0}^{t_1} \langle\varphi| i\frac{\partial}{\partial t} - W|\varphi\rangle\, dt \quad , \tag{5.2}$$

completed with a boundary condition defining the states of the system at t=t_0. The equivalence between the Schrödinger equation (5.1) and the variational expression (5.2) can be easily demonstrated. Indeed, let me first introduce a continuous or discrete basis of the Hilbert space: . Then (5.2) reads

$$I[\phi,\phi^*] = \int_{t_0}^{t_1} \sum_i \varphi_i^* \left(i\dot{\varphi}_i - \sum_j W_{ij}\varphi_j \right) dt \quad , \tag{5.3}$$

Since the coefficientsϕ_i^* are complex numbers we can either consider the variations of their real and imaginary parts independently or we can rather use ϕ^* and ϕ as two independent variables. Therefore, the requirement that the action is stationary when we add a small variation $\delta\phi^*$ to ϕ^* leads to

$$\delta I[\phi,\phi^*] = 0 = \int_{t_0}^{t_1} \sum_i \delta\varphi_i^* \left(i\dot{\varphi}_i - \sum_j W_{ij}\varphi_j \right) dt \quad , \tag{5.4}$$

If we apply no restriction on the wave functions this relation should hold for any variation $\delta\phi^*$ this implies that

$$0 = i\dot{\varphi}_i - \sum_j W_{ij}\varphi_j \tag{5.5}$$

which is nothing but the Schrödinger equation.

5.2 Variational Derivation of TDHF using density matrices

Among the many derivations of the TDHF equations, we will adopt the variational method presented in ref. [Ba84, Ba85a, Ba88]. Let us introduce the generalized action

$$I[\mathcal{D},\mathcal{A}] \equiv \mathrm{Tr}\mathcal{A}(t_1)\mathcal{D}(t_1) - \int_{t_0}^{t_1} dt \mathrm{Tr}\mathcal{A}(t)\left(\frac{d\mathcal{D}(t)}{dt} + i[H,\mathcal{D}(t)] \right) \quad , \tag{5.6}$$

where the variational parameters are the time dependent operators $\mathcal{D}(t)$ and $\mathcal{A}(t)$, respectively akin to a density operator and to an observable. The action (5.6) must be complemented with the boundary conditions: $\mathcal{D}(t_0) = D(t_0)$ and $\mathcal{A}(t_1) = A$ where $D(t_0)$ is the known density matrix of the system at the initial time t_0 and where A is the observable which one wants to measure at the final time t_1. When no restrictions are imposed on $\mathcal{D}(t)$ and $\mathcal{A}(t)$ the stationarity condition yields exact quantum equations of motion, i.e. the usual Liouville-Von Neumann equation for the density and the backward Heisenberg equation for the observable. Moreover, the stationary value of I corresponds to the result of the observation at time t_1:

$$I_{st} = < A > |_{t_1} \equiv Tr A(t_1) D(t_1) \quad . \tag{5.7}$$

If one restricts the trial sets to independent-particle density matrices

$$\mathcal{D}(t) = \exp\left(d(t) + \sum_{ij} d_{ij}(t) a_i^\dagger a_j \right) \quad , \tag{5.8}$$

and to one-body operators

$$\mathcal{A}(t) = a(t) + \sum_{ij} A_{ij}(t) a_i^\dagger a_j \quad , \tag{5.9}$$

the TDHF evolution [Ke76, Ri81, Ba85a]:

$$i\dot{\rho} = [W(\rho),\rho] \tag{5.10}$$

is provided as the stationarity condition of the action I with respect to the variations of $\mathcal{A}(t)$. In equation (5.10) the mean-field Hamiltonian W is found to be:

$$W(\rho) = \frac{\partial E(\rho)}{\partial \rho^*} \quad , \tag{5.11}$$

where E is the total energy $E(\rho) =< H >= TrHD$. In equation (5.10) we have introduce ρ, the one-body density matrix defined as

$$\rho_{ij} \equiv< a_j^\dagger a_i >\equiv \mathrm{Tr} D a_j^\dagger a_i \quad , \tag{5.12}$$

where a_i and $a_i^\dagger$ are respectively annihilation and creation operators associated with the single particle orbital i

5.3 the RPA and the Response of the System

In chapter 3.2.3 we have discussed the small amplitude motion around a given density $\rho^{(0)}$ and we have derived the RPA equation

$$i\|\dot{\rho}^{(1)} \gg = \mathcal{K}\|\rho^{(1)} \gg \ , \tag{5.13}$$

by expanding the TDHF equation (3.26) to the first order in ρ, $\rho = \rho^{(0)} + \rho^{(1)} + \cdots$. This approach leads to the definition of the RPA matrix

$$\mathcal{K} = \mathcal{E} + \mathcal{F}\mathcal{L} \ , \tag{5.14}$$

where the super matrices $\mathcal{E}, \mathcal{F}, \mathcal{L}$ are defined by:

$$\begin{array}{lcl} \mathcal{E}\|\sigma \gg & = & \|[W^{(0)}, \sigma] \gg \\ \mathcal{F}\|\sigma \gg & = & -\|[\rho^{(0)}, \sigma] \gg \\ \mathcal{L}_{\alpha\beta} & = & \frac{\partial W_\alpha}{\partial \rho_\beta} = \frac{\partial^2 E}{\partial \rho_\alpha^* \partial \rho_\beta} \end{array} \ . \tag{5.15}$$

In the following we will also need to introduce the eigenmodes, $\mathcal{X}^\nu$, of the RPA matrix $\mathcal{K}$:

$$\mathcal{K}\|\mathcal{X}^\nu \gg = \omega_\nu \|\mathcal{X}^\nu \gg \ . \tag{5.16}$$

Linear Response

If we are now interested in the response of the system to an external perturbation described by a one-body field F we must solve a new linearized TDHF equation which reads:

$$i\|\dot{\rho}^{(1)} \gg = \mathcal{K}\|\rho^{(1)} \gg + \mathcal{F}\|F \gg \ . \tag{5.17}$$

If we now specify a given frequency ω for the external field we can formally invert equation (5.17) into

$$\|\rho^{(1)} \gg = \mathcal{G}_{RPA}\|F \gg \ , \tag{5.18}$$

where we have introduced the finite-temperature RPA Green's function defined by:

$$\mathcal{G}_{RPA}(\omega) = \frac{1}{\omega - i\eta - \mathcal{K}}\mathcal{F} \ . \tag{5.19}$$

Using the definitions (3.33) and introducing the unperturbed HF Green's function,

$$\mathcal{G}_{HF}(\omega) = \frac{\mathcal{F}}{\omega - i\eta - \mathcal{E}} \ , \tag{5.20}$$

we can easily demonstrate that the so-called linearized Bethe-Salpeter relation holds:

$$\mathcal{G}_{RPA} = \mathcal{G}_{HF} + \mathcal{G}_{HF}\ \mathcal{L}\ \mathcal{G}_{RPA} \ . \tag{5.21}$$

Introducing the eigenmodes of the RPA, we realize that the RPA Green's function contains poles at the RPA energies and that the residues are the eigenmodes

$$\mathcal{G}_{RPA}(\omega) = \sum_\nu sgn(\omega_\nu)\frac{\|\mathcal{X}^\nu \gg \ll \mathcal{X}^\mu\|}{\omega - \omega_\nu - i\eta} \ . \tag{5.22}$$

Response Function

The result of the measurement of the perturbation induced by the external field F is given by the response function :

$$R_F(\omega) \equiv \mathrm{tr}F\rho^{(1)} \equiv \ll F\|\rho^{(1)} \gg = \ll F\|\mathcal{G}_{RPA}(\omega)\|F \gg \ . \tag{5.23}$$

Using the relation $1/(\omega - i\eta) = \mathcal{P}(1/\omega) + i\pi\delta(\omega)$, the imaginary part of $R_F(\omega)$ is the RPA strength function:

$$S(\omega) = \frac{1}{\pi}\Im m\ R_F(\omega) = \sum_\nu sgn(\omega_\nu)|\ll \mathcal{X}^\nu\|F \gg|^2\delta(\omega - \omega_\nu) \ . \tag{5.24}$$

Therefore, ω^ν must be interpreted as an eigenenergy while $\ll F\|\chi^\nu \gg$ can be related to a transition amplitude.

Strength Function

However to get the exact interpretation of these quantities we must study a physical process. For example, we can compute the excitation of a hot system induced by the operator F at a frequency ω. In the finite temperature $T = 1/\beta$ formalism the absorption probability is given by a statistical average over the initial states $|n>$ and a sum over the final states $|m>$ of the elementary transition probability $|<m|F|n>|^2$:

$$S_{abs}(\omega) = \frac{1}{Z}\sum_{mn} e^{-\beta(\omega_n - \mu N_n)}|<m|F|n>|^2\delta(\omega_{mn} - \omega) \quad . \tag{5.25}$$

In this equation indices m and n label the eigenstates of the many-body Hamiltonian H. This strength can be related to the exact two-body Green's function [Ab63, Fe71, Ch90] defined by :

$$\mathcal{G}_{ij,k\ell}(\omega) = \frac{1}{Z}\sum_{mn} e^{-\beta(\omega_n - \mu N_n)}\left\{\frac{\tilde{\mathcal{X}}_{ij}^{(mn)}\tilde{\mathcal{X}}_{k\ell}^{(mn)*}}{\omega - i\eta - \omega_{mn}} - \frac{\tilde{\mathcal{X}}_{ji}^{(mn)*}\tilde{\mathcal{X}}_{\ell k}^{(mn)}}{\omega - i\eta + \omega_{mn}}\right\} \quad , \tag{5.26}$$

where $\omega_{mn} = \omega_m - \omega_n$ and $\tilde{\mathcal{X}}_{ij}^{(mn)} =< m|a_i^+ a_j|n >$ are, respectively, the transition energies and densities. In terms of the Green's function the absorption strength reads :

$$S_{abs}(\omega) = \frac{1}{\pi}\frac{1}{1 - \exp(-\beta\omega)} \ll F\|\Im m\ \mathcal{G}(\omega)\|F \gg \quad . \tag{5.27}$$

The factor $1/(1 - \exp(-\beta\omega))$ is easily understood since $\mathcal{G}$ does not contain only the absorption mechanism but also the spontaneous emission which is equal to $\exp(-\beta\omega)$ times the absorption.

Since $\mathcal{G}_{RPA}$ is supposed to be a good approximation of $\mathcal{G}$ we get

$$S_{abs}(\omega) \approx \frac{1}{1 - \exp(-\beta\omega)} S(\omega) \quad . \tag{5.28}$$

Therefore, the RPA probability, $|\ll F\|\mathcal{X}^\nu \gg|^2$, can be identified with the absorption probability, $e^{-\beta(\omega_n - \mu N_n)}| < m|F|n > |^2/Z$, times a factor $(1 - exp(-\beta\omega))$, while ω^ν can be identify with the energy spacing between the two states $|\ m >$ and $|\ n >$.

Continuum RPA

The RPA Green's function can be directly computed from equation (5.21). For finite-range nuclear forces, this method presents enormous numerical difficulties. However, the problems become much simpler for zero-range effective interactions such as Skyrme forces [Be73, Sh75, Be75, Li76a, Ts78] because one can solve the Bethe-Salpeter equation (5.21) directly in coordinate space.

Indeed, using the definition of the super matrices $\mathcal{F}$ and $\mathcal{E}$ together with the $\mathbf{r}$ representation defined by the projection on the one-body operators $\|\mathbf{r}_1\mathbf{r}_2 \gg\equiv |\mathbf{r}_1 >< \mathbf{r}_2|$ the unperturbed Green's function (5.20) reads :

$$\mathcal{G}_{HF}(\omega, \mathbf{r}_1\mathbf{r}_2, \mathbf{r}_{1'}\mathbf{r}_{2'}) \equiv\ll \mathbf{r}_1\mathbf{r}_2\|\mathcal{G}_{HF}\|\mathbf{r}_{1'}\mathbf{r}_{2'} > \quad , \tag{5.29}$$

$$\mathcal{G}_{HF}(\omega, \mathbf{r}_1\mathbf{r}_2, \mathbf{r}_{1'}\mathbf{r}_{2'}) =< \mathbf{r}_1\mathbf{r}_{2'}|\frac{I(1)\rho^{(0)}(2) - \rho^{(0)}(1)\ I(2)}{\omega - i\eta +\ I(1)W(2) - W(1)\ I(2)}|\mathbf{r}_{1'}\mathbf{r}_2 > \quad , \tag{5.30}$$

where I represents the identity operator. Introducing the single particle Green's function

$$G^0(\omega, r, r') =< r|\frac{1}{\omega - i\eta - W}|r' >= 2m\frac{v(r_>)\ w(r_<)}{\mathcal{W}(v, w)} \quad , \tag{5.31}$$

where $r_<$ and $r_>$ denote the greater and the lesser of r and r' and v and w are two solutions, one regular and the other irregular of $(W - \omega)\nu = 0)$, $\mathcal{W}(\ v,\ w)$ being their Wronskian, one gets

$$\mathcal{G}_{HF}(\omega, \mathbf{r}_1\mathbf{r}_2, \mathbf{r}_{1'}\mathbf{r}_{2'}) = \sum_i n_i\phi_i(\mathbf{r}_1)\phi_i^*(\mathbf{r}_{1'})G^0(\varepsilon_i - \omega, r_{2'}, r_2) + (\mathbf{r}_1 \leftrightarrow\ \mathbf{r}_{2'})(\mathbf{r}_{1'} \leftrightarrow\ \mathbf{r}_2) \quad . \tag{5.32}$$

In this equation ϕ_i represents the single-particle orbital at the energy ε_i occupied by n_i nucleons. For a pure δ force the Bethe-Salpeter equation (5.21) becomes, for the local response $r_1 = r_2 \equiv r$, $r_{1'} = r_{2'} \equiv r'$, :

$$\mathcal{G}_{RPA}(\omega, \mathbf{r}, \mathbf{r}') = \mathcal{G}_{HF}(\omega, \mathbf{r}, \mathbf{r}') + \int d\mathbf{r}"\mathcal{G}_{HF}(\omega, \mathbf{r}, \mathbf{r}")\mathcal{L}(\mathbf{r}")\mathcal{G}_{RPA}(\omega, \mathbf{r}", \mathbf{r}') \quad . \tag{5.33}$$

These Green's functions can be easily computed on a lattice using expressions (5.31) and (5.32) and give directly access to the strength function (3.58).

5.4 Adiabatic TDHF Approximation

The basic idea of ATDHF is to introduce a velocity field and a set of collective coordinates. Since the coordinates are usually time reversal invariant quantities, Baranger and Véneroni [Ba78] proposed to decompose the density using two time-even Hermitian matrices, a density $\rho^{(0)}(t)$ and a velocity field $\chi(t)$:

$$\rho(t) = e^{i\chi(t)}\rho^{(0)}(t)e^{-i\chi(t)} \quad . \tag{5.34}$$

They also proposed the adiabatic approximation assuming that $\rho(t)$ is very close to $\rho^{(0)}(t)$, i.e. that the velocity field is small enough to be treated perturbatively. Therefore expanding the exponential operators in Eq. (5.34) , the density can be written as

$$\rho = \rho^{(0)} + \rho^{(1)} + \rho^{(2)} + \dots \quad , \tag{5.35}$$

where

$$\rho^{(1)} = i[\chi, \rho^{(0)}] \qquad (i.e.\ \|\rho^{(1)} \gg = i\mathcal{F}\|\chi \gg) \tag{5.36}$$

and

$$\rho^{(2)} = -\frac{1}{2}\left[\chi, [\chi, \rho^{(0)}]\right] \quad . \tag{5.37}$$

The collective Hamiltonian can be deduced from the energy of the system in a manner very similar to the illustration presented in section 2.2.1.2 where the classical collective Lagrangian was derived from the projection of the quantum action on a family of trial function (the so-called "collective path").

Using the density (5.35) the Hartree-Fock energy can be expanded as :

$$E(\rho) = E(\rho^{(0)}) + \frac{\partial E}{\partial \rho}\rho^{(2)} + \frac{\partial^2 E}{\partial \rho \partial \rho}\rho^{(1)}\rho^{(1)} + \dots \quad . \tag{5.38}$$

Using the RPA notation, this energy, (Eq. (5.38)), can be recast as

$$E(\rho) = E(\rho^{(0)}) + \frac{1}{2} \ll \chi\|\mathcal{M}^{-1}\|\chi \gg \quad , \tag{5.39}$$

where we have introduced the mass tensor defined as

$$\mathcal{M} = (\mathcal{K}\mathcal{F})^{-1} \quad . \tag{5.40}$$

The first term in equation (5.39) can be interpreted as a potential energy $V(\rho^{(0)})$ whereas the second one corresponds to a kinetic energy term $T(\chi, \rho(0))$. The energy E plays the role of a classical Hamiltonian for which $\rho^{(0)}$ and χ appear as conjugate variables. Therefore, the dynamical equations for $\dot{\rho}^{(0)}$ and $\dot{\chi}$ can be derived from the Hamiltonian equations: $\|\dot{\rho}^{(0)} \gg \equiv \|\partial E/\partial \chi^* \gg$ and $-\|\dot{\chi} \gg \equiv \|\partial E/\partial \rho^{(0)^*} \gg$, which lead to the equations

$$\dot{\rho^{(0)}} = \mathcal{M}^{-1}\chi \tag{5.41}$$

and

$$-\dot{\chi} = W + \frac{1}{2} \ll \chi\|\frac{\partial \mathcal{M}^{-1}}{\partial \rho^{(0)^*}}\|\chi \gg \quad . \tag{5.42}$$

These equations together with the definition (5.39) of the collective Hamiltonian form the most general formulation of the ATDHF approximation. However, they are often too difficult to solve without further approximations. In fact this approach is really useful if we can assume that the density $\rho^{(0)}(t)$ is driven by an ensemble of collective coordinates $Q(t)$

$$\|\rho^{(0)}(t) \gg = \|\rho^{(0)}(Q(t)) \gg \quad . \tag{5.43}$$

In such a case, we can directly express the velocity as

$$\|\dot{\rho}^{(0)}(t) \gg = \dot{Q}\|\frac{\partial \rho^{(0)}}{\partial Q} \gg \quad . \tag{5.44}$$

Using the ATDHF equation (5.41), $\|\chi \gg = \mathcal{M}\|\dot{\rho}^{(0)} \gg$we can write the kinetic energy as

$$T = \frac{1}{2}\dot{Q}M\dot{Q} \quad , \tag{5.45}$$

where the mass tensor is defined by[1]

$$M_{\mu\nu} = \ll \frac{\partial \rho^{(0)}}{\partial Q_\mu}\|\mathcal{M}\|\frac{\partial \rho^{(0)}}{\partial Q_\nu} \gg \quad . \tag{5.46}$$

[1] *One can recognize in the Mass Tensor $M_{\mu\nu}$(5.46) the polarizability tensor $M_{\mu\nu} = \ll \partial\rho^{(0)}/\partial Q_\mu\|$ $(i\mathcal{F}^{-1})$ $\mathcal{G}_{RPA}(\omega = 0)$ $(i\mathcal{F}^{-1})$ $\|\partial\rho^{(0)}/\partial Q_\nu \gg$ which corresponds to the static deformation induced by the operator $i\mathcal{F}^{-1}\partial\rho^{(0)}/\partial Q_\nu$ and measured according to the operator $i\mathcal{F}^{-1}\partial\rho^{(0)}/\partial Q_\mu$. It should be noticed that if we are considering the dynamics of Slater determinants, $\rho^2 = \rho$ these operators reduce to $i[\rho^{(0)}, \partial\rho^{(0)}/\partial Q_\mu]$. and $i[\rho^{(0)}, \partial\rho^{(0)}/\partial Q_\nu]$.*

Therefore, if we define the momentum $P = M\dot{Q}$, equation (5.39) yields the collective Hamiltonian

$$E(\rho) \equiv H(P,Q) = \frac{1}{2}PMP + V(Q) \quad , \tag{5.47}$$

where the potential is the mean value of the energy associated with $\rho^{(0)}$: $V(Q) \equiv E(\rho^{(0)})$. Therefore, the ATDHF approximation leads to a classical Hamiltonian similar to the one of the macroscopic approaches.

5.5 Periodic Orbits of TDHF

Iterative Construction of Periodic Orbits

The method proposed in ref. [Ch86] is an iterative method based on the existence of a distance in the Liouville space constructed from the scalar product (3.28)

$$\ell(\rho,\varrho) = \ll \rho - \varrho \| \rho - \varrho \gg \quad . \tag{5.1}$$

Therefore, if one starts with an arbitrary solution $\rho(0)$, one can first find the period T for which this distance, $\ell(\rho(0),\rho(T))$, is minimum. One can thus look for the small variation $\delta\rho(0)$ which will reduce the distance $\ell(\rho(0),\rho(T))$. The evolution of $\delta\rho(t)$ is given by the RPA equation (3.30) which can be integrated formally as

$$\|\rho^{(1)}(t) \gg = \mathcal{T}\left(-i\int_0^t dt' \mathcal{K}(t')\right) \|\delta\rho(0) \gg \equiv \mathcal{U}(t) \|\delta\rho(0) \gg \quad , \tag{5.2}$$

where $\mathcal{T}$ is the time-ordering symbol. So the variation of distances ℓ is given at the first order in $\delta\rho$:

$$\delta\ell = 2 \ll \rho(0) - \rho(T) \| \; 1 - \mathcal{U}(T) \; \|\delta\rho(0) \gg \quad . \tag{5.3}$$

Therefore, the idea is to choose $\delta\rho(0)$ to be

$$\|\delta\rho(0) \gg = \epsilon \; \mathcal{P}(1 - \mathcal{U}^\dagger) \; \|\rho(T) - \rho(0) \gg \quad , \tag{5.4}$$

where ϵ is a real positive number small enough to ensure the validity of the linear response theory. In equation (5.4), $\mathcal{P}$ is a projector which ensures the conservation of the particle number and, if required, of the constraint: $\rho^2 = \rho$. In this case, the distance will always be reduced and will eventually converge to 0.

We know that the linear evolution preserves the simplectic form $\mathcal{F}$ (see discussion of eq. (3.35)). This property implies that $\mathcal{U}$ is a simplectic operator, as in classical mechanics [Ar74],

$$\mathcal{U}^\dagger(T) = \mathcal{F}^{-1}(0) \; \mathcal{U}^{-1}(T) \; \mathcal{F}(T) \quad . \tag{5.5}$$

Therefore, one may use this relation to construct the variation $\|\delta\rho(0) \gg$

$$\|\delta\rho(0) \gg = \epsilon \; \|\rho(T) - \rho(0) \gg + \epsilon \; \mathcal{F}^{-1}(0) \; \mathcal{U}^{-1}(T) \; \mathcal{F}(T) \; \|\rho(T) - \rho(0) \gg \quad . \tag{5.6}$$

The second term is constructed by propagating backward the perturbation
$\|\delta\varrho(T) \gg = \epsilon \; \mathcal{F}(T) \; \|\rho(T) - \rho(0) \gg = \epsilon \; \|[\rho(T),\rho(0)] \gg$ and by taking $\mathcal{F}^{-1}(0)\|\delta\varrho(0) \gg$ at the time 0. If only Slater determinants are considered, this reduces to $[\delta\varrho(0),\rho(0)]$. If we want to keep the constraint $\rho^2 = \rho$, we can project $\delta\rho(0)$ on the particle hole space. Iterating this method eventually yields a periodic orbit since the distance ℓ is reduced after each iteration.

Perturbative Construction of Periodic Orbits

The basic idea of this method is to expand the density in powers of a small number, the amplitude of the oscillations ϵ

$$\rho(t) = \rho^{(0)} + \varepsilon\rho^{(1)}(\frac{\omega t}{\omega^{(0)}}) + \varepsilon^2\rho^{(2)}(\frac{\omega t}{\omega^{(0)}}) + \varepsilon^3\rho^{(3)}(\frac{\omega t}{\omega^{(0)}}) + \cdots \quad , \tag{5.7}$$

where the frequency is also expanded in a power series of ϵ :

$$\omega = \omega^{(0)} + \varepsilon\omega^{(1)} + \varepsilon^2\omega^{(2)} + \varepsilon^3\omega^{(3)} + \cdots \tag{5.8}$$

The dynamical equations for $\rho^{(n)}$ are obtained from the expansion of the TDHF equations (3.26) at the n'th order in ε:

$$0 = \mathcal{W} \; \|\rho^{(0)} \gg \tag{5.9}$$

$$i \; \|\dot\rho^{(1)} \gg = \mathcal{K} \; \|\rho^{(1)} \gg \tag{5.10}$$

$$i \; \|\dot\rho^{(2)} \gg = \mathcal{K} \; \|\rho^{(2)} \gg + \|[W^{(1)},\rho^{(1)}] \gg - i\frac{\omega^{(1)}}{\omega^{(0)}} \; \|\dot\rho^{(1)} \gg \tag{5.11}$$

$$i \; \|\dot\rho^{(3)} \gg = \mathcal{K} \; \|\rho^{(3)} \gg + \cdots \tag{5.12}$$

where the mean-field W has been expanded in series:

$$W = W^{(0)} + \varepsilon W^{(1)} + \varepsilon^2 W^{(2)} + \varepsilon^3 W^{(3)} + \cdots \tag{5.13}$$

In equations 5.9, we have explicitly introduced the RPA matrix $\mathcal{K}$. It should be noticed that the equations (5.9) only define the p.h. components of $\rho^{(n)}$, the particle-particle or hole-hole components being defined by the relation $\rho^2 = \rho$.

The equation for $\rho^{(1)}$ implies that $\delta\rho$ is proportional to the RPA eigenstates

$$\|\rho^{(1)}(t) \gg = \sum_\nu a_\nu \left(\|\mathcal{X}^\nu \gg e^{-i\omega_\nu^{(0)}t} + \|\mathcal{X}^{\nu\dagger} \gg e^{i\omega_\nu^{(0)}t} \right) \quad , \tag{5.14}$$

where the a_ν are free parameters. If we are looking for periodic solutions we can only mix commensurable frequencies. The equation for $\rho^{(2)}$ contains a source term proportional to $\rho^{(1)}\rho^{(1)}$, so it contains frequencies which are sums or differences of the ω_ν 's. Therefore, in order to avoid a linearly increasing solution which is non-physical, one needs to set $\omega^{(1)} = 0$. The situation is different in the next order, $\rho^{(3)}$, because equation (5.9) reads

$$(i\frac{\partial}{\partial t} - \mathcal{K})\rho^{(3)} = [W^{(1)}, \rho^{(2)}] + [W^{(2)}, \rho^{(1)}] - i\frac{\omega^{(2)}}{\omega^{(0)}}\dot{\rho}^{(1)} \quad , \tag{5.15}$$

or specifying only the p.h. components

$$(i\frac{\partial}{\partial t} - \mathcal{K})\mathcal{P}\rho^{(3)} = \mathcal{P}\sigma^{(3)} - i\frac{\omega^{(2)}}{\omega^{(0)}}\dot{\rho}^{(1)} \quad , \tag{5.16}$$

with $\sigma^{(3)} = [W^{(1)}, \rho^{(2)}] + [W^{(2)}, \rho^{(1)}] + \mathcal{K})(1 - \mathcal{P})\rho^{(3)}$ and where $\mathcal{P}$ projects on the p.h. components. The commutators on the right-hand side of equation (5.15) contain sums or differences of three frequencies ω_ν and in particular contain a resonant term ω_ν. The terms coming from the modifications of ω are there to cancel these resonant terms which otherwise would yield non-physical solutions. This condition defines the frequency correction $\omega^{(2)}$ requiring that the projection on the eigenstates $\|\mathcal{X}^\nu \gg$ does not contain the frequency ω_ν, i.e. $0 = \int_0^T dt \left(\ll \mathcal{X}^\nu \|\mathcal{F}^{-1} \|\sigma^{(3)} \gg -i\frac{\omega^{(2)}}{\omega^{(0)}} \ll \mathcal{X}^\nu \|\mathcal{F}^{-1} \|\dot{\rho}^{(1)} \gg \right)$ so that

$$\omega^{(2)} = \omega^{(0)} \frac{\int_0^T dt \ \mathrm{tr}\sigma^{(3)}[\rho^{(0)}, \rho^{(1)}]}{\int_0^T dt \ \mathrm{tr}i\dot{\rho}^{(1)}[\rho^{(0)}, \rho^{(1)}]} \quad . \tag{5.17}$$

This procedure can be iterated in order to find all the the frequencies $\omega^{(n)}$ requiring that no resonant terms appear in the equation of evolution of $\rho^{(n+1)}$. The last step is to apply the quantization rule which reads

$$I \equiv \sum_h -\Theta_h + \int_0^T dt < h(t)|i\frac{\partial}{\partial t} - W|h(t) >= n \quad , \tag{5.18}$$

where the Θ_h are the Floquet-Lyapounov phase defined as the phase acquired by the orbital h after one period. In ref. [Ab91, Ab92, Ab92a] the action I is approximated by

$$I \approx \varepsilon^2 \int_0^T dt \ \mathrm{tr}W^{(1)}\rho^{(1)} + W^{(0)}\rho^{(2)} = \varepsilon^2 T E^{(2)} \quad , \tag{5.19}$$

where $E^{(2)}$ is the second order correction to the energy $E = E^{(0)} + \varepsilon^2 E^{(2)} + \varepsilon^3 E^{(3)} + \cdots$. Using the expansion of the period $T = 1/2\pi\omega$, we get for the n quantified states:

$$\varepsilon_n^2 = n\frac{\omega^{(0)}}{E^{(2)} - n\omega^{(2)}} \quad , \tag{5.20}$$

and so the excitation energy reads :

$$E_n^* \equiv E_n - E^{(0)} = n\omega_n = n(\omega(0) + \varepsilon_n^2\omega(2)) \quad . \tag{5.21}$$

These equations give corrections to the one phonon state ω_1 and also to the two phonon states ω_2.

In realistic calculations, one needs to introduce the angular momentum. This can be done by introducing the quantum numbers λ and μ. $\rho^{(1)}$ contains a sum over μ and $\rho^{(2)}$ and $\omega^{(2)}$ can be expressed as

$$\rho^{(2)} = \sum_{\lambda'=0}^{\lambda} \sum_{\mu'=-2\lambda'}^{2\lambda'} \rho^{(2)}_{2\lambda',\mu'} \tag{5.22}$$

and

$$\omega^{(2)} = \sum_{\lambda'=0}^{\lambda} \sum_{\mu'=-2\lambda'}^{2\lambda'} \omega^{(2)}_{2\lambda',\mu'} \quad . \tag{5.23}$$

However, the equations (5.20) and (5.21) do not predict any splitting of the two phonon states. In refs. [Ab91, Ab92, Ab92] the following ansatz is proposed in analogy with the idea of the projection onto a good angular momentum : the splitting of the two phonon states is obtained replacing $\omega^{(2)}$ by $\omega^{(2)}_\lambda$ in equations (5.20) and (5.21).

5.6 Example of a Boson Mapping of the Hamiltonian of Fermions

With the transformation (3.107) , the fermion Hamiltonian is mapped onto:

$$
\begin{aligned}
H_f \xrightarrow{\mathcal{M}} H_b &= E_0 + \sum_{ph}(\epsilon_p - \epsilon_h) b^\dagger_{ph} b_{ph} + \sum_{php'h'} V_{ph'hp'} b^\dagger_{ph} b_{p'h'} \\
&+ \tfrac{1}{2\sqrt{2}} \sum_{pp'hh'} [V_{pp',hh'} b^\dagger_{ph} b^\dagger_{p'h'} + h.c.] \\
&+ \tfrac{1}{2\sqrt{2}} \sum_{\substack{pp'p'' \\ hh'}} [V_{pp',hp''} b^\dagger_{ph} b^\dagger_{p'h'} b_{p''h'} + h.c.] \\
&+ \tfrac{1}{2\sqrt{2}} \sum_{\substack{pp' \\ hh'h''}} [V_{ph,h'h''} b^\dagger_{ph''} b^\dagger_{p'h'} b_{p'h} + h.c.] \\
&- \sum_{\substack{pp'p'' \\ hh'h'''}} V_{ph,hp'} b^\dagger_{ph''} b^\dagger_{p''h} b_{p''h''} b_{p'h'} \\
&- \tfrac{1}{4} \sum_{\substack{pp'p''p''' \\ hh'}} V_{pp',p''p'''} b^\dagger_{ph} b^\dagger_{p'h'} b_{p'''h} b_{p''h'} \\
&- \tfrac{1}{4} \sum_{\substack{pp' \\ hh'h''h'''}} V_{hh',h''h'''} b^\dagger_{ph'''} b^\dagger_{p'h''} b_{ph} b_{p'h'} \\
&+ \tfrac{1-\sqrt{3}}{2\sqrt{2}} \sum_{\substack{pp'p'' \\ hh'h''}} V_{pp',hh'} [b^\dagger_{ph} b^\dagger_{p'h''} b^\dagger_{p''h'} b_{p''h''} + h.c.] \\
&+ \ldots
\end{aligned}
\tag{5.24}
$$

On the right hand side of Eq.(5.24) the first four terms correspond to a harmonic Hamiltonian with particle-hole interactions. Comparing this part with the quasi-boson Hamiltonian, we find that they are quite similar, differing only by some numerical factors [Ri81]. In that sense, the RPA can be considered as an approximation where H_b is truncated at second-order in boson operators [Ri81].

Bibliography

[Ab63] A.A. Abrikosov, L.P. Gorkov and I.E. Dzyaloshinski, *Methods of Quantum Field Theory in Statistical Physics*, Prentice - Hall Cliffs (1963)

[Ab75] Y. Abgrall and E. Caurier, Phys. Lett. **56B** (1975) 229

[Ab90] S. Aberg, H.Flocard and W.Nazarewicz, Annu. Rev. Nucl. Part. Sci. (1990) 439

[Ab91] A. Abada and D. Vautherin, Phys. Lett. **B258** (1991) 1

[Ab92] A. Abada and D. Vautherin, Phys. Rev. **C45** (1992) 2205

[Ab92a] A. Abada, These, IPNO-T-92-03, IPN-Orsay (France) (1992)

[Al56] K. Alder, A. Bohr, T. Huus, B. Mottelson and A. Winther, Rev. Mod. Phys. **28** (1956) 432

[Al96] N. Alamanos and P. Roussel-Chomaz, Ann. Phys. (Paris) **21** (1986) 601

[Ar60] R. Arvieu and M. Véneroni, Comp. Rend. Ac. des Sci. (Paris) **250** (1960) 992

[Ar74] V.I. Arnold, *Méthodes Mathématiques de la Mécanique Classique*, Mir, Moscow (1974)

[Au82] N. Auerbach, Phys. Rev. Lett. **49** (1982) 913

[Au90] N. Auerbach, Ann. of Physics **197** (1990) 376

[Au93] T. Aumann et al. Phys. Rev. **C 47** (1993) 1728

[Ba47] G.C.Baldwin and G.Klaiber, Phys. Rev. **71** (1947) 3

[Ba60] M. Baranger, Phys. Rev.**120** (1960) 957

[Ba62] V. Bargmann, Rev. Mod. Phys. **34** (1962) 829

[Ba72] M. Baranger, J. Phys. (Paris) **33** (1972) C5-61

[Ba72] R. Balian and C. Bloch, Ann. Phys. (N.Y.) **69** (1972) 76

[Ba73] B. Banerjee and D.M. Brink, Z. Phys. **258** (1973) 46

[Ba74] R. Balian and C. Bloch, Ann. Phys. (N.Y.) **85** (1974) 514

[Ba78] M. Baranger and M. Véneroni, Ann. Phys. (N.Y.) **114** (1978) 123

[Ba81] R. Balian and M. Véneroni, Ann. Phys. (N.Y.) **135** (1981) 270

[Ba83] H.W. Baer, R. Bolton, J.D.Bowman, M.D. Cooper, F. Cverna, N.S.P. King, M.Leitch, H.S. Matis, J.Alster, A. Doron, A. Erell, M.A. Moinester, E. Blackmore and E.R. Siciliano, Nucl. Phys. **A396** (1983) 437c

[Ba84] R. Balian and M. Véneroni, Phys. Lett. **B136** (1984) 301

[Ba85] M. Barranco, A. Polls, S. Marcos, J. Navarro and J. Treiner, Phys. Lett.B154 (1985) 96 M. Barranco, A. Polls and J. Martorell Nucl. Phys.A444 (1985) 445

[Ba85a] R. Balian and M. Véneroni, Ann. Phys. (N.Y.) **164** (1985) 334

[Ba85b] J. Bar Touv, Phys. Rev.C32 (1985) 1369

[Ba88] R. Balian and M. Véneroni, Ann. Phys. (N.Y.) **187** (1988) 29

[Ba88a] G.P. Baur and C.A. Bertulani, Phys. Rep. **163** (1988) 299.

[Ba88b] B. Baur and C. Bertulani, Nucl. Phys. **A482** (1988) 313c

[Ba88c] J.Barrette et al., Phys. Lett. **B299** (1988) 182

[Ba92] J.Barrette et al., Phys. Rev. **C45** (1992) 2427

[Ba92] J. Bar Touv and S. Mordechai, Phys. Rev. **C 45** (1992) 197

[Be61] D.R. Bés, Mat. Fys. Medd. Dan. Vid. Selsk **33** (1961) nj2

[Be62] S.T. Beliaev and V.G. Zelevinsky, Nucl. Phys. **39** (1962) 582

[Be73] G.F. Bertsch. Phys. Rev. Lett. **31** (1973) 121

[Be74] M. Beiner, H. Flocard, N. Van Giai and P. Quentin, Physica Scripta **10A** (1974) 29

[Be75] G.F. Bertsch and S.F.Tsai, Phys. Rep **180** (1975) 125

[Be83]

[Be75a] B.L. Berman, S.C. Fultz, Rev. Mod. Phys. **47** (1975) 713

[Be75b] B.L. Berman, Atomic Data and Nuclear Data Tables **15** (1975) 319

[Be76] M.V. Berry and M. Taylor, Proc. R. Soc. London **A349** (1976) 101

[Be76a] F.E. Bertrand, Ann. Rev. Nucl. Part. Sci. **26** (1976) 457

[Bc77] M.V. Berry and M. Talor, J. Phys. **A10** (1977) 371

[Be81] F. E. Bertrand, Nucl. Phys. **A354** (1981) 129c

[Be83] G.F. Bertsch, P.F. Bortignon and R.A. Broglia, Rev. Mod. Phys. **55** (1983) 287.

[Be84] W. Besold, P.G. Reinhart and C. Toepffer, Nucl. Phys. A431 (1984) 1

[Be86] G.F. Bertsch and R.A. Broglia, Physic Today **39** n^o 8 (1986) 44

[Be87] F.E.Bertrand et al. Phys. Rev. **C35** (1987) 111

[Be88] G.F. Bertsch and S. Das Gupta, Phys. Reps **160** (1988)190

[Be89] F.E. Bertrand and J.R. Beene Proceeding of Int. Nucl. Phys. Conference, Sao Paulo (1989)

[Be91] J.R. Beene, et al. Phys. Rev. **C41** (1991) 920

[Be92] D. Beaumel and Ph. Chomaz, Ann. Phys. (N.Y.), **213** (1992) 405

[Be94] J.R. Beene, et al. Proc. of the Gull Lake Nucl. Phys. Conf., U.S. August (1993), to be published in Nucl. Phys. (1994)

[Bi89] L.Bianchi, B.Fernandez, J.Gastebois, A.Gillibert,W.Mittig and J.Barrette, Nucl. Inst. Meth. **A276** (1989) 509

[Bl76] J.P. Blaizot, D. Gogny end B. Grammaticos, Nucl. Phys. **A265** (1976) 315

[Bl76a] J. Blocki, J Randrup, W. H Swiatecki and C.F Tsang LBL-5014(1976)

[Bl77] J.P. Blaizot and D. Gogny, Nucl. Phys. **A284** (1977) 429

[Bl78] J. P. Blaizot and E.R. Marshalek, Nucl. Phys. **A309** (1978) 422,453

[Bl80] J.P. Blaizot, Phys. Rep. **64** (1980) 171

[Bl81] J.P. Blaizot, Phys. Lett. **107B** (1981) 331

[Bl85] Y. Blumenfeld, J.C. Roynette, Ph. Chomaz, N. Frascaria, J.P. Garron and J.C. Jacmart. Nucl. Phys. **A445** (1985) 151

[Bl88] Y. Blumenfeld and Ph. Chomaz, Phys. Rev. **C38** (1988) 2157

[Bl88a] J. Blocki et al, Nucl. Phys. **A477** (1988) 189

[Bl95] J.P. Blaizot,J.F. Berger, J. Dechargé and M. Girod, Nucl Phys. **A591** (1995) 435

[Bo37] N.Bohr and F.Kalchar, Mat. Fys. Medd. Dam. Vid. Lelrk **14** nj10(1937)

[Bo37a] W. Bothe and W. Gentner, Z. für Physik **106** (1937) 237

[Bo39] N. Bohr and J.A. Wheeler, Phys. Rev. **56** (1939) 426

[Bo53] D. Bohm and D. Pines Phys. Rev. **92** (1953) 609

[Bo65] J. de Boer, R.G. Stokstad, G.P. Symons and A.Winther, Phys. Rev. Lett **14** (1965) 564

[Bo69] A. Bohr and B. Mottelson, *Nuclear Physics*, Vol. I, Benjamin (N.Y), (1969)

[Bo75] A. Bohr and B. Mottelson, *Nuclear Structure* Vol II, Benjamin (N.Y.), (1975)

[Bo76] P. Bonche, S.Koonin and J.W. Negele, Phys. Rev **13** (1976) 1226

[Bo88] Recent developpements of the boson mapping methods are sumerized in D. Bonatsos, Interacting Boson Model of Nuclear Structure (chap. 15.), Oxford Science Publications, Oxford (1988).

[Bo84] J.D. Bowman et al. Journ. dee Phys. **45** (1984) C4 351

[Br59] G.E. Brown and M. Bolsterli, Phys. Rev. Lett. **3** (1959) 472

[Br61] G.E. Brown, J.A. Evans and D.J. Thouless, Nucl. Phys **24** (1961) 1

[Br62] D.M. Brink, Ph. D. Thesis University of Oxford (1955)
P. Axel, Phys. Rev. **126** (1962) 671

[Br65] D.M. Brink, A.F.R De Toledo Piza and A.K. Kerman Phys. Lett. **19** (1965) 413

[Br76] D.M. Brink, M.J. Giannoni and M. Vénéroni, Nucl. Phys. **A258** (1976) 237

[Br76a] R.A. Broglia, C.H.Dasso and A. Winter, Phys. Lett. **61B** (1976) 113

[Br78] R.A. Broglia, O. Civitarese, C H. Dasso and A. Winther, Phys Lett **73B** (1978)405

[Br78a] R.A. Broglia, C H. Dasso, G. Pollarolo and A. Winther, Phys. Rep. **48** (1978)331

[Br79] R.A. Broglia, C.U. Dasso and A.Winther proceeding of the Int. Sch. of Phys. Enrico Fermi Vienna (1979)

[Br79a] R.A. Broglia et al, Phys Lett. **B89** (1979) 22

[Br80] R.A. Broglia, C.H.Dasso and H.Erbensen, Prog. in Part. and Nucl. Phys. Vol 4, Pergamon (N.Y.) (1980) 345.

[Br81] R.A. Broglia, C.H.Dasso and A. Winter, Proc. Int. Sch. of Phys. E. Fermi, Course LXXVII eds R.A. Broglia, C.H.Dasso and R. Ricci (North-Holland) Amsterdam (1981) 327

[Br83] S. Brandenburg, R. De Leo, A.G. Drentje, M.N. Harakeh, H. Sakai and A. Van der Woude, Phys. Lett. **130B** (1983) 9

[Bu84] M.Buenerd, Journ. de Phys. **45** (1984) C4 115

[Bu94] A.Buda, PhD Thesis (1994) KVI (Groningen)

[Ca73] E. Caurier, B. Bourotte, Bilwes and Y. Abgrall, Phys. Lett. **44B** (1973) 411

[Ca84] E. Caurier et al, Nucl. Phys. **A425** (1984) 233

[Ca85] E. Caurier, M. Ploszajczak and S. Drozdz, Phys. Lett. **160B** (1985) 357

[Ca85a] E. Caurier et al, Nucl. Phys. **A437** (1985) 407

[Ca86] F. Catara and V. Lombardo, Nucl. Phys. **A 455** (1986) 158

[Ca87] F. Catara, Ph. Chomaz and A. Vitturi, Nucl. Phys. **A471** (1987) 661

[Ca88] F. Catara and Ph. Chomaz, Nucl. Phys. **A482** (1988) 271c.

[Ca89] F. Catara, Ph. Chomaz and N. V. Giai, Phys. Lett. **B233** (1989) 6

[Ca92] F. Catara, Ph. Chomaz and N.V. Giai, Phys. Lett. **B277** (1992) 1

[Ca93] F. Catara, Ph. Chomaz and N.V. Giai, to be published in Phys. Rev. **B** (1993)

[Ca94] F. Catara, Ph. Chomaz and N. Van Giai, to be published

[Ce89] L. Cerbaro, Thesis, Univ. of Padova, Italy (1989) unpublished and P. F. Bortignon, private comunication.

[Ch64] T.H. Chang, Acta Phys. Sinica **20** (1964) 159

[Ch76] E. Chacón, M. Moshinsky and R.T. Sharp, J. of Math. Phys. **17** (1976) 668

[Ch76a] E. Chacón and M. Moshinsky, J. of Math. Phys. **18** (1977) 870

[Ch84] Ph. Chomaz, N. Frascaria, Y. Blumenfeld, J.P. Garron, J.C. Jacmart, J.C. Roynette, W. Bohne, A. Gamp, W. Von Oertzen, M. Buenerd, D. Lebrun and Ph. Martin. Z. Phys. **A 318** (1984) 51

[Ch84a] Ph. Chomaz, Y. Blumenfeld, N. Frascaria, J.P. Garron, J.C. Jacmart, J.C. Roynette, W. Bohne, A. Gamp, W. von Oertzen, N.V. Giai and D. Vautherin Z. Phys. **A 319** (1984) 167

[Ch84b] Ph. Chomaz and D. Vautherin, Phys. Lett. **B139** (1984) 244

[Ch84c] Ph. Chomaz, Thèse de $3^{e}me$ cycle, IPNO-T84-01, Orsay, (1984)

[Ch86] Ph. Chomaz, H. Flocard and V. Vautherin, Phys. Rev. Lett. **56** (1986) 1787

[Ch86a] Ph. Chomaz, J. Phys. Paris **47** (1986) C4-155

[Ch86b] Ph. Chomaz and D. Vautherin, Phys. Lett. **B177** (1986) 9

[Ch87] Ph. Chomaz, N. V. Giai and S. Stringari, Phys. Lett. **B189** (1987) 4.

[Ch88] Ph. Chomaz, N. V. Giai and D. Vautherin, Nucl. Phys. **A476** (1988) 125.

[Ch90] Ph. Chomaz, D. Vautherin and N. Vinh Mau, Phys. Lett. **B242** (1990) 313

[Ch92] Ph. Chomaz and N. V. Giai, Phys. Lett. **B282** (1992) 13.

[Ch95] Ph. Chomaz and N. Frascaria; Phys. Rep. **252** (1995) 275

[Ch95a] Ph. Chomaz, Mémoire d'Habilitation, Caen, (1995)

[Ch96] Ph. Chomaz, Ann. Phys. (Paris) **21** (1986) 669

[Co73] C. Cohen-Tannoudji, B. Diu and F. Laloé, Mécanique Quantique, Paris Hermann (1973)

[Co92] G. Colò, P.F. Bortignon, N. V. Giai, A. Bracco and R.A. Broglia, Phys. Lett. **B276** (1992) 279.

[De81] J. Decharge, M. Girod, D. Gogny and B. Grammaticos, Nucl. Phys. **A358** (1981) 203

[De82] J. Decharge et al, Phys. Rev. Lett. **49** (1982) 982

[De83] J. Decharge and L. Sips, Nucl. Phys. **A407** (1983) 1-28

[Di30] P.A.M. Dirac, Proc. Cambridge Phil. Soc. **26** (1930) 376

[Do83] D.H. Dowell, G. Feldman, K.A. Snover, A.M. Sandorfi and M.T. Collins, Phys. Rev. Lett. **50** (1983) 1191

[Dr86] S. Drożdż, V. Klent, J. Speth and J. Wambach, Nucl. Phys. **A451** (1986) 11

[Dr86a] S. Drozdz et al, Ann. Phys. (N.Y.) **171** (1986) 108

[Dr88] S.Drozdz et al, Phys. Lett. **206B** (1988) 567

[Dy56] F.J. Dyson, Phys. Rev. **102** (1956) 1217

[Em94] H. Emling et al., Proc. of the Gull Lake Nucl. Phys. Conference - (USA) 1993, to be published in Nucl. Phys. A. (1994)

[En75] Y.M. Engel, D.M. Brink, K. Goeke, S.J. Krieger and L. Vautherin, Nucl. Phys. **A249** (1975) 215

[Fa59] S. Fallieros, Maryland Tech. Rept. N¡128 (1959)

[Fa59a] S. Fallieros and R.A. Ferrell, Phys. Rev. **116** (1959) 660

[Fa64] U. Fano, *Lectures on the Many-Body Problem*, (E. Caianiello, Ed.), Academic Press, N.Y., (1964)

[Fa82] S.A. Fayans,V.V Palichnik, N.I.Pyatov, Z.Phys. **A 308** (1982) 145

[Fa83] M. Faber, J.L. Egido and P. Ring, Phys. Lett. **B127** (1983) 5

[Fe34] E. Fermi, Z. Phys. **29** (1924) 315

[Fe57] R.A. Ferrell, Phys. Rev. **107** (1957) 1631

[Fe71] A.L. Fetter and J.D. Walecka, *Quantum Theory of many Particle Systems*, Mc Graw - Hill, New York (1971)

[Fe72] L.S. Ferreira and D.H. Caldeira, Nucl. Phys. **A189** (1972) 250

[Fe83] S.N. Fedotkin, I.N. Mikhailov and R.G. Nazmidinov, Phys. Lett.B121 (1983) 15

[Fl75] H. Flocard and D. Vautherin. Phys. Lett. **55B** (1975) 259

[Fl76] H. Flocard and D. Vautherin, Nucl. Phys. **A264** (1976) 197

[Fl81] H. Flocard and M. Weiss, Phys. Lett. **105B** (1981) 14

[Fo88] S.Fortier, S.Gales, S.M.Austin, W.Benenson, G.W. Crawley, C.Djalali, J.H. Lee, J.van der Plicht and J.S. Winfield, Phys. Rev. **C** (1988) 14

[Fr34] J. Frenkel *Wave Mechanics Advanced General Theory* Oxford Univ. Press, Clarendon Oxford (1934).

[Fr77] N. Frascaria, C. Stéphan, P. Colombani, J.P. Garron, J.C. Jacmart, M. Riou and L. Tassan-Got,Phys. Rev. Lett. **39** (1977) 918

[Fr80] N. Frascaria, P. Colombani, A. Gamp, J.P. Garron, M. Riou, J.C. Roynette, C. Stéphan, A. Amcaume, C. Bizard, J.L. Laville and M. Louvel. Z. Für Physik **A294** (1980) 167

[Fr82] N. Frascaria, Proceedings of the International Conf. on Nucl. Phys. Trieste (Italy) Ch. Dasso, A. Broglia, A. Winther, Eds North Holland, Amsterdam Nucl. Phys. (1982) 617.

[Fr86] N. Frascaria Proceeding of the XXIV International Winter Meeting on Nuclear Physics, Bormio, Italie (20-25 Janvier 1986)

[Fr87] N. Frascaria, Y. Blumenfeld, Ph. Chomaz, J.P. Garron, J.C. Jacmart, J.C. Roynette, T. Suomijarvi and W. Mittig. Nucl.Phys. **A474** (1987) 253

[Fr88] N. Frascaria Nucl. Phys. **A482** (1988) 245c

[Ga85] M. Gallardo, M. Dievel, T. Dossing and R. A. Broglia, Nucl. Phys.A443 (1985) 415

[Ga88] J.J. Gaardhøje, Nucl. Phys. **A482** (1988) 261c

[Ga92] J.J. Gaardhøje, Ann. Rev. Nucl. Part. Sci. **42** (1992) 483

[Gi75] B. Giraud and B. Grammaticos, Nucl. Phys. **A255** (1975) 141

[Gi76] M.J. Giannoni, F. Moreau, P. Quentin, D. Vautherin, M. Veneroni and D.M. Brink Phys. Lett. **65B** (1976) 305

[Gi80] M.J. Giannoni and P.Quentin, Phys. Rev. **C21** (1980) 2060, 2076

[Gi81] N.V. Giai and H. Sagawa, Nucl. Phys. **A371** (1981) 1

[Gi87] N. V. Giai, P.F. Bortignon, F. Zardi and R.A. Broglia, Phys. Lett. **B199** (1987) 155

[Gi88] N. V.Giai, Ph. Chomaz, P.F. Bortignon, F. Zardi and R.A. Broglia, Nucl. Phys. **A 482** (1988) 437

[Gl59] A.E. Glassgold, W. Heckrotte and K.M. Watson Ann. Phys. **6** (1959) 1

[Gl63] R. J. Glauber, Phys. Rev **130** (1963) 2529, 131 (1963)2766

[Go48] M.Goldhaber and E. Teller, Phys. Rev. **74** (1948) 1046

[Go59] F.K Gowan, in Compte- Rendus du Congrés Interne de Physique Nucléaire, ed. P Gargen berger, Dunod, Paris (1959) 225

[Go59a] J. Goldstone and K. Gottfried, Nuovo cimento **13** (1959) 849

[Go75] D. Gogny, Proc. of the Int. Conf. on Nucl. Selfconsistent Field, Trieste, G.Ripka and M. Porneuf, Eds. North Holland Amsterdam (1975)

[Go77] K. Goeke Phys. Rev. Lett. **38** (1977) 212

[Gr57] J.J. Griffin and J.A. Wheeler, Phys. Rev. **108** (1957) 311

[Gu67] M.C. Gutzwiller, J. Math. Phys. **8** (1967) 1979

[Gu69] M.C. Gutzwiller, J. Math. Phys. **10** (1969) 1004

[Gu70] M.C. Gutzwiller, J. Math. Phys. **11** (1970) 1791

[Gu71] M.C. Gutzwiller, J. Math. Phys. **12** (1971) 343

[Ha72] M. Hage-Hassan and M. Lambert, Nucl. Phys. **A188** (1972) 545

[Ha73] P.K. Haff and L. Willets, Phys. Rev. **C7** (1973) 951

[Ha77] M.N. Harakeh, K. van der Borg, T Ishimatsu, H.P. Morsch, A. van der Woude and F.E. Bertrand. Phys. Rev. Lett. **38** (1977) 676

[Hi53] D.L. Hill and J.A. Wheeler, Phys. Rev. **89** (1953) 1102

[Ho73] G. Holzwarth, Nucl. Phys. **A207** (1973) 545

[Ho76] T. Hoshino and A. Arima, Phys. Rev. Let. **37** (1976) 266

[Ia87] F. Iachello and A. Arima, The Interacting Boson Model,Cambridge Univ. Press. (1987)

[Ik59] K. Ikeda et al, Prog. Theor. Phys. (Kyoto) **22** (1959) 663

[Ja64] B. Jancovici and D.H. Schiff, Nucl. Phys. **58** (1964) 678

[Ja75] J.D. Jackson, *Classical Electrodynamics*, Wiley, N.Y., (1975)

[Ja84] D. Janssen, M. Militzer and R. Reif Nucl. Phys. **A425** (1984) 152

[Jo84] R.V. Jolos, R. Schmidt and J. Teichert, Nucl. Phys. **A429** (1984) 139

[Ka60] M. Kalagashi and T. Marumori, Prog. Theor. Phys. (Kyoto) **23** (1960) 387

[Ka68] A. Kamlah, Z. Phys.**216** (1968) 52

[Ka79] K.K. Kan, J.J. Griffin, P.C. Lichtner and M. Dworzecka, Nucl. Phys. **A332** (1979) 109

[Ke62] A.K. Kerman and CM Shakin, Phys Lett. **1** (1962) 151

[Ke76] A.K. Kerman and S.E. Koonin Ann. of Phys. (N.Y.) **100** (1976) 332

[Ko79] M.A. Kovash, S.L.Blatt, R.N. Boyd, T.R. Donoghue, H.J. Hausman, A.D. Bacher, Phys Rev. Lett. **42** (1979) 700

[Kr76] S. Krewald, R. Rosenfelder, J.E. Galonska and A. Faessler, Nucl. Phys. **A269** (1976) 112

[Kr77] S. Krewald, V. Klemt, J. Speth and A. Faessler, Nucl. Phys. **A281** (1977) 166

[Ku92] W. Kuhn, Proc. of the 8th. Int. Wint. Workshop on Nucl. Dyn., Jackson Hole, Wy-USA, jan. 1992, Ed. B.B. Back and W. Bauer, World Scientific. (1992),

[La41] L.D Landau, J. Phys. (USSR) **5** (1941) 71

[La64] A. M. Lane, *Nuclear theory*, Benjamin, New York (1964)

[La69] L.D. Landau and E.F. Lifschitz, *Mécanique Classique*, Mir, Moscow (1969) sect.28

[La74] L.F.F. Lathourvers, Nucl. Phys. **A226** (1974) 125

[La76] L.F.F. Lathourvers, Ann. Phys. (N.Y.) **102** (1976) 347

[La90] G. Lauritsch and P.G. Reinhard, Nucl. Phys. **A509** (1990) 287.

[La92] Land Collaboration, Nucl. Inst. Meth. **A314** (1992) 136

[La93] Land Collaboration, Phys. Rev. Lett. **70** (1993) 1767

[Le50] J.S. Levinger and H.A. Bethe, Phys. Rev. Lett. **42** (1950) 115

[Le79] C. Leclerc-Willain and K. Dietrich Phys. Lett. **87B** (1979) 21

[Le80] S. Levit, J.W. Negele and Z. Paltiel, Phys. Rev. **C21** (1980) 1603

[Le80a] S. Levit, J.W. Negele and Z. Paltiel, Phys. Rev. bf C22 (1980) 1979

[Lh93] I. Lhenry, T. Suomijarvi, Ph. Chomaz and N. Van Giai, Nucl. Phys. **A565** (1993) 524

[Li65] H.J. Lipkin, N. Meshkov and A.J. Glick, Nucl. Phys. **62** (1965) 188,199,211

[Li76] K.F. Liu and G.E.Brown, Nucl. Phys. **A265** (1976) 385

[Li76a] K.F. Liu and N. Van Giai Phys. Lett. **65B** (1976) 23

[Li89] E. Lipparini and S. Stringari, Phys. Rep. **175** (1989)103

[Ll92] W.J. Llope and P. Braun Munzinger, Phys. Rev. **C 45** (1992) 799

[Ma60] T. Marumori, Prog. Theor. Phys. **24** (1960) 331

[Ma64] T. Marumori, M. Yamamura, A. Tokunaga and K. Takad, Progr. Theor. Phys. **31** (1964) 1009 and **22** (1964) 726

[Ma71] E.R. Marshalek, Nucl. Phys. **A161** (1971) 401

[Ma74] E.R. Marshalek, Nucl. Phys. **A224** (1974) 221 and 245

[Ma76] E.R. Marshalek, Phys. Lett. **62B** (1976) 5

[Ma76a] N.Marty , A Willis, V. Comparat, R. Frascaria and M. Morlet, Orsay report IPNO76-03

[Ma80] E.R. Marshalek, Nucl. Phys. **A347** (1980) 253

[Ma80a] E.R. Marshalek, Phys. Lett. **95B** (1980) 337

[Ma84] G. Maino, A. Ventura, L. Zuffi, F. Iachello, Phys. Rev. **C 30** (1984) 2101

[Me39] O.L. Meitmer and O.R. Frirch, Nature **143** (1939) 239

[Me83] J. Meyer, P. Quentin and M. Brack, Phys. Lett.B133 (1983) 15

[Mi67] A.B.Migdal, *The theory of Finite Fermi systems and Aplications to Atomic Nuclei*, Wiley (Interscience) New York N.Y. (1917)

[Mo76] M.A. Morrison, T.L. Estle and N.F. Lane,*Quantum States of Atoms, Molecules and Solids*, Printice Hall, Englewood Cliffs, N.J., (1976)

[Mo88] S. Mordechai et al., Phys. Rev. Lett. **60** (1988) 408

[Mo88a] S. Mordechai, N. Auerbach, M. Burlein, H.T. Fortune, S.J. Greene, C. Fred Moore, C.L. Morris, J.M. O'Donnell, M.W. Rawool, J.D. Silk, D.L. Watson, S.H. Yoo and J.D. Zumbro, Phys. Rev. Lett. **61** (1988) 531

[Mo88b] S. Mordechai et al., Phys. Rev. **C38** (1988) 2709.

[Mo89] S. Mordechai et al, Phys. Rev. **C 40** (1989) 850

[Mo90] S. Mordechai, H.J. Fortune, J.M. O'Donnell, G. Liu, M. Burlein, A.H. Wuosmaa, S. Greene, C.L. Morris, N. Auerbach, S.H. Yoo and C. Fred Moore, Phys. Rev. **C41** (1990) 202.

[Mo91] S. Mordechai, H. Ward, K. Johnson, G. Kahrimanis, David Saunders, C. Fred Moore, J.M. O'Donnell, M.A. Kagarlis, D. Smith, H.T. Fortune, C.L. Morris, Phys. Rev. **C 43** (1991) R 1509

[Mo91a] S. Mordechai and C. Fred Moore, Nature **352** (1991) 393

[My95] W.D. Myers and W.J. Swiatecki, Nucl. Phys. **A587** (1995) 92

[Na95] R. Nayak et al, Phys. Rev. **C52** (1995) 711

[Ne82] J.W. Negele, Rev. Mod. Phys. **54** (1982) 913

[Ne83] J.O. Newton, B. Herskind, R.M. Diamond, E.L. Dines, J.E. Draper, K.L. Lindenberger, C. Schuck, S. Shih, F.S. Stephens, Phys. Rev. Lett. **46** (1981) 1383

[Ot78] T. Otsuka, A. Arima and F. Iachello, Nucl. Phys. **A309** (1978) 1

[Pa68] S.C. Pang, A. Klein and R.M. Dreizler, Ann. Phys. **49** (1968) 477

[Pe62] R.E. Peierls and D.J. Thouless, Nucl. Phys. **38** (1962) 154

[Pe77] I. Percival, Adv. Chem. Phys. **36** (1977) 3A

[Pe77a] A M. Perelomov, Sov. Phys. Ups **20(9)** (1977) 703.

[Pi66] D.Pines P.Nozieres, *The Theory of Quantum Liquids* , Benjamin New York (1966) N.Y.

[Po1892] H. Poincaré, *Les méthodes nouvelles de la mécanique céleste*, Gauthier-Villars, Paris (1892)

[Po84] E.C. Pollacco, J.C. Jacmart, Y. Blumenfeld, Ph. Chomaz, N. Frascaria, J.P. Garron and J.C. Roynette, Nucl. Inst. and Meth. **225** (1984) 51

[Po86] G. Pollarolo, R.A. Broglia, and C.H.Dasso, Nucl. Phys. **A 451** (1986) 1212

[Pr65] J. Da Providencia, Nucl. Phys. **65** (1965) 87

[Pr68] J. Da Providencia, Nucl. Phys. **A108** (1968) 589

[Pu77] F.Pühlhofer, Nucl. Phys. **A280** (1977) 267// M.N. Harakeh, extended version

[Ra1877] J.W.S. Rayleigh, *Theory of Sound*, (1877), Mac Millan London

[Ra78] J. Randrup, Nucl. Phys. **A307** (1978)319

[Re76] P.G. Reinhard, Nucl. Phys. **A261** (1976) 291

[Ri81] P.Ring and P.Schuck, *The Nuclear many body problem*, (1981) (Springer-Verlag N.Y.)

[Ri84] P. Ring, L.M. Robledo, J.L. Egido and M. Faber, Nucl. Phys.A419 (1984) 261

[Ri93] J. Ritman et al.,Phys. Rev. Lett. **70** (1993) 533

[Ro81] J.C. Roynette, N. Frascaria, Y. Blumenfeld, J.C. Jacmart, E. Plagnol, J.P. Garron, A. Gamp and H. Fuchs. Z. Phys. **A299** (1981) 73

[Sa62] J. Sawicki, Phys. Rev. **126** (1962) 2231

[Sa83] T. Saito, Y. Fujii, K. Saito, Y. Torizuka, T. Tohei and J. Hirota, Phys. Rev. **C28** (1983) 652

[Sa84] H. Sagawa and G.F. Bertsch, Phys. Lett.B146 (1984) 138

[Sc73] P. Schuck and S. Ethofer, Nucl. Phys. **A212** (1973) 269

[Sc91] J. A. Scarpaci, Y. Blumenfeld, Ph. Chomaz, N. Frascaria, J. P. Garron, J. C. Roynette, T. Suomijärvi, N. Alamanos, B.Fernandez, A. Gillibert, A. Lepine, A. Van der Woude, Phys. Lett. **258B** (1991) 279

[Sc91b] R. Schmidt, Ph. D. Dissertation, University of Mainz (1991) GSI report n^o 9-91 (to be published)

[Sc91c] J. A. Scarpaci, These Orsay (1991)

[Sc93] J. A. Scarpaci, Y. Blumenfeld, Ph. Chomaz, N. Frascaria, J. P. Garron, J. C. Roynette, T. Suomijärvi, N. Alamanos, B.Fernandez, A. Gillibert, A. Lepine, A. Van der Woude, Phys. Rev. Lett. **71** (1993) 3766

[Sc93a] R.Schmidt et al., Phys. Rev. Lett. **70** (1993) 1767.

[Sh75] S. Shlomo and G.F. Bertch Nucl. Phys. **A243** (1975) 507

[Sh93] S. Shlomo and D.H. Youngblood, Phys. Rev. **C47** (1993) 529

[Sn86] K.A. Snover, Ann. Rev. Nucl. Part. Sci. **36** (1986) 545

[So83] M. Sommermann, Ann. Phys. 151 (1983) 163

[So94] U. Sonnadara et al. Proc. of the Gull Lake Nucl. Phys. Conf. August 1993 (USA) and to be published in Nuc. Phys A. (1994)

[Sp81] J. Speth and A. Van der Woude, Rep. Progr. Phys. **44** (1981) 719

[Sp91] J.Speth, *Electric and Magnetic Giant Resonances in Nuclei*, World Scientific (1991)

[St50] H.Steinwedel and J.H.D. Jensen, Z. Nat. **5a** (1950) 413

[Su61] H. Suhl and N. R. Werthamer, Phys. Rev. **122** (1961) 359

[Su89] T. Suomijärvi, D. Beaumel, Y. Blumenfeld, Ph. Chomaz, N. Frascaria, J.P. Garron, J.C. Jacmart, J.C. Roynette, J. Barrette, B. Berthier, B. Fernandez, J. Gastebois, P. Roussel-Chomaz, W. Mittig, L. Kraus, and I.Linck, Nucl.Phys. **A491** (1989) 314

[Su90] T. Suomijärvi, D. Beaumel, Y. Blumenfeld, Ph. Chomaz, N. Frascaria, J.P. Garron, J.C. Roynette, J. A. Scarpaci, J. Barrette, B. Fernandez, J.Gastebois and W. Mittig, Nucl. Phys. **A509** (1990) 369

[Ta59] S. Takagi, Prog. Theor. Phys. (Kyoto) **21** (1959) 174

[Th61] D.J. Thouless, *The Quantum Mechanics of Many Body Systems*, Academic Press, New York (1961)

[Th61a] D.J. Thouless, Nucl. Phys **22** (1961) 78

[To77] A.F.R. De Toledo Piza et al, Phys. Rev. **C15** (1977) 1477

[To78] A.F.R. De Toledo Piza and E.J.V. De Passos, Nuovo Cimento **45B** (1978) 1

[Tr81] H. Tricoire, C. Marty and D. Vautherin Phys. Lett. **100B** (1981) 106

[Tr81a] H. Tricoire, H. Flocard and D. Vautherin Phys. Lett. **100B** (1981) 103

[Ts78] S.F. Tsai, Phys. Rev. **C17** (1978) 1862

[Um84] S.A. Umar, M.R. Strayer and D.J. Ernst, Phys. Lett. **140B** (1984) 290

[Us60] T. Usui, Progr. Theor. Phys. **23** (1960) 787

[Va75] D. Vautherin, Phys. Lett. **57 B** (1975) 425

[Va84] D. Vautherin and N. Vinh Mau, Nucl. Phys.A422 (1984) 140

[Vi72] F. Villars, Proc. of the Int. Conf. on Dyn. Struct. of Nucl. States, Mont Tremblant, 1971, D.J. Rowe, L.E. Trainor, S.S.MS. Wong, T.W . Donnelly, Eds. Toronto, Univ. Press, (1972)

[Vi75] F. Villars, Proc. of the Int. Conf. on Nucl. Selfconsistent Fields, Trieste, G.Ripka and M. Porneuf, Eds. North. Holland. Amsterdam (1975)

[Vi77] F. Villars, Nucl. Phys **A285** (1977) 269

[Wa92] H. Ward, K. Johnson, G. Kahrimanis, D. Saunders, C. Fred Moore, S. Mordechai, C.L. Morris, H.T. Fortune, M. Akagarlis, D.A. Smith, J.M. O'Donnell, N. Auerbach, Phys. Rev. **C 45** (1992) 2723

[Wa93] H. Ward, J. Johnson, K. Johnson, S. Greene, Y. Grof, C. Fred Moore, S. Mordechai, C.L. Morris, J.M. O'Donnell and C. Whitley, Phys. Rev. Lett **70** (1993) 3209

[We34] C. F. Weiszacker, Z. Phys. **88** (1934) 612

[Wi34] E. J. Williams, Phys. Rev. **45** (1934) 729

[Wi35] E. J. Williams, K. Dan Vidensk and S. Selsk, Math. Fys. Med **13** (1935) 4

[Wi79] A. Winther and K. Alder, Nucl. Phys. **A319** (1979) 518

[Wo87] A. Van der Woude, Prog. in Part. and Nucl. Phys. **18** (1987) 217

[Ya83] C. Yannouleas, M. Dworzecka and J. J. Griffin, Nucl. Phys. **A397** (1983) 239

[Ya85] C. Yannouleas, S. Jang and Ph. Chomaz, Phys. Lett. **163B** (1985) 55

[Yo77] D.H.Youngblood, C.M. Rosza, J.M. Moss, D.R. Brown and J.D. Bronson, Phys. Rev. Lett. **39** (1977) 1188

[Yu94] V.Yu.Ponomarev et al., Phys. Rev. Lett. **72** (1994) 1168.

[Za84] I. Zahed and M. Baranger, Phys. Rev. **C29** (1984) 1010

[Ze93] V. Zelevinsky, Nucl. Phys. (in press) C.A. Bertulani and V. Zelevinsky Preprint MSUCL-891 (1993)

[Zw60] R. Zwanzig, *Lectures in Theoretical Physics*, Vol. III (Boulder, 1960), Interscience, N.Y. (1961)